

Journal of Experimental Biology
Colonial Architecture Modulates the Speed and Efficiency of Multi-Jet Swimming in Salp Colonies
--Manuscript Draft--

Manuscript Number:	jeb.249465R1
Article Type:	Research Article
Full Title:	Colonial Architecture Modulates the Speed and Efficiency of Multi-Jet Swimming in Salp Colonies
Abstract:	<p>Salps are marine pelagic tunicates with a complex life cycle including a solitary and colonial stage. Salp colonies are composed of asexually budded individuals that coordinate their swimming by multi-jet propulsion. Colonies develop into species-specific architectures with distinct zooid orientations. These distinct colonial architectures vary in how frontal area scales with the number of zooids in the colony. Here, we address how differences in frontal area drive differences in swimming speed and the relationship between swimming speed and cost of transport in salps. We (1) compare swimming speed across salp species and architectures, (2) evaluate how swimming speed scales with the number of zooids across colony in architectures, and (3) compare the metabolic cost of transport across species and how it scales with swimming speed. To measure swimming speeds, we recorded swimming salp colonies using in situ videography while SCUBA diving in the open ocean. To estimate the cost of transport, we measured the respiration rates of swimming and anesthetized salps collected in situ using jars equipped with non-invasive oxygen sensors. We found that linear colonies swim faster, which supports idea that their differential advantage in frontal area scales with an increasing number of zooids. We also found that higher swimming speeds predict lower costs of transport in salps. These findings underscore the importance of considering propeller arrangement to optimize speed and energy efficiency in bioinspired underwater vehicle design, leveraging lessons learned from the diverse natural laboratory provided by salp diversity.</p>
Corresponding Author:	Alejandro Damian-Serrano, Ph.D. University of Oregon Oregon Institute of Marine Biology Eugene, OR UNITED STATES
Other Authors:	Kaiden A. Walton, B.S. Anneliese Bishop-Perdue, B.S. Sophie Bagoye Kevin T. Du Clos, Ph.D. Bradford J. Gemmell, Ph.D. Sean P. Colin, Ph.D. John H. Costello, Ph.D. Kelly R. Sutherland, Ph.D.
Keywords:	salps; colonial architecture; multi-jet propulsion; swimming; cost of transport
Additional Information:	
Question	Response
Editor Suggestions You may request that your submission is assigned to a specific <u>editor</u> . Please suggest no more than three editor names in order of preference. Although you may suggest an editor for your submission, the journal will make the final assignment. If you do not request an editor, your	Sheila Patek (previous editor for first submission)

submission will be assigned to the most appropriate editor as determined by the editorial staff.	
Companion Paper	No
Is your paper a companion paper (part of a group of papers being submitted)?	
Special Issue	No, this article is not part of a special themed issue
Open Access	Green Open Access
Please check your funder requirements carefully and select the appropriate Open Access publication route below. A quote for your Open Access publication charges will be available to view on the final submission page, revealing any institutional discounts and providing you with another chance to select Open Access. See Instructions for further information.	
Word Count	8041
Number of Figures	7
Number of Tables	0

Dear Dr Damian-Serrano,

...

As you will see, the reviewers gave favourable reports but raised some critical points that will require amendments to your manuscript. Both reviewers (and I) appreciate the extensive revisions based on the first round of reviews. However, there still remain a considerable number of areas needed revision. The reviewers provide clear and constructive feedback about which areas need additional work.

>We thank the Editor for her generous feedback.

I also emphasize the need to be clear about sample sizes (N, n, df, test statistics) when reporting the statistical results.

>We added details on sample sizes everywhere where p-values are reported across the results.

Also, there appears to be a misconception by the authors about why phylogenetic comparative methods are used. The most crucial reason is to address the non-independence of data points when species are more or less closely related (independence of data points is required of all the statistics used in this manuscript). Please fix that section of the manuscript and clearly state how violating the rule of non-independence of data points may have influenced your statistics-based findings. Or, include a phylogeny and perform the statistics correctly using appropriate statistical methods.

>Please see response to the last point raised by Reviewer 1.

Please make sure to plot all data points on the box plots (data transparency requirement of JEB).

>We added jittered data points to the boxplots in Figs. 3 and 7 and now all data points are plotted in all plots.

Lastly, I encourage the authors to upload their R code to accompany the data spreadsheet. The code would further enhance the replicability of the study.

>We have now included the R code in the resubmission.

Provided you are able to fully address the reviewers' comments, we hope you won't mind the extra work involved in revising your manuscript and adhering to our formatting instructions below. Please ensure that you clearly highlight all changes made in the revised manuscript. Please avoid using 'Track changes' in Word files as these are lost in PDF conversion.

I would be grateful if you would also list how you have dealt with the points raised by the editor and reviewers in the 'Response to Reviewers' box. Please attend to all of the editor's and

reviewers' comments. If you do not agree with any of their criticisms or suggestions please explain clearly why this is so.

In order to promote timely publication, we generally ask that the revision be completed within 90 days from the date of this letter. However, we recognise that this may not always be possible so we will be happy to grant an extension where this is needed: please just contact the Editorial Office.

I look forward to receiving your revised manuscript.

With best wishes,

S. Patek

Handling Editor

Comments from the Reviewers:

Reviewer 1: Damian-Serrano et al have considered a comparison of swimming and metabolic-rate measurements across numerous species of salp to address a hypothesis that differences in swimming speed are driven by frontal area differences between different colony formations. I reviewed an earlier version of this manuscript and find this version to be a great improvement. However, I still have number of suggestions for improving the presentation of this work. Most importantly, the statistical analysis requires greater transparency in its presentation in the methods and through reporting of sample size in the Results.

>We thank Reviewer 1 for their generous feedback and for their willingness to re-review our manuscript.

SPECIFIC COMMENTS

(Line numbers are the ones on the right)

L45 - Given the hypothesis, seems like you'd want to see how COT scales with frontal area too.

>Since COT was only different in a few of the architectures based on Tukey's posthoc pairwise comparisons and was mostly unrelated to frontal area (Table S2B), we chose to focus on the more robust relationship between swimming speed and COT.

L49 - The statement about "due to their differential advantage in frontal area scaling" is in interpretation is written in the tone of an observation. Given the evidence, I think it would be more appropriate to say sometime like "We found that linear colonies generally swim faster, which supports the idea that . . ."

>We rephrased the statement to "We found that linear colonies swim faster, which supports idea that their differential advantage in frontal area scales with an increasing number of zooids."

L63 - Maybe "drawing" and "ejecting" instead of "inhaling" and "exhaling"?

>We modified the statement to "Zooids in the colony feed and propel themselves by drawing water in through the oral siphon, using muscle contraction to compress their pharyngeal chamber, and ejecting a jet of water from their atrial siphon (Bone & Trueman 1983)."

L91 - I think Alexander and Vogel only makes sense as a citations if they offered a unique statement about drag in salps, which may be the case. They are not really strong sources on the origins of drag.

>We chose to omit this statement all together when we streamlined the Introduction in response to Reviewer 2's comments.

L139 - Nothing against Vogel, but there many options in the primary literature, and reviews, to support this statement, which would more directly point to the source of the information.

>We replaced this citation with Andersen et al 2016.

Andersen, K. H., Berge, T., Gonçalves, R. J., Hartvig, M., Heuschele, J., Hylander, S., ... & Kiørboe, T. (2016). Characteristic sizes of life in the oceans, from bacteria to whales. Annual review of marine science, 8(1), 217-241.

L168 - The statement about "scaling drive disparities between colonial architectures" is important because it articulates a major aim of the study. So, I recommend using more precise language: disparities in what respect?

>We rewrote this statement to be more precise and concise: "...we investigate how swimming speed varies with the number of propeller zooids and differences in frontal area scaling between colonial architectures."

I believe JEB requires that you provide the location of manufacturers.

>We added the locations of manufacturers to the products throughout the Methods wherever possible.

I do not think Eqns. 1 and 2 are necessary, but fine to include.

>We kept the equations for completeness.

L288 - Readers may wonder why dried mass was not selected as the means of normalizing the metabolic measurements by animal size, given the presumably large volume of these gelatinous organisms that is not comprised of living tissue. Isn't it possible that differences in the measurements could be due to differences in the proportion of metabolically-active tissue. A concise mention of these considerations would be helpful.

>We added the following explanation: "Biovolume was used instead of dry mass to normalize measurements due to the inherent difficulties of accurately measuring dry mass of these fragile gelatinous organisms in the field. Biovolume provides a consistent and reliable measure of the

live size of the colony, which is directly relevant to the volume of water being displaced during swimming."

L323 - This section requires a more expansive description of the statistical analysis. What particular linear models? Which continuous variables, in particular? How are repeated measures taken into account? I'm not sure if testing relative to a zero slope makes sense (vs. comparing regressions between species), but I am not sure what variables are being referenced here.

>We added the following text in the Methods to state more precisely how we used statistical methods.

Linear model: "To test the relationships between pairs of continuous variables across architectures (e.g. swimming speed vs. number of zooids), we used linear regressions."

Testing against zero slope: "We evaluated the significance of the slope parameter when compared against a flat slope (one-tailed t-test) to test whether changes in the independent variable (e.g. number of zooids) were associated with changes in the dependent variable (e.g. swimming speed)."

Repeated measures: "Owing to the patchiness of some species despite 80+ hours spent underwater (Table S1), we used replicate measurements (n) from each specimen (N) in swimming speed ANOVAs and regressions. We used an exponential regression to test the relationship between speed and COT. Specimen means (N) were used for all COT comparisons and regressions. Individual measurements (n) were used up to determine oxygen consumption rates. To evaluate the relative contribution of zooid size, pulsation rate, zooid number, and architecture type on swimming speed, we fitted a generalized linear model and evaluated the significance and proportion of variance explained by each factor using their partial R^2 ."

Sample sizes should be reported in the Results. It should be made clear when p-values are reported what the sample sizes are. Supplemental tables and mention in the methods is insufficient.

>We added sample sizes everywhere where p-values were reported throughout the ms, including in the figure legends.

Fig. 5 - zooids/pulse — Does this mean zooid length/pulse? Perhaps this could be phrased more specifically?

>We updated the y-axis label to read "zooid lengths per pulsation".

L408-415 - These details should be offered in the Methods.

>We briefly describe the generalized linear model (GLM) in the Methods and then name the model variables again in Results-- salp swimming speed (U) from zooid length (L), pulsation

rate (P), number of zooids (Z), and colonial architecture represented as frontal area scaling mode (A) -- so that the reader won't have to backtrack to the Methods.

L439 - Paragraphs should be 3 or more sentences.

>We adjoined this paragraph to the next one, which is also about energetic investment.

L442-446 - Run on sentence.

>We split the sentence into three sentences. The new wording reads: "We then compared the proportion of energetic investment in swimming to the COT values across species (Fig. S3A,B). We found no relationship with absolute COT (N = 74, 14 species, p = 0.24). We found a positive relationship with zooid-length scaled COT (N = 74, 14 species, Swimming % = 0.11*COT per zooid length + 34.4, adjusted R² = 0.22, p < 0.001), indicating that species with more costly locomotion per zooid length invest a larger proportion of their energy budget in swimming."

L479 - size, by what metric?

>We rephrased the wording to be more precise "...suggesting an underlying relationship between pulsation rate and zooid length..."

Please cite the results supporting all of the statements of findings in the Discussion. This appears more towards the end of the Discussion than at the beginning.

>We added relevant figure and table citations throughout the Discussion.

L497 - There is no such thing as a "less hydrodynamic configuration." L603 Says "highly hydrodynamic forms". These are misuses of the term "hydrodynamic". By analogy, one would not say that one animal is more mechanical than another.

>We removed these mentions of "more/less hydrodynamic" and replaced them with the term "streamlined".

L631-634 - I do not follow the logic of the co-evolution of traits as reason for a phylogenetic analysis as being inappropriate. This merits a more clear explanation or perhaps it is a non-essential point that could be avoided.

>We thank the Reviewer for raising this important point. We understand the importance of addressing the non-independence of data points when dealing with species that are related to varying degrees and acknowledge that our statement was not sufficiently clear. We have revised the text to clarify our reasoning and acknowledge the potential influence of phylogenetic history on residual variation as follows: "In the current study we did not use phylogenetic comparative methods in our analysis because like other investigators comparing biomechanical properties across species (e.g. Dabiri et al. 2010, Di Santo et al. 2021) we were

interested in inherent mechanical relationships dictated by the colony architectures. For instance, a linear arrangement of zooids inherently reduces drag compared to a cluster arrangement, leading to faster swimming speeds and potentially higher efficiency regardless of phylogenetic history. In other words, any phylogenetic inertia is irrelevant in instantaneous relationships between traits (Felsenstein 1985). Moreover, independence of data is often incorrectly assumed to be an assumption of standard (nonphylogenetic) regressions (Uyeda et al. 2018), when in reality the assumptions relate to the independence and distribution of the error terms. Thus, when all the phylogenetic signal is present in the predictor, as it is in the case with colonial architecture (Damian-Serrano et al. 2022) and its associated characteristics, there is no need for any “phylogenetic correction” (Uyeda et al. 2018). However, there may be unaccounted factors explaining the residual variation in our analyses that may bear phylogenetic signal. For example, tunic stiffness, tunic smoothness, muscle band number, muscle fiber density, swimming behavior, as well as metabolic and physiological baselines may be more similar between more closely related species, potentially erasing some of the architecture-specific signal. Future studies could address the role of phylogeny and heritable factors in salp swimming speed and cost of transport using phylogenetic comparative methods. These analyses could reveal whether these factors have co-evolved with each other and/or with respiration rate or colonial architecture.”

Dabiri, J. O., Colin, S. P., Katija, K., & Costello, J. H. (2010). A wake-based correlate of swimming performance and foraging behavior in seven co-occurring jellyfish species. *Journal of experimental biology*, 213(8), 1217-1225.

Di Santo, V., Goerig, E., Wainwright, D. K., Akanyeti, O., Liao, J. C., Castro-Santos, T., & Lauder, G. V. (2021). Convergence of undulatory swimming kinematics across a diversity of fishes. *Proceedings of the National Academy of Sciences*, 118(49), e2113206118.

Felsenstein, J. (1985). Phylogenies and the comparative method. *The American Naturalist*, 125(1), 1-15.

Uyeda, J. C., Zenil-Ferguson, R., & Pennell, M. W. (2018). Rethinking phylogenetic comparative methods. *Systematic Biology*, 67(6), 1091-1109.

Damian-Serrano, A., Hughes, M., & Sutherland, K. R. (2023). A new molecular phylogeny of salps (Tunicata: thalicea: salpida) and the evolutionary history of their colonial architecture. *Integrative Organismal Biology*, 5(1), obad037.

Reviewer 2: The primary aim of the paper is to determine what effect, if any, the architectures of salps colonies have on the swimming speed and metabolic costs of the organisms. The stated motivation for the work is to provide insight into bio-inspired designs, such as for underwater vehicles.

The authors' experimental measurements of difficult-to-obtain quantities and their contribution to the body of knowledge regarding salps are impressive. They have also made a conscious effort to clarify and strengthen many points, which indicates a desire to be clear, open, and honest in their reporting. Below I have tried to balance recognition of the enormous challenges involved in

obtaining the data and the limited number of available data points for analysis with gauging the appropriateness of the strength of the claims.

>We thank Reviewer 2 for their generous feedback.

There are two main outstanding issues of the paper as I read it. First is the number of predictions and expectations in the introductory part of the paper, which tend to take away from rather than strengthen the main hypotheses.

>We have eliminated the predictions and expectations in the Introduction and now focus on a single expectation based on frontal area (p. 3): "Salp colonial architectures differ in how the number of zooids in the colony scales with their frontal area relative to motion (Madin 1990). Some architectures (linear, bipinnate, and helical) have a constant frontal area, regardless of zooid number. These architectures may benefit from increased thrust delivered by larger numbers of zooids while maintaining a constant frontal area. However, the rest of the architectures (oblique, transversal, whorl, and cluster) have an increasing (directly proportional) frontal area as the number of zooids increases (Fig. 1). Therefore, we expect the latter architectures to not only obtain more thrust, but to also experience more frontal water resistance as zooid number increases. As a result, we anticipate that swimming speed will be greater in colonies that bear a larger number of zooids, but only (or more so) for species with architectures that have a constant frontal area."

The second is a claim of a causal relationship based on indirect rather than direct evidence. It's possible these questions/issues could be addressed within the current architecture of the paper. Statement of hypotheses. The introduction contains at least 12 expectations/predictions (Lines 84, 85, 90, 91, 98, 102, 106, 129, 137, 142, 146, 158, 162.)

> Instead of stating expectations based on previous literature in the Introduction, we now discuss the Results in light of previous literature in the Discussion. The paper reads more smoothly.

The last paragraph (Lines 309-318) of the introduction states that the following will be studied: how swimming speed varies with the number of propellers and whether there are differences in frontal scaling drive [which?] disparities between architectures, assessing how cost of transport varies, and how COT varies with swimming speed and pulsation effort.

We have edited the last paragraph in the Introduction to say: "In addition, we investigate how swimming speed varies with the number of propeller zooids and differences in frontal area scaling between colonial architectures. Finally, we compare cost of transport (COT) across salp species and assess how COT scales with swimming speed and pulsation effort."

Is one or more of these the main hypothesis of the paper? Many measurements are made and many tests run, but they don't seem to address a single (or maybe two) clearly stated question or line of inquiry. This may be in part due to the fact that there is limited data in some cases, so

there may be a desire to present the case from many different angles. And I think the paper does have an intention (see below), but the number of side predictions obscures it. I suggest moving the predictions/expectations to the discussion as part of the analysis if they support the central thesis while leaving the introduction clear to lay the groundwork for the primary aim. If the authors feel the predictions lay this ground work, they may have a different notion of how to tighten the focus.

>We have streamlined the Introduction and now have a single prediction regarding scaling of frontal area. After re-visiting the literature, we determined that there are not enough data on the relationship between swimming speed and COT to have an a priori hypothesis. We therefore have re-worded the Introduction such that studying COT is a research objective rather than addressing a specific hypothesis. The end of the Introduction now reads: "we compare cost of transport (COT) across salp species and assess how COT scales with swimming speed and pulsation effort."

Statement of causal relationships. If a clear purpose were to be identified, it appears to be the main result from the abstract which reads (Lines 49-53): "We found that linear colonies generally swim faster due to their differential advantage in frontal area scaling with an increasing number of zooids." I agree with the findings to an extent, but the cause is less clear. The qualifier on lines 525-542 acknowledges that there may be confounding factors, but the strength of the statement in the abstract belies that notion.

>We rephrased this to: "We found that linear colonies generally swim faster, which is consistent with the hypothesis that their differential advantage in frontal area scaling contributes to their increased speed."

Focusing on Figure 5 A for example, I agree that this shows linear colonies tend to swim faster as the number of zooids increases when only considering linear colonies. However, it would be a strong statement to state that linear colonies swim faster than bipinnate and helical as number of zooids grow (line 503) based on these data because 1) there is only one helical specimen and 2) that pattern is not necessarily clear in the range where you have data for all three types of specimens, and you only have linear specimens in the region where you see a clear increase in speed on the right.

In figure 5 B, there is a similar concern with the oblique data point, but also the gap in colony numbers for the cluster data is concerning. Ignoring the point on the right, there appears to be an upward trend in swimming speed, even if more slight than the left. This could indicate the right-hand point is an outlier, or there is likely a non-monotonic relationship between swimming speed and a number of colonies in some of the architectures. This means there is possibly a region where larger frontal areas swim as fast or faster than architectures with lower frontal areas. The data presented here neither confirm nor deny this.

>We agree with the reviewer that there is patchiness in sample sizes and gaps in zooid numbers. And, we originally had a figure showing number of zooids vs. swimming speed for each individual species in the Supplemental section but we removed it to comply with JEB's

figure limits (the raw data are still available in Dataset S1). We added a sentence to the Results associated with Fig. 5 to acknowledge the uncertainties associated with low specimen numbers: "However, the limited sample sizes for helical and oblique chains prevent us from drawing firm conclusions about these architectures."

Questions about data comparison:

*In table S1, there is a lot of variation in the mean length of zooids between species. Is there a lot of variation within a species? It might be appropriate to report the standard deviation.

>The raw data including all of the zooid lengths and showing the full variability is available now in Dataset S1A and S1B.

*I couldn't open/find the Dataset S1, so this might have been addressed already. There is some discussion about the 2D versus stereo measurements and that the 2D measurements gave slower speeds. I didn't see that it was specified which species were measured with which apparatus. Using obtainable footage is reasonable, especially when the specimens are hard to collect/track/find. But if speed is a primary part of the argument, it should be obvious where the differences in speed measurements lie.

>We were sorry to hear that the reviewer couldn't access Dataset 1; please do let us know of there are any challenges with access this time. Dataset S1A specifies each video file analyzed, species and camera system (3D or 2D). Both measurement types were used for *S. zonaria* and *S. maxima*. However, *Brookssia*, *Ritteriella* spp., *Pegea*, *I. cylindrica*, *M. hexagona*, *S. fusiformis*, *S. aspera*, *C. bakeri*, *C. polae*, and *C. sewelli* were 3D-only; whereas *Helicosalpa*, *Thalia*, *C. affinis*, and *C. quadriluminis* were 2D-only.

Minor things:

*It might be more appropriate to refer to these as all of the known architectures throughout rather than all of the architectures unless it is definitively known that no other configurations are possible.

>We modified the wording in the Introduction to: "In this study, we compare swimming speeds across 17 salp species and energetic costs of swimming across 15 species, encompassing all seven known salp colony architectures"

*Different marker point shapes would make the graphs more color-/resource accessibility friendly. The results would be hard to discern for someone with a different color perception or who can only access a black-and-white copy. Similarly, using different striping patterns on bar charts would make the graphs more accessible. This might be something for the publisher to address.

>We appreciate this point and agree that the different markers might be hard to distinguish in a greyscale print version of Figs. 4, 5 and 7. On the other hand, since electronic versions are more accessible and widely read, we will leave the plotting requirements up to the publisher.

1 **Title: Colonial Architecture Modulates the Speed and
2 Efficiency of Multi-Jet Swimming in Salp Colonies**

3
4 **Authors:** Alejandro Damian-Serrano¹, Kai A. Walton¹, Anneliese Bishop-Perdue¹, Sophie
5 Bagoye¹, Kevin T. Du Clos², Bradford J. Gemmell³, Sean P. Colin^{4,5}, John H. Costello⁶, Kelly R.
6 Sutherland¹

7
8 **Author Affiliations:**
9

10 (1) Institute of Ecology and Evolution, Department of Biology, University of Oregon. 473 Onyx
11 Bridge, 5289 University of Oregon, Eugene, OR 97403-5289, USA.

12 (2) Louisiana Universities Marine Consortium, 8124 Highway 56, Chauvin, LA 70344, USA.

13 (3) Department of Integrative Biology, University of South Florida, 4202 East Fowler Avenue,
14 Tampa, FL 33620, USA.

15 (4) Marine Biology and Environmental Science, Roger Williams University, Bristol, RI 02809, USA.

16 (5) Whitman Center, Marine Biological Laboratory, Woods Hole, MA 02543, USA.

17 (6) Biology Department, Providence College, Providence, RI 02918, USA.

18
19 **Running title:** Architecture Modulates Salp Swimming
20

21 **Summary Statement (30 words)**

22
23 Linear arrangements in multi-jet propelled marine colonial invertebrates are faster than less
24 streamlined architectures without incurring in higher costs of transport, offering insights for
25 bioinspired underwater vehicle design.

26
27
28
29
30
31
32
33

34 **Abstract**

35
36 Salps are marine pelagic tunicates with a complex life cycle including a solitary and colonial stage.
37 Salp colonies are composed of asexually budded individuals that coordinate their swimming by
38 multi-jet propulsion. Colonies develop into species-specific architectures with distinct zooid
39 orientations. These distinct colonial architectures vary in how frontal area scales with the number
40 of zooids in the colony. **Here, we address how** differences in frontal area drive differences in
41 swimming speed and **the relationship between** swimming speed **and** cost of transport in salps.
42 We (1) compare swimming speed across salp species and architectures, (2) evaluate how
43 swimming speed scales with the number of zooids across colony in architectures, and (3)
44 compare the metabolic cost of transport across species and how it scales with swimming speed.
45 To measure swimming speeds, we recorded swimming salp colonies using in situ videography
46 while SCUBA diving in the open ocean. To estimate the cost of transport, we measured the
47 respiration rates of swimming and anesthetized salps collected in situ using jars equipped with
48 non-invasive oxygen sensors. We found that linear colonies swim faster, **which supports idea that**
49 **their** differential advantage in frontal area **scales** with an increasing number of zooids. We also
50 found that higher swimming speeds predict lower costs of transport in salps. These findings
51 underscore the importance of considering propeller arrangement to optimize speed and energy
52 efficiency in bioinspired underwater vehicle design, leveraging lessons learned from the diverse
53 natural laboratory provided by salp diversity.

54

55 **Keywords:** salps, colonial architecture, multi-jet propulsion, swimming, cost of transport

56

57 **Introduction**

58 Salps (Tunicata: Thaliacea: Salpida) are planktonic invertebrates that have a two-phase
59 life cycle comprised of a solitary oozooid that asexually buds colonies of sexually reproducing
60 blastozooids. Salp colonies are composed of up to hundreds of genetically identical, physically
61 and neurophysiologically integrated pulsatile zooids (Bone et al. 1980, Mackie 1986). Zooids in
62 the colony feed and propel themselves by **drawing** water **in** through the oral siphon, using muscle
63 contraction to compress their pharyngeal chamber, and **ejecting** a jet of water from their atrial
64 siphon (Bone & Trueman 1983). While solitary oozooids move using single-jet propulsion, salp
65 blastozooid colonies integrate multiple propelling jets, which increases their thrust and reduces
66 the drag that results from periodical acceleration and deceleration via asynchronous swimming
67 (Sutherland & Weihs 2017).

68 Currently, there are 48 described species of salps (WoRMS, 2024) and while salps are
69 widely distributed, most species are restricted to open ocean environments, far from the coast,
70 which poses unique challenges to accessing them for direct study in their environment (Hamner
71 et al 1975, Haddock 2004). Moreover, salps cannot be maintained alive in containers beyond a
72 few hours since they are extremely fragile and sensitive to the presence of solid walls. Therefore,
73 many morphological, ecological, and functional aspects of salp diversity, such as swimming
74 speeds and metabolic demands, have remained unexplored. One such aspect is colonial
75 architecture or the way that the zooids are arranged relative to each other in the colony. Salp
76 colonies develop into species-specific architectures with distinct zooid orientations, including
77 transversal, oblique, linear, helical, and bipinnate chains; as well as whorls, and clusters (Damian-
78 Serrano & Sutherland, 2023). These architectures **likely drive aspects of** swimming performance
79 (Madin 1990, Damian-Serrano et al. 2023).

80 Linear salp chains have been **described as** more efficient swimmers due to the reduction
81 of drag associated with a more streamlined form (Bone & Trueman 1983). In a multi-jet system,
82 having a larger number of propellers **can** improve the hydrodynamic and inertial benefits granted
83 by asynchronous multijet propulsion, in addition to providing additional thrust to the colony (Madin
84 1990, Sutherland & Weihs 2017). The effect of varying numbers of propeller zooids on swimming
85 speed has never been investigated in salps, nor how this relationship may vary across their
86 diverse colonial architectures. Salp colonial architectures differ in how the number of zooids in
87 the colony scales with their frontal area relative to motion (Madin 1990). Some architectures
88 (linear, bipinnate, and helical) have a constant frontal area, regardless of zooid number. These
89 architectures **may** benefit from increased thrust delivered by larger numbers of zooids while
90 maintaining a constant frontal area. However, the rest of the architectures (oblique, transversal,
91 whorl, and cluster) have an increasing (directly proportional) frontal area as the number of zooids
92 increases (Fig. 1). Therefore, we expect the latter architectures to not only obtain more thrust, but
93 to also experience more frontal water resistance **as zooid number increases**. As a result, we
94 **anticipate** that swimming speed will be greater in colonies that bear a larger number of zooids,
95 but only (or more so) for species with architectures that have a constant frontal area.

96

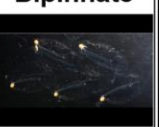
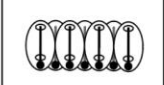
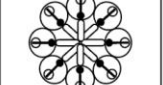
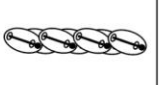
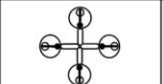
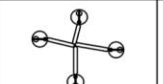
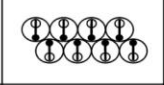
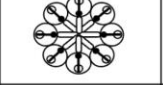
	Transversal	Whorl	Cluster	Helical	Oblique	Linear	Bipinnate
Architecture							
							
Frontal area 4 zooids							
Frontal area 8 zooids							
Scaling	2	2	2	1	1×2	1	1

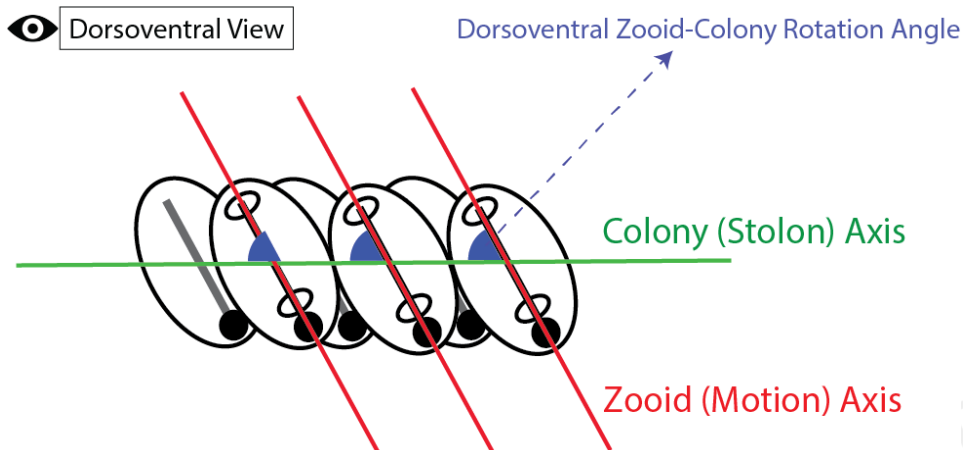
Figure 1. Salp colonial architectures with representative species photos (*Pegea* sp. for transversal, *Cyclosalpa affinis* for whorl, *Cyclosalpa sewelli* for cluster, *Helicosalpa virgula* for helical, *Thalia cicatricosa* for oblique, *Soestia zonaria* for linear, and *Ritteriella retracta* for bipinnate) and diagrams showing the distinct zooid orientations. The subsequent rows show the frontal view of colonies with four and eight zooids, with the final row indicating the expected frontal area increase factor between the four and the eight zooid colonies. Full black circles in the diagrams represent viscerae (guts) while the open circle represent siphons. Black straight lines inside the zooids indicate gill bars while gray straight lines represent endostyles.

Linearity of colonies, as well as zooid size and pulsation rates, are additional factors that could influence swimming performance. The degree of linearity in a colony can be expressed as the degree of parallelism between the zooids and the elongation axis of the colony (Fig. 2). This angle is determined by the degree of developmental dorsoventral zooid rotation, which can span from 90°, in transversal chains with no rotation, to 0° (perfect linearity), in some linear chains such as those from the species *Soestia zonaria* (Damian-Serrano & Sutherland, 2023). Strong reductions in the dorsoventral zooid rotation angle toward linear forms have evolved multiple times independently (Damian-Serrano et al. 2023), possibly due to adaptive advantages related to their swimming efficiency. Body size predicts swimming velocity in many animals (Andersen et al. 2016), however colonies with multiple swimming units may circumvent this size-speed relationship by having multiple propellers. Pulsation rates may also influence swimming speed as has been shown in solitary salps (Madin 1990). Pulsation by salps serves the dual role of locomotion and filter feeding. The relationship between pulsation and speed might therefore be particularly relevant for species that undergo diel vertical migration (Madin et al. 1996) and in other species pulsation may serve to maximize filtration rates. Considering the tradeoffs between

121 swimming and filtering, the eco-evolutionary relevance of swimming speed, and the hydrodynamic
122 efficiency likely varies between species (Damian-Serrano et al. 2023).

123

124



125
126 Figure 2. Schematic of an oblique chain from the dorsoventral perspective showing the zooid and
127 stolon axes and the zooid rotation angle (degree of linearity) relative to those axes. Black lines
128 indicate gill bars (mostly occluded by zooid axis) while gray lines represent endostyles.

129 The energetic costs of salp locomotion from mechanically estimated propulsive efficiency
130 suggest that like other jet-propelled swimmers, salps are hydrodynamically efficient (Sutherland
131 & Madin 2010, Gemmell et al. 2021, Trueman et al. 1984). The few metabolic measurements of
132 swimming salps show that more active species-- in terms of swimming speed and pulsation rates--
133 have the highest respiration rates (Cetta et al. 1986) and that salps have higher respiration rates
134 than other gelatinous taxa (Biggs 1977, Schneider 1992, Mayzaud et al. 2005, Trueblood 2019).
135 However, the specific costs incurred by their swimming activity and their relationship to swimming
136 speed have never been examined across the diversity of salp species.

137 In this study, we compare swimming speeds across 17 salp species and energetic costs
138 of swimming across 15 species, encompassing all seven known salp colony architectures (Fig. 1,
139 Table S1). In addition, we investigate how swimming speed varies with the number of propeller
140 zooids and differences in frontal area scaling between colonial architectures. Finally, we compare
141 cost of transport (COT) across salp species and assess how COT scales with swimming speed
142 and pulsation effort.

143

144 Materials and Methods

145 *Fieldwork* – We observed salps via 48 bluewater SCUBA dives (Haddock & Heine, 2005)
146 from a small vessel off the coast of Kailua-Kona (Hawai'i Big Island, 19°42'38.7" N 156°06'15.8"
147 W), over 2000 m of offshore water during September 2021, April 2022, September 2022 and May
148 2023. We spent a total of 42.2 hours (84.4 person hours: ADS & KRS) collecting and imaging
149 salp colonies. Some dives were diurnal, where we collected most of the specimens of *Iasis*
150 *cylindrica*, *Cyclosalpa affinis*, *Cyclosalpa sewelli*, and *Brooksia rostrata*. We observed and
151 collected most specimens of other species during night dives (blackwater diving). We recorded in
152 situ underwater videos of salp colonies swimming using a variety of cameras including primarily
153 a dark field stereovideography system (Sutherland et al. 2024), as well as a lightweight dual
154 GoPro stereo system, a brightfield single-camera system (Colin et al. 2022), and a darkfield
155 single-camera system. The primary stereovideography system was comprised of two
156 synchronized high-resolution cameras (Z Cam E2, Nan Shan, Shenzhen, China and Sync Cable;
157 4K at 60 or 120 fps) with 17mm f/1.8 lenses (Olympus M.Zuiko Digital) housed in custom
158 aluminum housings (Sexton Company, Salem, OR, USA). Each field of view was 23 x 42 mm and
159 in-focus depth was 20-25 mm. The image from the right-hand camera was viewed using an
160 external monitor (Aquatica Digital, Montreal, Quebec, Canada), and illumination was provided
161 with two 10,000-lumen lights (Keldan, Bruegg, Switzerland). An L-shaped plastic framer helped
162 the videographer position colonies in the field of view of both cameras. Before diving, the stereo
163 system was calibrated in a swimming pool using a cube with reflective landmarks. Calibration
164 images were processed using the CAL software package (SeaGIS measurement science,
165 Bacchus Marsh, Victoria, Australia). Over the course of the study, we observed 241 salp colonies
166 (N) from 18 species and recorded 1,946 measurements (n) (Dataset1A, Table S1). Throughout
167 the manuscript, we refer to the number of specimens as N and the number of measurements as
168 n.

169 *Measuring salp colony swimming speed* – For most species, we collected and analyzed
170 footage from multiple specimens (Dataset1A, Table S1). We analyzed the swimming behavior of
171 salp colonies arranged in linear (six species, 64 specimens), bipinnate (three species, 17
172 specimens), whorl (three species, 10 specimens), cluster (two species, eight specimens), and
173 transversal (one species, two specimens) architectures, with oblique and helical architectures
174 represented by a single specimen. We used a combination of spatially calibrated stereo video
175 and 2D videos with a reference scale in the frame. From the stereo videos, we manually selected
176 and measured the relative XYZ positions of salp colony zooids in EventMeasure (SeaGIS). We
177 implemented a cutoff in the RMS (root mean squared) point error estimate of < 2 mm.

178 We complemented gaps in taxon sampling with archived 2D videos in the lab from
179 previous expeditions to West Palm Beach (FL, USA) and the Pacific coast of Panama. These two-
180 dimensional single-camera videos were collected using a Sony FDR-AX700 4K Camcorder
181 (3840x2160 pixels, 60-120 fps) with a Gates Underwater Housing (**Poway, CA, USA**) using
182 brightfield illumination (Colin et al 2022) or darkfield illumination. For these 2D videos, we used
183 the FFmpeg plugin in ImageJ to manually select and measure the relative XY positions of salp
184 zooids in sequences where the colony was swimming horizontally within the focal plane. The
185 colonies were assumed to be in the same plane as the scale bar so at same distance from the
186 camera. However, in videos with a broad focal depth, this may not always had been the case,
187 thus potentially introducing some measurement error.

188 We tracked and manually selected the position of the first zooid's viscera (using a contrast-
189 based centering macro to mark the center point) as well as the position of a reference particle in
190 the water (methods described in Sutherland et al. 2024) in 10-30 frames across 50-500 frame
191 windows spanning 2-4s of swimming on the synchronized left and right videos in EventMeasure.
192 The reference particle was a non-swimming organism (such as a foraminiferan or radiolarian) or
193 a non-living particle. In addition, we recorded the pulsation rates of the specimens measured by
194 counting the number of times the atrial siphon contracted in a known period. For each analyzed
195 frame, we calculated the horizontal x, vertical y, and depth z (in the case of the stereo video
196 measurement files) components of the relative positions of the frontal zooid to the reference
197 particle as shown in Eq. 1.

$$\begin{aligned} x &= n_{animal} - n_{particle} \\ y &= n_{animal} - n_{particle} \quad \text{Eq. 1} \\ z &= n_{animal} - n_{particle} \end{aligned}$$

203 Then we calculated the instantaneous relative speeds of the frontal zooid using Eq. 2
204 (without the z component in the case of the 2D videos) given the known frame rate of each video.
205

$$U = \frac{\sqrt{(x_2-x_1)^2 + (y_2-y_1)^2 + (z_2-z_1)^2}}{t_2-t_1} \quad \text{Eq. 2}$$

207
208 *Salp colonial architecture* – To examine the relationships between locomotory variables
209 and colonial architecture, we adopted the species-specific architecture characterizations and
210 dorsoventral zooid rotation angle measurements for each species from Damian-Serrano et al.

211 (2023). Using stills from the underwater videos, we measured zooid length, zooid width, and
212 number of zooids in ImageJ manually selecting the point coordinates. These measurements were
213 repeated in at least three locations from each colony. When a distinct zooid size gradient was
214 observed, we measured zooids in locations from the proximal, middle, and distal regions to
215 capture the full range of variation in the specimen.

216 *Respiration measurements* – We collected healthy, adult blastozooid (aggregate stage)
217 colonies across 18 salp species (Dataset S1B) during blue- and black-water SCUBA dives off the
218 coast of Kona (Hawaii, USA) between September 2021 and May 2023. We analyzed the
219 respiration rates of salp colonies arranged in linear (seven species, N = 46), bipinnate (three
220 species, N = 29), whorl (three species, N = 23), cluster (two species, N = 18), and transversal
221 (one species, N = 13) architectures, oblique chains (*Thalia* sp., N = 7), and helical architectures
222 represented by *Helicosalpa virgula* (N = 2). Specimens were sealed *in situ* with their surrounding
223 water in plastic jars equipped with a PreSens oxygen sensor spot (Regensburg, Germany) and a
224 self-healing rubber port to allow for the injection of solutions without the introduction of air bubbles.
225 We removed as many symbiotic animals from the salps as possible before closing the lid without
226 damaging the colony. The same method was applied to one or more seawater controls to account
227 for the oxygen demand of the local seawater's microbiome. Several collection events occurred
228 during each 20-60 min long SCUBA dive. Jars with larger animals were opened during the safety
229 stop to allow them to re-oxygenate. Upon the divers' return to the boat, we measured the initial
230 oxygen concentration (mg/l) and temperature, and then repeated the measurements at intervals
231 between 15min and 3h, for total periods ranging between 2h and 5h, depending on logistic
232 constraints in the field and the rate of oxygen depletion. The exact interval time for each
233 measurement was variable but recorded (Dataset S1B).

234 To estimate the energetic expenditure of different salp species while actively swimming,
235 we recorded the oxygen consumption of intact specimens while swimming inside the jar. To obtain
236 a baseline of basal respiration rate (while not swimming), we anesthetized some specimens
237 before the start of the first oxygen measurement time. A few specimens were used for paired
238 experiments, where their swimming respiration was recorded for a few hours, then inoculated with
239 the anesthetic, and recorded anesthetized for another set of hours. To anesthetize salps, we
240 injected their jars with small volumes of concentrated (50 g/l) bicarbonate-buffered MS-222
241 through the rubber ports on the lids. We tailored the injection volume to the jar size aiming for a
242 final concentration of 0.2g/l, following the methods in Trueman et al. (1984). We also injected
243 some seawater control jars to evaluate the effect of MS-222 on oxygen concentration in seawater
244 and found no effect.

When multiple seawater controls were collected using jars of different sizes, we paired each jar with the control that had the most similar volume. If among multiple controls only some were jars injected with anesthetic, we paired the anesthetized specimen jars with the injected controls and the intact specimen jars with the intact controls. In experiment 26 (see Dataset S1B for experiment numbers), the control jar was lost due to an encounter with an oceanic white tip shark, thus we paired those measurements with the nearest relative time points from the control jar in experiment 25, collected the same day hours earlier. At the end of each experiment, we identified the salp specimens used in the experiments to the species level, counted the number of zooids, measured the zooid length (total length including projections), and measured the biovolume of the colony using a graduated cylinder. For those specimens where colony or zooid volume was not measured directly, we estimated the colony volume from their zooid length and the number of zooids using a Generalized Additive Model with the measured specimens.

We estimated the oxygen consumption rate for each specimen by fitting a linear regression of consumed oxygen mass (concentration by container volume) against the duration of the measurement series. We subtracted the slope calculated for the relevant control jar to the estimated slope of the animal jar. Since our seawater controls were not filtered, some experiments had abnormally high estimated background respiration rates, leading to negative values. We removed these data points before the analysis. To estimate biovolume-specific rates, we divided the rates by the colony volumes. We then compared the biovolume-specific respiration rates of active (swimming) and anesthetized specimens within each species, calculating the difference as a measure of biovolume-specific swimming cost respiration rate. Biovolume was used instead of dry mass to normalize measurements due to the inherent difficulties of accurately measuring dry mass of these fragile gelatinous organisms in the field. Biovolume provides a consistent and reliable measure of the live size of the colony, which is directly relevant to the volume of water being displaced during swimming. We also calculated the relative investment in swimming as the proportion of biovolume-specific respiration rate comprised by the swimming-specific rate. To capture variability within species, we calculated the mean respiration rate of anesthetized specimens for each species and subtracted it from each intact specimen's total respiration rate to get multiple swimming-specific rate values within each species. We noticed that some species had higher average respiration rates among the anesthetized specimens than among the swimming specimens, leading to negative swimming-specific respiration estimates. We interpreted this anomaly as a systematic error due to the extremely low respiration rates of some species that fall within the effective detection limit of our experimental setup given the random variation range of respiration rates in seawater both in experimental jars and in control jars. Small

279 absolute negative values get amplified into large relative values, especially in small animals with
280 a minuscule biovolume denominator. Therefore, we removed the swimming specimens that had
281 lower respiration rates than the mean anesthetized respiration rate for their species. We also
282 removed two respirometry outliers of *Thalia* sp. which had extremely high swimming respiration
283 rates (>7500 pgO₂/ml/min, whereas all other measurements across species including other
284 *Thalia* sp. were limited to 0-1700 pgO₂/ml/min), which were likely due to amplification of
285 experimental error (presence of organic matter or symbionts, underestimation of colony volume
286 due to loss of tiny zooids in the sieves) with the small biovolume denominators in this species.

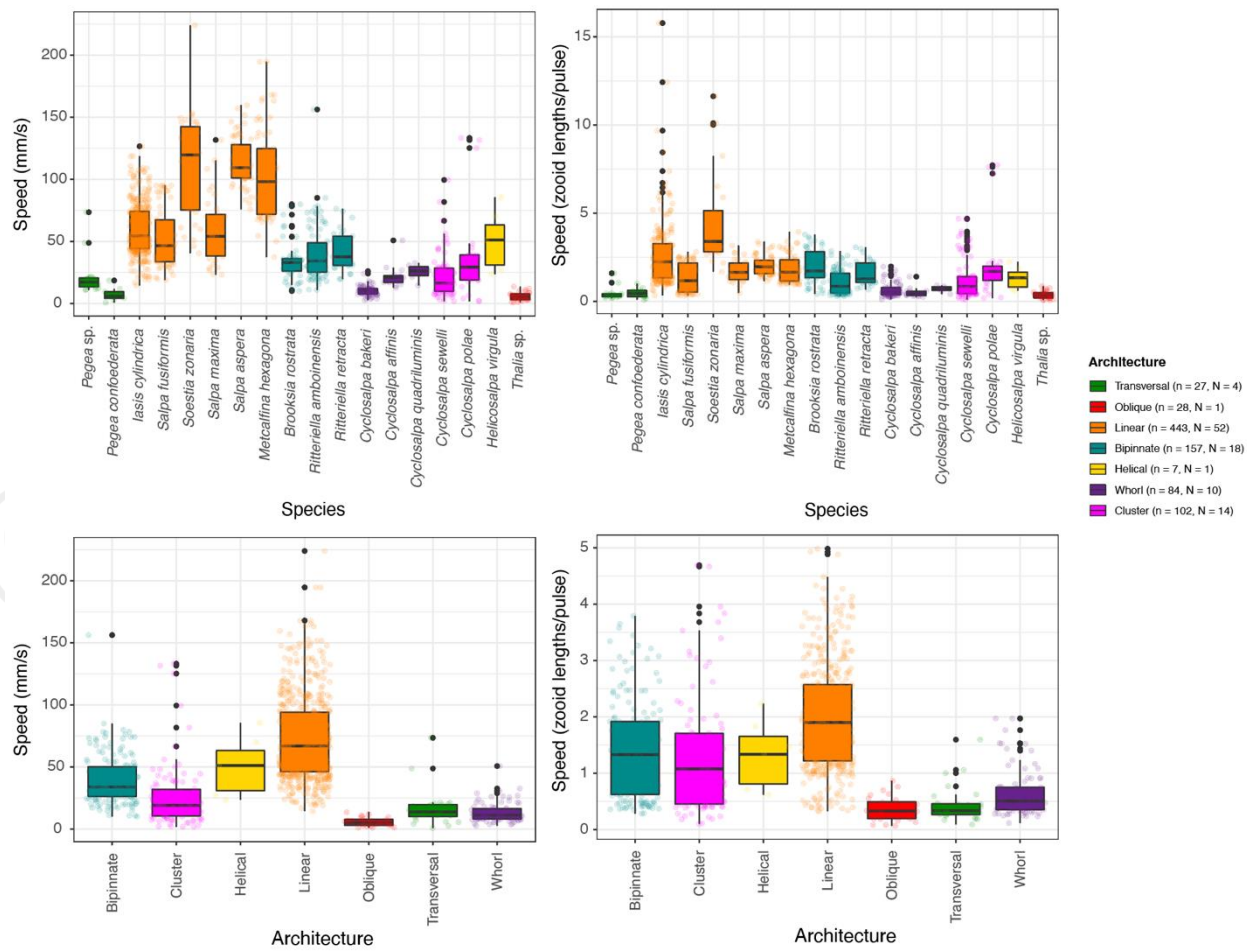
287 *Estimating costs of transport* – We define the cost of transport (COT) as the amount of
288 oxygen consumed per tissue volume per distance traveled by the colony. To estimate the COT,
289 we divided the swimming-specific respiration rates by the mean swimming speed for each species
290 measured from the stereo and 2D video data. Since the specimens used for speed measurements
291 in the videos and those used in the respirometry experiments had different zooid sizes, we used
292 the mean zooid-lengths per second speeds from the video measurements and then multiplied
293 them by the actual zooid lengths of the respirometry specimens to estimate their absolute (mm/s)
294 speeds. Pulsation rate estimates were taken from species averages from the video specimens.
295 We also calculated the size-specific COT by transforming the swimming distances into zooid
296 lengths measured from the respirometry specimens.

297 *Statistical Analyses* – All data wrangling and statistics were carried out in R 3.6.3 (R Core
298 Team 2021). To test for differences between architectures, we used ANOVAs with Tukey's post-
299 hoc pairwise contrasts, reporting the difference magnitude and the adjusted p-value in
300 supplementary tables S2A and S2B. To test the relationships between pairs of continuous
301 variables **across architectures** (e.g. swimming speed vs. number of zooids), we used **linear**
302 **regressions**. We evaluated the significance of the slope parameter when compared against a flat
303 slope (one-tailed t-test) **to test whether changes in the independent variable** (e.g. number of
304 zooids) **were associated with changes in the dependent variable** (e.g. swimming speed). Owing
305 to the patchiness of some species despite 80+ hours spent underwater (Table S1), we used
306 replicate measurements (n) from each specimen (N) in swimming speed ANOVAs and
307 regressions. We used an exponential regression to test the relationship between speed and COT.
308 Specimen means (N) were used for all COT comparisons and regressions. Individual
309 measurements (n) were used up to determine oxygen consumption rates. To evaluate the relative
310 contribution of zooid size, pulsation rate, zooid number, and architecture type on swimming
311 speed, we fitted a generalized linear model and evaluated the significance and proportion of
312 variance explained by each factor using their partial R².

313

314 **Results**

315 Salp colony swimming speeds, pulsation rates, and respiration rates varied within and
 316 across species and colony architectures. When considering speed in terms of mm/s, we found
 317 a relationship between pulsation rate (effort) and absolute speed ($n = 947$, $N = 111$, 18
 318 species, Speed mm/s = $0.41 \times \text{Pulsation rate} + 52.14$, $p < 0.0001$, Fig. S1A), as well as with
 319 zoid-size corrected swimming speed ($n = 848$, $N = 100$, 18 species, Speed zoid lengths/s
 320 = $0.96 \times \text{Pulsation rate} + 1.73$, adjusted $R^2 = 0.18$, $p < 0.0001$, Fig. S1B). Normalized swimming
 321 speeds (zoid lengths per pulse) allow for a more direct comparison of swimming speed across
 322 colonial architectures.



323

324 Figure 3. Boxplots showing the absolute (A) and corrected for body size and pulsation rate (B)
 325 swimming speeds recorded for each salp species and architecture (C, D) respectively. Colors
 326 correspond to colonial architecture types. Sample sizes are included in the legend and Tukey's

327 post-hoc pairwise comparisons across architecture types are listed in Dataset 1A and Table S2A,
328 respectively.

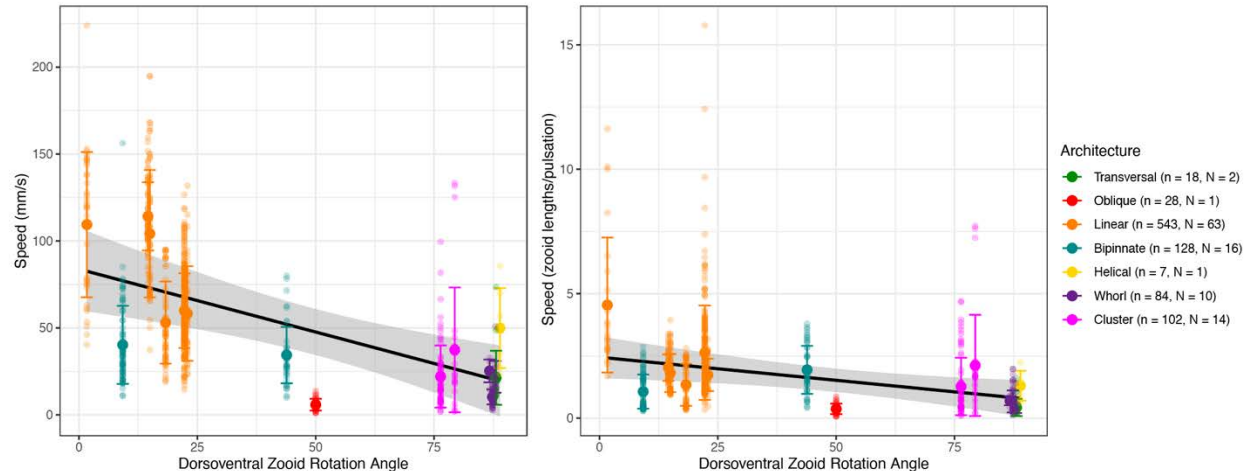
329

330 *Swimming speeds across salp architectures*

331 Swimming speed varied significantly (5 architectures, 16 species, N = 109, n = 913,
332 ANOVA F > 38, p < 0.001) between colonial architecture types (Fig. 3C, D, Table S2A). Speeds
333 measured with 2D methods were slightly slower than those measured with 3D methods within the
334 species in which they overlapped. This is to be expected since 2D methods cannot account for
335 the z (depth) component of the speed vector. Measurements of helical and oblique chains were
336 limited to a single specimen, so they were excluded from the analysis. In terms of absolute speed
337 (mm/s), linear architectures were significantly faster than every other architecture (Tukey's p <
338 0.001). While bipinnate chains were significantly slower than linear chains, they were significantly
339 faster than transversal chains, clusters, and whorls (Tukey's p < 0.002). Clusters were not
340 significantly faster than transversal chains nor whorls. Transversal chains were on par to whorls,
341 with no significant differences between them.

342 In terms of relative speed (zooid lengths/pulse), linear architectures were significantly
343 faster than every other architecture (Tukey's p < 0.001). Bipinnate chains were significantly faster
344 than whorls and transversal chains (Tukey's p < 0.01), but not significantly different from clusters.
345 Clusters were significantly faster than whorls (Tukey's p < 0.001) in relative speed. Whorls and
346 transversal chains presented similar relative swimming speeds with no significant differences.

347 Since linear architectures had the fastest mean swimming speeds (Fig. 3C, D), we
348 investigated the relationship between swimming speeds with the dorsoventral zooid rotation
349 angle, which represents the degree of linearity of the colony (Fig. 4). Species with more parallel
350 (lower angles) dorsoventral zooid rotation presented faster absolute speeds (n = 910, N = 107,
351 16 species, Speed mm/s = -0.78*DV Zoid angle + 81.25, adjusted R² = 0.33, p < 0.0001) and
352 faster size-and-effort corrected swimming speeds (n = 810, N = 96, 16 species, Speed
353 zooids/pulse = -0.016*DV Zoid angle + 2.37, adjusted R² = 0.09, p < 0.0001).

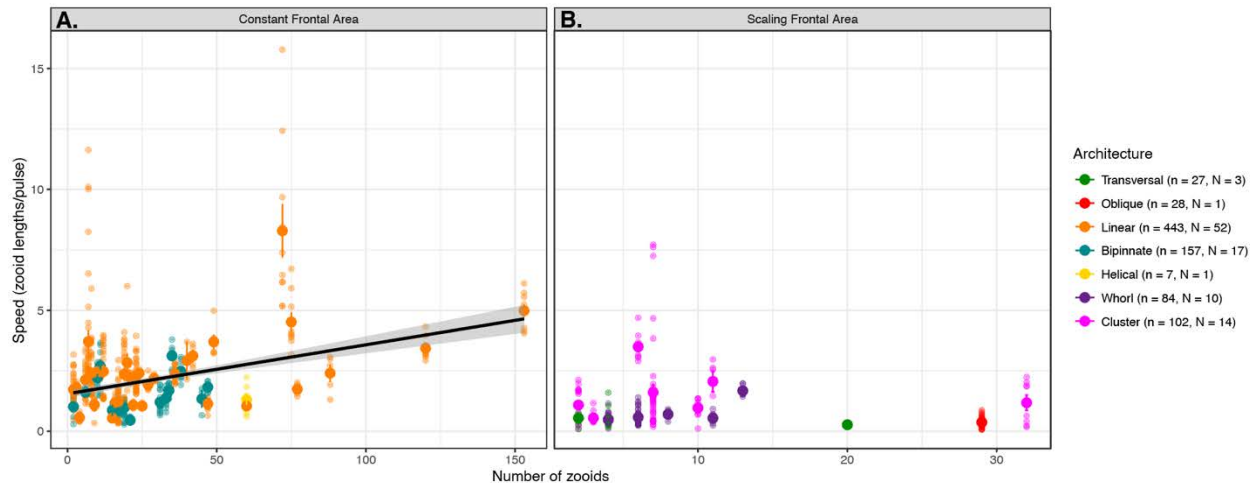


354
355 Figure 4. Absolute (A) and relative (B) colony swimming speed (specimen mean with standard
356 errors, total n=103) for each salp species across their degree of dorsoventral zooid rotation. Error
357 bars indicate standard error. The color indicates colonial architecture. Gray areas indicate the
358 95% confidence interval of the linear regression (black line).

359
360 We compared how swimming speeds scale with the number of zooids in the colony and
361 found differences between colonial architectures. Swimming speed in whorls increased with
362 number of zooids ($n = 84$, $N = 10$, 3 species, Speed mm/s = $0.08 \times \text{Number of zooids} + 0.12$,
363 adjusted $R^2 = 0.3$, $p < 0.0001$), though the data for this architecture was limited to small numbers
364 of zooids (4 to 13) and relatively slow speeds (under 51 mm/s). Linear chain architectures did
365 increase in relative speed with the number of zooids ($n = 443$, $N = 52$, 6 species, Speed mm/s =
366 $0.02 \times \text{Number of zooids} + 1.77$, adjusted $R^2 = 0.14$, $p < 0.001$), as did bipinnate chains ($n = 157$,
367 $N = 18$, 3 species, Speed mm/s = $0.015 \times \text{Number of zooids} + 1.05$, adjusted $R^2 = 0.04$, $p < 0.02$).
368 This relationship was not significant for any of the other architectures.

369 We pooled the data from multiple architectures into scaling modes to evaluate the overall
370 relationship in colonies with a constant frontal area (linear, bipinnate, and helical species) and in
371 colonies with scaling frontal area (transversal, whorl, cluster, and oblique species) with linear
372 regressions (Fig. 1). This aggregation allowed the inclusion of data from architectures for which
373 we only have one specimen (helical and oblique). When pooled by scaling mode (Fig. 5), the
374 regression on colonies with a constant frontal area had a higher intercept on the swimming speed
375 axis than in those with a scaling frontal area (1.54 and 1.09 zoid lengths/pulse, respectively),
376 reflecting the generally higher swimming speed of the former. Moreover, the regression on
377 colonies with constant frontal area had a significant positive slope ($n = 607$, $N = 71$, 10 species,
378 Speed mm/s = $0.02 \times \text{Number of zooids} + 1.55$, adjusted $R^2 = 0.12$, $p < 0.001$), while the regression

379 on those with scaling frontal area was not significant ($n = 241$, $N = 29$, 8 species, $p = 0.073$).
 380 However, the limited sample sizes for helical and oblique chains prevent us from drawing firm
 381 conclusions about these architectures.



382
 383 Figure 5. Linear relationships between relative swimming speed (zoid lengths per pulsation,
 384 specimen mean with standard errors) and number of zooids in the colony for constant (A) and
 385 scaling (N=71) (B) frontal motion-orthogonal frontal area (N=29) scaling modes. Gray areas
 386 represent the 95% confidence intervals of the regressions.
 387

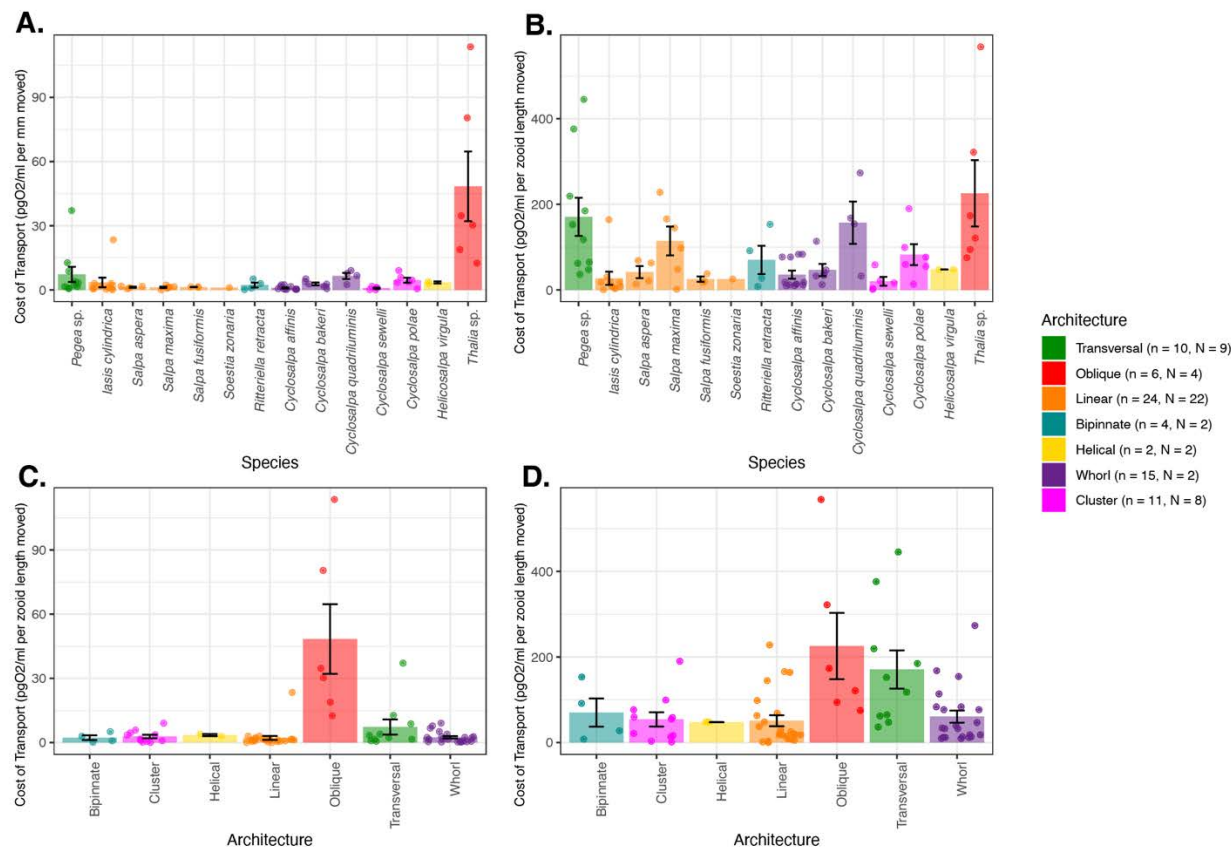
388 Putting together all the different organismal factors that we analyzed in this study, we
 389 calculated a generalized linear regression model to predict absolute salp swimming speed (U)
 390 from zooid length (L), pulsation rate (P), number of zooids (Z), and colonial architecture
 391 represented as frontal area scaling mode (A) as expressed in Eq. 3. While our results suggest
 392 that the effect of Z depends on A , we favored this simpler regression formula because it had a
 393 significantly lower ($\Delta > 70$) AIC score than those with interaction terms between Z and A .

394
$$U \sim L + P + Z + A \quad \text{Eq. 3}$$

395 In this global model, we found significant effects on swimming speed (848 measurements,
 396 100 videos, 18 species, $U = 0.29L - 0.60P - 0.2Z - 50.34A$, pseudo- $R^2 = 0.37$, $p < 0.001$) for L ,
 397 Z , and A . We found that our global regression explains 36.8% of the variance in our swimming
 398 speed data: 5.8% is explained by zooid size, 3.5% by pulsation rate, 0.8% from zooid number,
 399 and 26.6% by the frontal scaling mode.

400
 401 *Respiration rates and cost of transport (COT)*
 402 The respiration rates of swimming and anesthetized salps revealed broad differences
 403 between species (Fig. 6, S2A). After estimating COT, we found a few significant differences

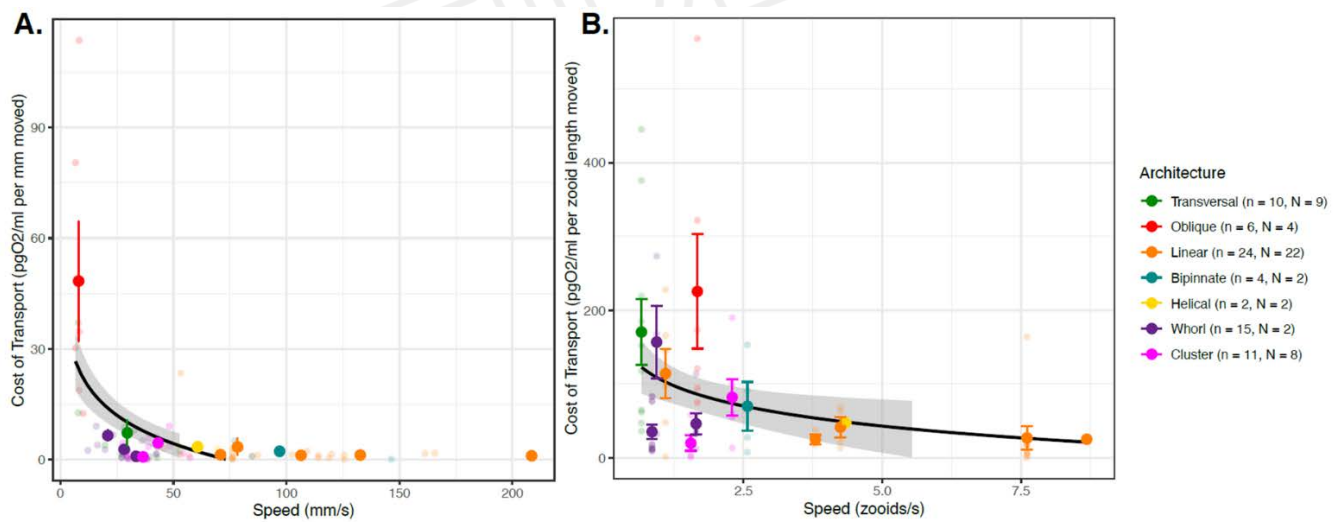
404 between architectures (Fig. 6, ANOVA $F > 5.9$, $p < 0.001$, Table S2B). In terms of absolute COT
 405 per mm traveled, all architectures except oblique chains had similar high transport efficiencies
 406 under 13 pgO₂/ml. Every one of these architectures was significantly more efficient per mm
 407 traveled than oblique architectures (Tukey's $p < 0.001$). In terms of relative COT per zooid length
 408 traveled, linear chains, clusters, and whorls had similar transport efficiencies that are significantly
 409 faster than transversal and oblique chains (Tukey's $p < 0.05$). Some of the differences between
 410 COT per mm and COT per zooid length are likely due to scaling with body size, as can be
 411 observed with the relative shift in the minuscule *Thalia* sp. (5.2 mm zooids) and the massive *Salpa*
 412 *maxima* (93.4 mm zooids).



413
 414 Figure 6. Mean cost-of-transport per mm (A) and per zooid length (B) moved for each salp
 415 species, and for each colonial architecture (C, D) with standard errors. Bar colors indicate colonial
 416 architecture. Sample sizes and Tukey's post-hoc pairwise comparisons across architecture types
 417 are listed in Dataset 1B and Table S2B, respectively.
 418

419 When comparing the proportion of investment of metabolic costs into swimming
 420 (compared to the species mean baseline) across salp species (Fig. S2B), eight species had
 421 locomotion budgets under 50%, and the other seven have budgets above 50%. We then

422 compared the proportion of energetic investment in swimming to the COT values across species
 423 (Fig. S3A,B). We found no relationship with absolute COT ($N = 74$, 14 species, $p = 0.24$). We
 424 found a positive relationship with zooid-length scaled COT ($N = 74$, 14 species, Swimming % =
 425 $0.11 \times \text{COT per zooid length} + 34.4$, adjusted $R^2 = 0.22$, $p < 0.001$), indicating that species with
 426 more costly locomotion per zooid length invest a larger proportion of their energy budget in
 427 swimming. Finally, we compared the proportion of energetic investment in swimming with speed
 428 (Fig. S3C,D). We found no relationship (neither in mm/s nor in zooids/s), indicating that faster
 429 swimmers do not invest more of their energy budget into their locomotion efforts. We found that
 430 regardless of whether we consider transport in terms of absolute distances (Fig. 7A, $N = 64$, 14
 431 species, linear regression: COT per mm = $-0.12 \times \text{Speed mm/s} + 13.46$, adjusted $R^2 = 0.09$, $p <$
 432 0.005 ; exponential regression: $\log\text{COT per mm} = -0.015 \times \text{Speed mm/s} + 1.39$, adjusted $R^2 = 0.14$,
 433 $p < 0.001$) or relative to body lengths (Fig. 7B, 64 specimens, 14 species, linear regression COT
 434 per zooid length = $-12.9 \times \text{Speed zooid lengths/s} + 116.1$, adjusted $R^2 = 0.07$, $p < 0.01$, exponential
 435 regression $\log\text{COT per zooid length} = -0.24 \times \text{Speed zooid lengths/s} + 4.28$, adjusted $R^2 = 0.14$ p
 436 < 0.001), the COT decreases in species with faster swimming speeds.
 437
 438



439
 440 Figure 7. COT (specimen mean with standard error, $n=75$) per mm (A) and zooid length (B) moved
 441 across the specimen mean absolute (A) or relative (B) swimming speeds. The dot color indicates
 442 colonial architecture. Gray areas represent the 95% confidence intervals of the exponential
 443 regressions (black lines).

444

445 Discussion

446 We compared the swimming speeds and costs of transport of salp colonies across the
447 most comprehensive representation of salp species diversity. Our results show a wide range of
448 colonial swimming speeds across salp species and architectures **with linear species swimming**
449 **fastest (Fig. 3)**. Moreover, this study shows for the first time how salp colonial swimming speed
450 scales with the number of zooids in the colony (**Fig. 5**), suggesting that incremental propulsive
451 power from additional zooids does **can produce higher swimming speeds for species with a**
452 **constant frontal area. Across species, salps have a low COT (Fig. 6) and as speed increases,**
453 **COT decreases (Fig. 7), which may be a unique advantage of multi-jet swimmers.**

454 *Architectural determinants of salp swimming speed*

455 Colonial architecture was the strongest predictor of swimming speed, though there is a
456 large amount of unexplained variation which may relate to species-specific differences,
457 behavioral, or environmental factors (see global GLM results). We expected that swimming speed
458 in colonial salps would be predicted by pulsation rate as a measure of swimming effort. Our results
459 indicate that this relationship only exists when accounting for zooid size (**Fig. S1B**), suggesting
460 an underlying relationship between pulsation rate and zooid **length** that may be masking its
461 predictive power over absolute speeds. This is consistent with the distribution of our data and our
462 observations in the field where larger salps pulsate at a slower rate than smaller ones. **We find a**
463 **significant increase in speed with larger zooid sizes (Fig. S1C,D), consistent with previous findings**
464 **of jet propelled invertebrates (Gemmell et al 2021; Bone and Trueman 1983) and more broadly**
465 **across aquatic swimmers (Andersen et al. 2016).**

466 The relationship between the number of zooids and speed in linear chains is complicated
467 by shifts in zooid orientation during development. Salp colonies start their free-living phase when
468 the developing buds detach from the solitary oozooid. **The newly released colony has** the
469 maximum number of zooids since the zooid number only gets reduced as the colony splits or
470 loses zooids to turbulence, disease, or predation. Therefore, colonies with higher numbers of
471 zooids are typically composed of smaller, younger zooids. In linear architectures, these younger
472 colonies could still be developing their dorsoventral rotation (Damian-Serrano & Sutherland 2023),
473 thus effectively being more like oblique architecture. A less acute dorsoventral rotation angle
474 would explain why these more numerous linear chains are not as fast as we would expect, given
475 that our results support a significant relationship between this angle and swimming speed (**Fig.**
476 **4**). Finding a strong relationship between zooid number and speed in whorls was surprising given
477 their less **streamlined configuration (Fig. 5)**. This could be due to the smaller range of slow speeds
478 and few zooids in the data we obtained for these species. Our regression results on pooled
479 architectures, as well as finding a significant relationship between number of zooids and speed

480 for linear and bipinnate chains but not for clusters nor transversal chains, support our primary
481 hypothesis that the different frontal area scaling relationships across architectures has an impact
482 on swimming speed.

483 Linear chains swam faster than all other architectures, including those that share a
484 constant frontal area feature like bipinnate chains ([Fig. 3, Table S2](#)). One potential explanation
485 for this difference could come from the relative thrust provided by the jets. Linear chains eject
486 their jet plumes at very small angles (near parallel) to the axis of locomotion (Sutherland et al.
487 2024), just wide enough to avoid interaction between jet plumes (Sutherland & Weihs 2017).
488 Bipinnate and helical chains (both with constant frontal area) have the atrial siphons (point of jet
489 ejection) of their constituent blastozooids oriented at a wider angle (Madin 1990), which may lead
490 to wider angles of their jets relative to the axis of locomotion. This in turn would result in a larger
491 proportion of the force exerted by the jet to be applied as torque rather than thrust onto the colony.
492 This hypothesis could be tested by measuring the 3D angles of the actual jets instead of the
493 angles of the zooids since salps can use their atrial muscles and siphon morphology to direct the
494 angle of their jets.

495 Finding that clusters can swim at speeds comparable to those of bipinnate and helical
496 chains, even faster than whorls, defies our intuitive understanding of the mechanical properties
497 of these colonies and thus warrants further investigation into how these species coordinate their
498 jets to produce forward thrust. While oblique chains are architectural intermediates between
499 transversal and linear chains ([Damian-Serrano & Sutherland 2023](#)), our data indicate that oblique
500 chains may be the slowest swimmers among salps. This incongruence may be explained by the
501 fact that we only had speed data from one oblique specimen (of *Thalia* sp.) with very small zooid
502 sizes. Small salps might operate at notably lower Reynolds numbers than large ones, which may
503 require a non-linear size correction for meaningful speed comparisons. Swimming speed data
504 from the much larger oblique chains of *Thetys vagina* may provide a more comparable example
505 of the locomotory performance of this oblique colonial configuration.

506 The questions addressed in this study focus on the effect of frontal area of colonial
507 architectures on swimming speed. This effect may be associated with form and pressure drag
508 differences between more and less streamlined colony shapes. To test whether these are the
509 forces responsible for differences in swimming speed, drag would have to be measured or
510 calculated, which is beyond the scope of this study. Other unaccounted forces may be significant
511 energetic contributors to the system that explain the remainder of the observed variation. Chain
512 length for the streamlined forms (helical, linear, and bipinnate chains) could have negative effects
513 on swimming speeds that may partially counteract the positive effect of increased propeller thrust.

514 For example, skin drag increases proportionally to the surface area of the system, and the
515 smoothness of the chain may increase pressure drag through vortex shredding (Vogel 1981).
516 While added (virtual) mass could also be an issue, asynchronously swimming colonies do not
517 suffer as much from these acceleration-related costs, since their speed is maintained near
518 constant while cruising (Bone & Trueman 1983). Chain length could also lead to reduced stability
519 and efficiency, though some linear species capitalize on this by swimming in corkscrew orbital
520 spirals (Sutherland et al. 2024). However, if friction drag, chain stability, or vortex shredding were
521 indeed more important contributors than frontal form drag, we would predict that linear chains
522 would appear slower than other more stable and compact architectures. Future studies may
523 unravel these potential confounding effects on the biomechanics of colonial salp swimming.
524

Salp swimming speed and diel vertical migration

525 Salps are important players in the oceanic carbon cycle, grazing upon both phytoplankton
526 and bacteria (Henschke et al. 2016). Their carcasses and fecal pellets export large quantities of
527 fixed carbon into the deep sea, accelerating carbon sequestration in the biological carbon pump
528 (Wiebe et al. 1979, Décima et al. 2023). Part of this process is enhanced by the diel vertical
529 migrations by some salp species though the distribution of this behavior across species diversity
530 is poorly known. Off Bermuda, Madin et al. (1996) reported *Pegea* spp., *B. rostrata*, and *C. polae*
531 as non-migratory, all of which we found to have slow swimming speeds. Other slow-swimmer
532 species like *C. affinis* were found to only migrate a few meters through the diel cycle. The species
533 *S. aspera*, *S. fusiformis*, *S. zonaria*, *I. punctata*, and *R. retracta* have been observed vertically
534 migrating off Bermuda (Madin et al 1996, Stone & Steinberg 2014), which is congruent with our
535 observations during fieldwork. These species all have constant frontal area and fast swimming
536 speeds.

537 Vertical migrators need to be fast enough to follow the dark isolumes as they shift during
538 dawn and dusk in time to maximize their exploitation of the food resources near the surface. Thus,
539 absolute speed is important to the autoecology of these animals. Other *Salpa* species have also
540 been reported as strong vertical migrators throughout the literature (Henschke et al. 2021, Madin
541 et al. 2006, Pascual et al. 2017). A species that does not fit this pattern is *I. cylindrica*, a fast-
542 swimming non-migratory species that spends night and day near the surface (Madin et al 1996;
543 and pers. obs.). However, other studies do report moderate diel vertical migration for this species
544 (Stone & Steinberg 2014), so it may be adapted for facultative vertical migration under specific
545 oceanographic conditions. Some migratory species, such as *S. aspera*, are known to travel
546 distances of over 800m at dawn and dusk, at rates predicted to require 5-10 m/min (83-166 mm/s)

547 based on MOCNESS trawl intervals (Wiebe et al. 1979). These predictions are consistent with
548 the speeds we recorded for this species (88-145 mm/s) and similar congeners.

549 *Ecophysiological implications*

550 While the importance of a few well-studied linear chain salp species in the biological
551 carbon pump has been delineated, the question of whether this ecological role is generalizable to
552 other salp species remains unanswered. In addition to vertical migration behavior, another likely
553 important factor in their carbon flow is their respiration rate. The higher their respiration rate, the
554 larger the proportion of assimilated carbon that will be released back into the water as dissolved
555 carbon dioxide. This study provides the broadest taxonomic perspective on respiration rates (18
556 species, Fig. S2A) and swimming cost of transport (14 species), finding 17-fold differences in their
557 respiration rates and over 77-fold differences in their mean COT. Except for a few species with
558 extremely high and low values, most respiration rates are centered between 0.2 and 1
559 $\mu\text{mol/g/hour}$, assuming a salp tissue density of 1.025 g/ml. In general, the respiration rates we
560 estimated for salps are within the range of those reported in the literature (Trueblood 2019, Iguchi
561 and Ikeda 2004). Compared to the metabolic rates estimated for the broader diversity of marine
562 pelagic animals (Seibel & Drazen 2007), the rates that we measured for salps are in a similar
563 range to those measured for *Salpa thompsoni* (Iguchi and Ikeda 2004). Our values are also similar
564 to those measured by Seibel & Drazen (2007) in nemerteans, chaetognaths, and most fishes (0.1-
565 1 $\mu\text{molO}_2/\text{g/h}$), which are generally higher than other gelatinous animals like ctenophores or
566 scyphomedusae (0.01-0.1 $\mu\text{molO}_2/\text{g/h}$), but generally lower than those of cephalopods,
567 crustaceans, or large fish (1-10 $\mu\text{molO}_2/\text{g/h}$). Salp species known to have strong vertical migration
568 behaviors (*Salpa* spp., *S. zonaria*, *I. punctata*, and *R. retracta*) have low basal metabolic rates
569 (Fig. S2A) and low costs of transport. These results indicate that many non-migratory species,
570 while likely still being important players in the biological carbon pump via their fecal pellet
571 production, are releasing more of the consumed carbon as carbon dioxide near the surface than
572 their more metabolically efficient relatives. The ultimate ecological outcome of each species
573 needs to be assessed holistically, considering their microbial filtration and pellet deposition rate
574 as well as their relative abundance in the water column.

575 Our metabolically calculated costs of transport range between 5-50 J/kg/m when
576 converting the mg of oxygen to J via aerobic respiration free energy equations at 23°C. **These**
577 values are higher than the highly efficient 1-2 J/kg/m reported for salps in the literature (Bone &
578 Trueman 1983, Gemmell et al. 2021), **and approach** the less-efficient values found in single jet-
579 propelled invertebrates like scallops or squids. We suspect that COT calculated from mechanical
580 parameters such as the displacement of water mass is not directly comparable to the COT

581 calculated from respiration rates. Furthermore, the standard aerobic respiration free-energy
582 equation based on glucose may not fully represent the metabolic energy-conversion processes
583 in salps, which could rely on a combination of sugars and fatty acids derived from their
584 microscopic prey.

585 While COT increases with swimming speed fishes (Rubio-Gracia et al. 2020) and jet-
586 propelled squid (Bi & Zhu 2019), multi-jet swimmers may circumvent this tradeoff by having
587 multiple swimming units. In colonial siphonophores, as zooid number increases swimming speed
588 increases together with a decrease in COT (Du Clos et al. 2022). Our results show that faster
589 swimming species have lower COT (Fig. 6), which suggests that faster speeds and higher
590 locomotory efficiency have a common cause, where both speed and efficiency depend on frontal
591 area which may partly drive form and pressure drag forces. However, this hypothesis is not
592 supported by the distribution of COT across architectures (Fig 6C, D), where except for oblique
593 and transversal chains, all architectures present similarly efficient COT values. Perhaps there are
594 other underlying explanatory factors linking swimming speed and swimming efficiency, such as
595 shared ancestry, muscle content, jet coordination, or jetting angles (thrust-to-torque ratios).

596 *Evolutionary implications*

597 Across the evolutionary history of salps, linear chains have evolved multiple times
598 independently from oblique ancestors (Damian-Serrano et al. 2023), suggesting the adaptive role
599 of this architecture as a functional trait. Linear chain architectures evolved independently in *M.*
600 *hexagona*, *S. zonaria*, *I. punctata*, and before the common ancestor of *Iasis* and *Salpa*. Our results
601 show that going from an oblique form to a linear one may confer significant advantages in
602 locomotory speed and energetic efficiency. However, multiple colonial architectures, which we
603 find to be slower swimmers (such as transversal chains, helical chains, whorls, and clusters in
604 the genus *Pegea* and the Cyclosalpidae family) had also evolved from oblique and linear
605 ancestors. This is incongruent with a scenario where natural selection strongly favors locomotion
606 efficiency across all ecological niches of salps. Therefore, the evolution of colonial architecture
607 may be driven by ecological trade-offs with other non-locomotory functions. Alternatively, in some
608 of these lineages, locomotion at the colonial stage may not be important enough for selection to
609 maintain these highly streamlined forms, allowing for neutral evolutionary processes to produce
610 a diversity of non-adaptive forms. In the current study, we did not use phylogenetic comparative
611 methods in our analysis because like other investigators comparing biomechanical properties
612 across species (e.g. Dabiri et al. 2010, DiSanto et al. 2021) we were interested in inherent
613 mechanical relationships dictated by the colony architectures. For instance, a linear arrangement
614 of zooids inherently reduces drag due to a cluster arrangement, leading to faster swimming

615 speeds and potentially higher efficiency regardless of phylogenetic history. In other words, any
616 phylogenetic inertia is irrelevant in instantaneous relationships between traits (Felsenstein 1985).
617 Moreover, independence of data is often incorrectly assumed to be an assumption of standard
618 (nonphylogenetic) regressions (Uyeda et al. 2018), when in reality the assumptions relate to the
619 independence and distribution of the error terms. Thus, when all the phylogenetic signal is present
620 in the predictor, as it is in the case with colonial architecture (Damian-Serrano et al. 2022) and its
621 associated characteristics, there is no need for any “phylogenetic correction” (Uyeda et al. 2018).
622 However, there may be unaccounted factors explaining the residual variation in our analyses that
623 may bear phylogenetic signal. For example, tunic stiffness, tunic smoothness, muscle band
624 number, muscle fiber density, swimming behavior, as well as metabolic and physiological
625 baselines may be more similar between more closely related species, potentially erasing some of
626 the architecture-specific signal. Future studies could address the role of phylogeny and heritable
627 factors in salp swimming speed and cost of transport using phylogenetic comparative methods.
628 These analyses could reveal whether these factors have co-evolved with each other and/or with
629 respiration rate or colonial architecture.

630 *Insights for bioinspired underwater vehicle design*

631 Pulsatile jet propulsion is a promising avenue for bioinspired aquatic vehicles and robots
632 (Mohensi 2006, Gohardini 2014, Yue et al. 2015). Multijet propulsion systems with multiple
633 propellers akin to salp colonies have been explored in an engineering context (Chao et al. 2017,
634 Costello et al. 2015) with direct inspiration from gelatinous animals (Marut 2014, Krummel 2019,
635 Bi et al 2022, Du Clos et al. 2022). Salp diversity provides a natural laboratory to explore the
636 hydrodynamic implications of different multijet arrangement designs. Our findings underscore the
637 importance of considering the scaling hydrodynamic properties of propeller arrangements to
638 optimize speed and energy efficiency in bioinspired underwater vehicle design. While linear chain
639 arrangements were the fastest and among the most energy efficient, robot (or vehicle)
640 configurations such as a cluster form may confer unique object manipulation or maneuverability
641 advantages. Our results show that these seemingly inefficient propeller configurations do not
642 impose large disadvantages in terms of speed and fuel efficiency.

643 **Acknowledgments:**

644 We are grateful to the crew of Aquatic Life Divers, Kona Honu Divers for their assistance
645 and support in hosting our offshore diving operations. We also wish to thank Marc Hughes, Jeff
646 Milisen, Rebecca Gordon, Matt Connelly, Clint Collins, Paul Richardson, and Anne Thompson for
647 their assistance during diving, collections, and filming operations in the field. We would like to

648 thank Tiffany Bachtel for her valuable advice on the respirometry experiment design. We thank
649 the associate editor and two anonymous reviewers for their helpful comments.

650 **Funding**

651 This research was supported by the Gordon and Betty Moore Foundation [grant number
652 8835] and the Office of Naval Research [grant number N00014-23-1-2171].

653 **Data availability**

654 Data used to generate the results presented in this paper are available in the supplementary
655 information. Any other datasets used directly or indirectly for this study are available from the
656 authors upon reasonable request.

657 **Competing interests**

658 No competing interests declared.

659 **Literature cited**

660 Alexander, A. J. (1968). Forward Speed Effects on Annular Jet Cushions. *The Aeronautical
661 Journal*, 72(689), 438-441.

662 Andersen, K. H., Berge, T., Gonçalves, R. J., Hartvig, M., Heuschele, J., Hylander, S., ... &
663 Kiørboe, T. (2016). Characteristic sizes of life in the oceans, from bacteria to whales.
664 *Annual review of marine science*, 8(1), 217-241.

665 Bi, X., & Zhu, Q. (2019). Dynamics of a squid-inspired swimmer in free swimming. *Bioinspiration
666 & Biomimetics*, 15(1), 016005.

667 Bi, X., Tang, H., & Zhu, Q., 2022. Feasibility of hydrodynamically activated valves for 416 salp-
668 like propulsion. *Physics of Fluids*, 34(10), 101903.

669 Biggs, D. C. (1977). Respiration and ammonium excretion by open ocean gelatinous zooplankton
670 1. *Limnology and Oceanography*, 22(1), 108-117.

671 Bone, Q., Anderson, P. A. V., & Pulsford, A. (1980). Morphology of salp chain communication.
672 *Proceedings of the Royal Society of London. Series B. Biological Sciences*, 210(1181),
673 549-558.

674 Bone, Q., & Trueman, E. R. (1983). Jet propulsion in salps (Tunicata: Thaliacea). *Journal of
675 Zoology*, 201(4), 481-506.

676 Cetta, C. M., Madin, L. P., & Kremer, P. (1986). Respiration and excretion by oceanic salps.
677 *Marine Biology*, 91, 529-537.

678 Chao, S., Guan, G., & Hong, G. S., 2017, September. Design of a finless torpedo-shaped micro
679 AUV with high maneuverability. In OCEANS 2017-Anchorage (pp. 425 1-6). IEEE.

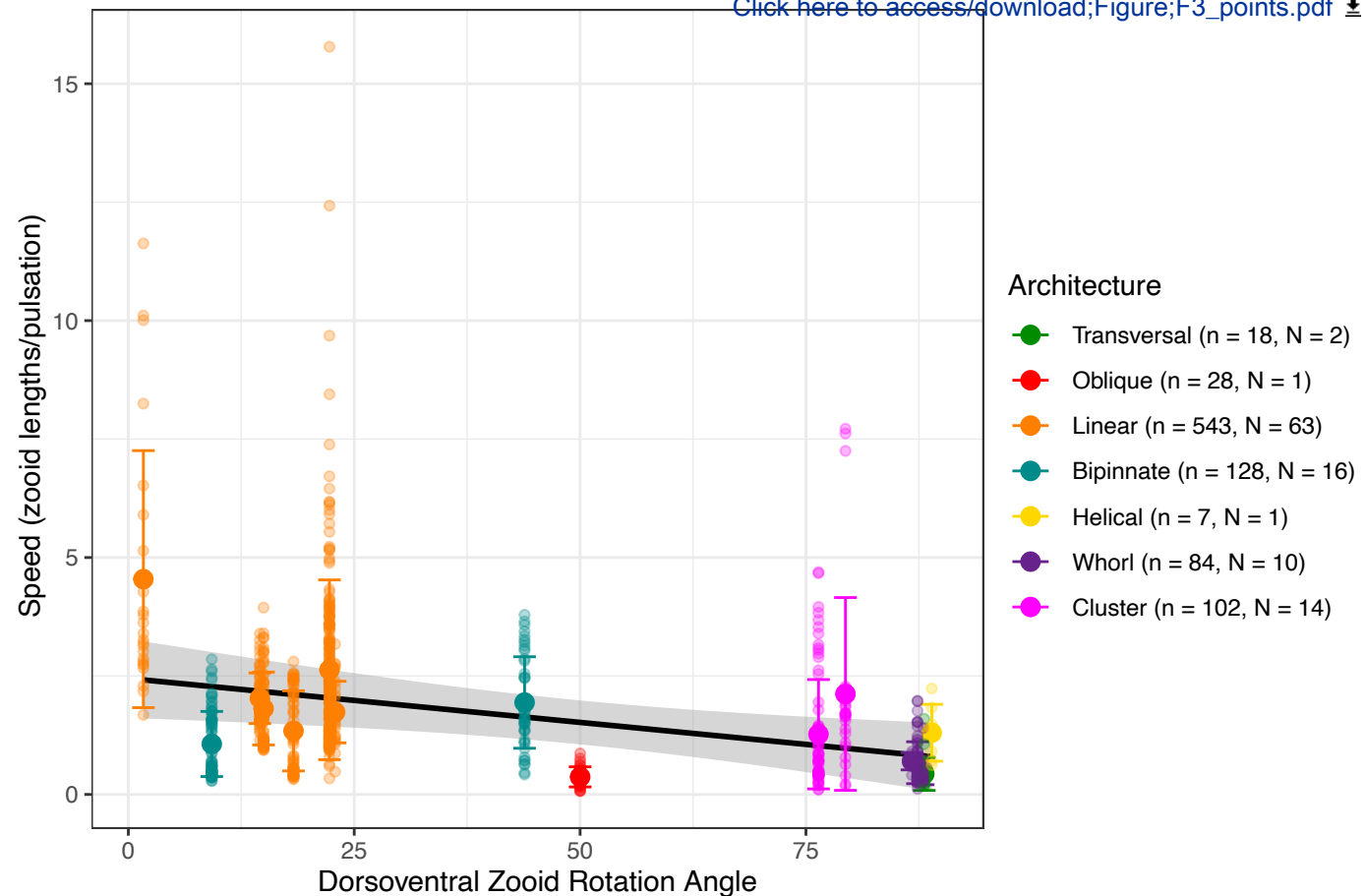
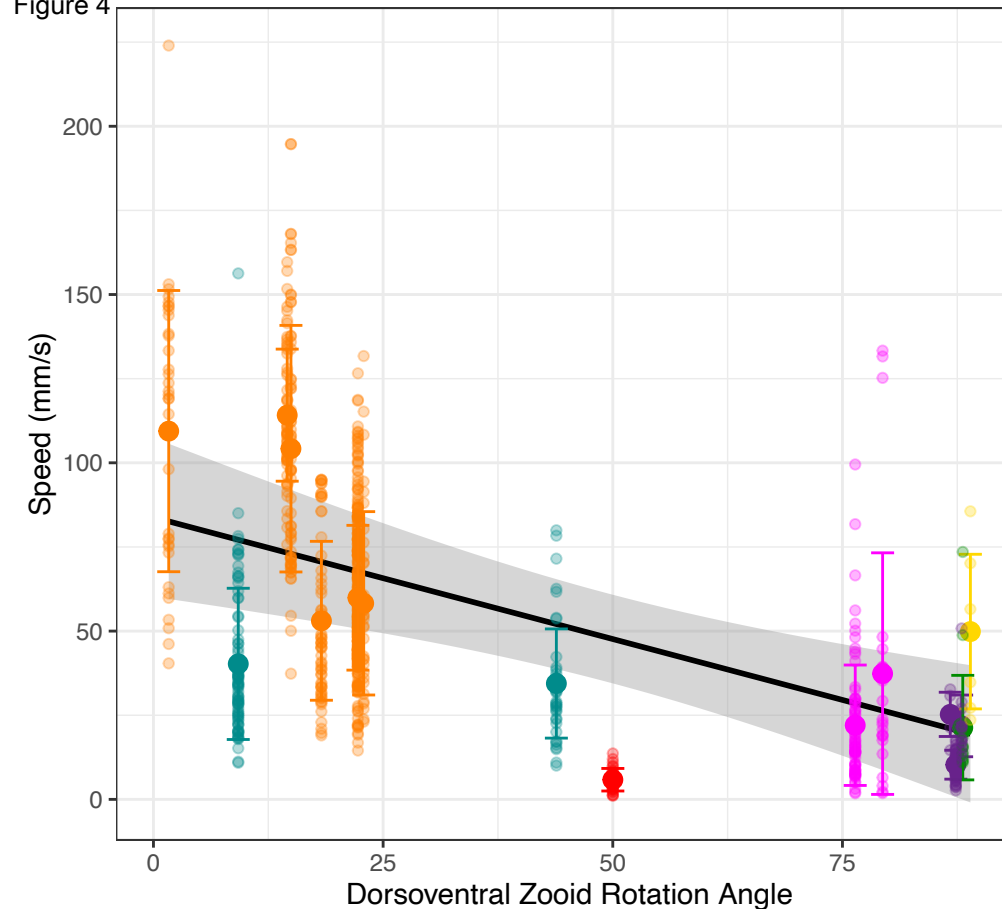
680 Colin, S. P., Gemmell, B. J., Costello, J. H., & Sutherland, K. R. (2022). In situ high-speed
681 brightfield imaging for studies of aquatic organisms. *Protocols.io*.

- 682 Costello, J. H., Colin, S. P., Gemmell, B. J., Dabiri, J. O., & Sutherland, K. R., 2015. 429 Multi-jet
683 propulsion organized by clonal development in a colonial siphonophore. 430 *Nature*
684 communications, 6(1), 8158.
- 685 Dabiri, J. O., Colin, S. P., Katija, K., & Costello, J. H. (2010). A wake-based correlate of
686 swimming performance and foraging behavior in seven co-occurring jellyfish species.
687 *Journal of experimental biology*, 213(8), 1217-1225.
- 688 Damian-Serrano, A., & Sutherland, K. R. (2023). A developmental ontology for the colonial
689 architecture of salps. *The Biological Bulletin*, 245(1), 9-18..
- 690 Damian-Serrano, A., Hughes, M., & Sutherland, K. R. (2023). A new molecular phylogeny of salps
691 (Tunicata: thalicea: salpida) and the evolutionary history of their colonial architecture.
692 *Integrative Organismal Biology*, 5(1), obad037.
- 693 Décima, M., Stukel, M. R., Nodder, S. D., Gutiérrez-Rodríguez, A., Selph, K. E., Dos Santos, A.
694 L., ... & Pinkerton, M. (2023). Salp blooms drive strong increases in passive carbon export
695 in the Southern Ocean. *Nature communications*, 14(1), 425.
- 696 Di Santo, V., Goerig, E., Wainwright, D. K., Akanyeti, O., Liao, J. C., Castro-Santos, T., & Lauder,
697 G. V. (2021). Convergence of undulatory swimming kinematics across a diversity of fishes.
698 *Proceedings of the National Academy of Sciences*, 118(49), e2113206118.
- 699 Du Clos, K. T., Gemmell, B. J., Colin, S. P., Costello, J. H., Dabiri, J. O., and Sutherland, K. R.
700 2022. Distributed propulsion enables fast and efficient swimming modes in physonect
701 siphonophores. *Proceedings of the National Academy of Sciences*. 119:e2202494119.
- 702 Felsenstein, J. (1985). Phylogenies and the comparative method. *The American
703 Naturalist*, 125(1), 1-15.
- 704 Gemmell, B. J., Dabiri, J. O., Colin, S. P., Costello, J. H., Townsend, J. P., & Sutherland, K. R.
705 (2021). Cool your jets: biological jet propulsion in marine invertebrates. *Journal of
706 Experimental Biology*, 224(12), jeb222083.
- 707 Gohardani, A. S. Distributed Propulsion Technology Nova Science Publishers (2014).
- 708 Haddock, S. H. (2004). A golden age of gelata: past and future research on planktonic
709 ctenophores and cnidarians. *Hydrobiologia*, 530, 549-556.
- 710 Haddock, S. H., & Heine, J. N. (2005). Scientific blue-water diving.
- 711 Hamner, W. M., Madin, L. P., Alldredge, A. L., Gilmer, R. W., & Hamner, P. P. (1975). Underwater
712 observations of gelatinous zooplankton: Sampling problems, feeding biology, and
713 behavior 1. *Limnology and Oceanography*, 20(6), 907-917.

- 714 Henschke, N., Cherel, Y., Cotté, C., Espinasse, B., Hunt, B.P. and Pakhomov, E.A., 2021. Size
715 and stage specific patterns in *Salpa thompsoni* vertical migration. *Journal of Marine*
716 *Systems*, 222, p.103587.
- 717 Krummel, G. M. (2019). Locomotion and Control of Cnidarian-Inspired Robots (Doctoral
718 dissertation, Virginia Tech).
- 719 Mackie, G. O. (1986). From aggregates to integrates: physiological aspects of modularity in
720 colonial animals. *Philosophical Transactions of the Royal Society of London. B, Biological*
721 *Sciences*, 313(1159), 175-196.
- 722 Madin, L. P. (1990). Aspects of jet propulsion in salps. *Canadian Journal of Zoology*, 68(4), 765-
723 777.
- 724 Madin, L. P., & Deibel, D. (1998). Feeding and energetics of Thaliacea. *The biology of pelagic*
725 *tunicates*, 81-104.
- 726 Madin, L. P., Kremer, P., & Hacker, S. (1996). Distribution and vertical migration of salps
727 (Tunicata, Thaliacea) near Bermuda. *Journal of Plankton Research*, 18(5), 747-755.
- 728 Madin, L.P., Kremer, P., Wiebe, P.H., Purcell, J.E., Horgan, E.H. and Nemazie, D.A., 2006.
729 Periodic swarms of the salp *Salpa aspera* in the Slope Water off the NE United States:
730 Biovolume, vertical migration, grazing, and vertical flux. *Deep Sea Research Part I:*
731 *Oceanographic Research Papers*, 53(5), pp.804-819.
- 732 Marut, K. J. (2014). Underwater Robotic Propulsors Inspired by Jetting Jellyfish (Doctoral
733 dissertation, Virginia Tech).
- 734 Mayzaud, P., Boutoute, M., Gasparini, S., Mousseau, L., & Lefevre, D. (2005). Respiration in
735 marine zooplankton—the other side of the coin: CO₂ production. *Limnology and*
736 *Oceanography*, 50(1), 291-298.
- 737 Mohensi, K., 2006. Pulsatile vortex generators for low-speed maneuvering of small 482
738 underwater vehicles. *Ocean Eng.* 33, 2209–2223.
- 739 Pascual, M., Acuña, J.L., Sabatés, A., Raya, V. and Fuentes, V., 2017. Contrasting diel vertical
740 migration patterns in *Salpa fusiformis* populations. *Journal of Plankton Research*, 39(5),
741 pp.836-842.
- 742 R Core Team, R. (2021). R: A language and environment for statistical computing.
- 743 Rubio-Gracia, F., García-Berthou, E., Guasch, H., Zamora, L., & Vila-Gispert, A. (2020). Size-
744 related effects and the influence of metabolic traits and morphology on swimming
745 performance in fish. *Current Zoology*, 66(5), 493-503.

- 746 Schneider, G. (1992). A comparison of carbon-specific respiration rates in gelatinous and non-
747 gelatinous zooplankton: a search for general rules in zooplankton metabolism.
748 *Helgoländer Meeresuntersuchungen*, 46, 377-388.
- 749 Seibel, B. A., & Drazen, J. C. (2007). The rate of metabolism in marine animals: environmental
750 constraints, ecological demands and energetic opportunities. *Philosophical Transactions
751 of the Royal Society B: Biological Sciences*, 362(1487), 2061-2078.
- 752 Stone, J. P., & Steinberg, D. K. (2014). Long-term time-series study of salp population dynamics
753 in the Sargasso Sea. *Marine Ecology Progress Series*, 510, 111-127.
- 754 Sutherland, K. R., & Weihs, D. (2017). Hydrodynamic advantages of swimming by salp chains.
755 *Journal of The Royal Society Interface*, 14(133), 20170298.
- 756 Sutherland, K. R., Damian-Serrano, A., Du Clos, K. T., Gemmell, B. J., Colin, S. P., Costello, J.
757 H. (2024). Spinning and corkscrewing of oceanic macroplankton revealed through in situ
758 imaging. *Science Advances* 10(20).
- 759 Sutherland, K. R., & Madin, L. P. (2010). Comparative jet wake structure and swimming
760 performance of salps. *Journal of Experimental Biology*, 213(17), 2967-2975.
- 761 Trueblood, L. A. (2019). Salp metabolism: temperature and oxygen partial pressure effect on the
762 physiology of *Salpa fusiformis* from the California Current. *Journal of Plankton Research*,
763 41(3), 281-291.
- 764 Trueman, E. R., Bone, Q., & Braconnor, J. C. (1984). Oxygen consumption in swimming salps
765 (Tunicata: Thaliacea). *Journal of Experimental Biology*, 110(1), 323-327.
- 766 Uyeda, J. C., Zenil-Ferguson, R., & Pennell, M. W. (2018). Rethinking phylogenetic comparative
767 methods. *Systematic Biology*, 67(6), 1091-1109.
- 768 Vogel, S. (1981). Life in moving fluids. *Princeton University Press*, Princeton, NJ.
- 769 Vogel, S. (2008). Modes and scaling in aquatic locomotion. *Integrative and Comparative Biology*,
770 48(6), 702-712.
- 771 Wiebe, P. H., Madin, L. P., Haury, L. R., Harbison, G. R., & Philbin, L. M. (1979). Diel vertical
772 migration by *Salpa aspera* and its potential for large-scale particulate organic matter
773 transport to the deep-sea. *Marine Biology*, 53, 249-255.
- 774 World Register of Marine Species (WoRMS). (2024). WoRMS Editorial Board. Accessed January
775 30, 2024. Available online at <http://www.marinespecies.org>
- 776 Yue, C. et al., 2015. Mechantronic system and experiments of a spherical underwater 510 robot:
777 SUR-II. *J. Intell. Robot Syst.* Doi:10.1007/s10846-015-0177-3.

Figure 4

[Click here to access/download;Figure;F3_points.pdf](#)


- Architecture**
- Transversal (n = 18, N = 2)
 - Oblique (n = 28, N = 1)
 - Linear (n = 543, N = 63)
 - Bipinnate (n = 128, N = 16)
 - Helical (n = 7, N = 1)
 - Whorl (n = 84, N = 10)
 - Cluster (n = 102, N = 14)

Figure 5

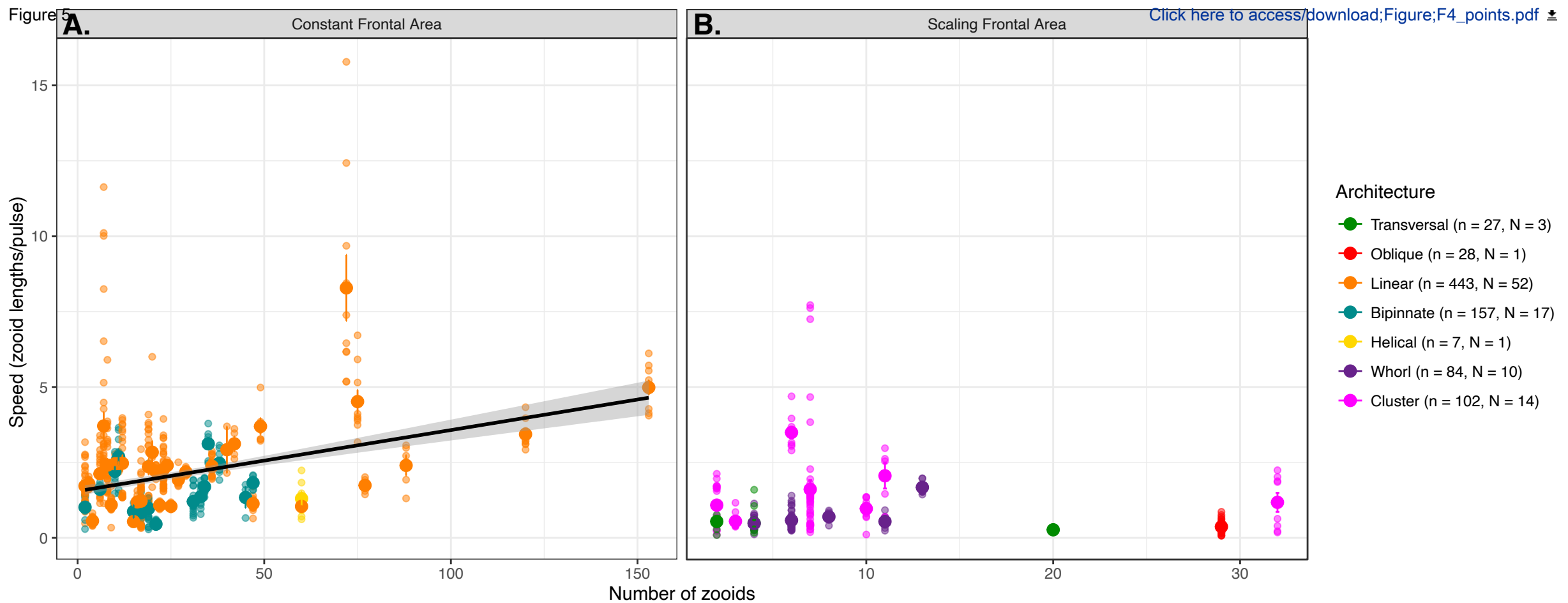
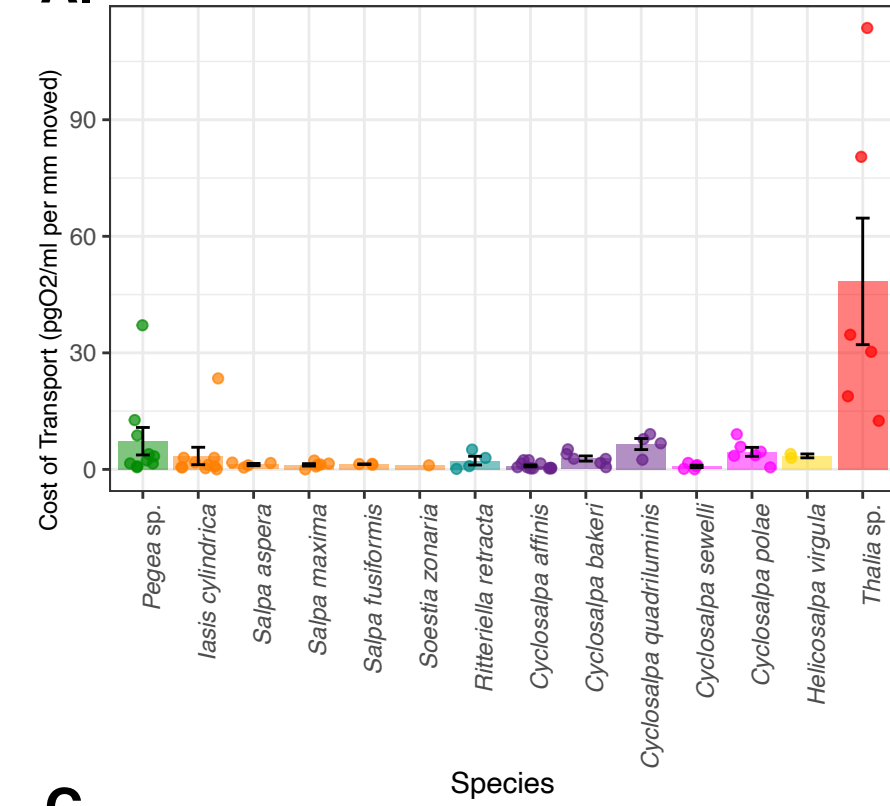
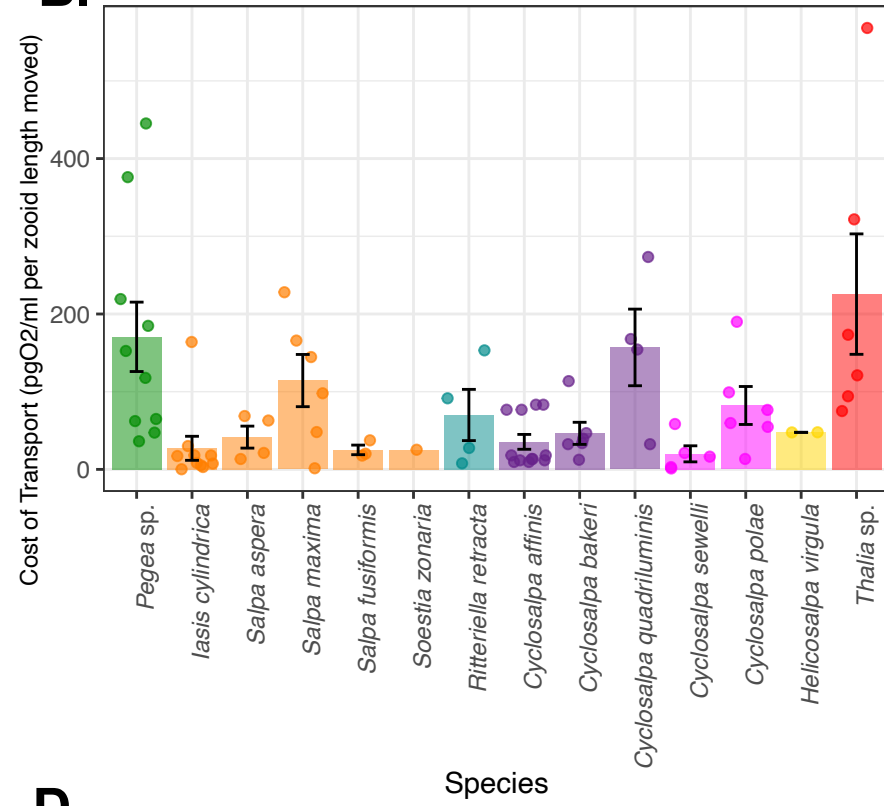


Figure 6

[Click here to access/download;Figure;F5_jitter.pdf](#)
A.**B.****Architecture**

- Transversal (n = 10, N = 9)
- Oblique (n = 6, N = 4)
- Linear (n = 24, N = 22)
- Bipinnate (n = 4, N = 2)
- Helical (n = 2, N = 2)
- Whorl (n = 15, N = 2)
- Cluster (n = 11, N = 8)

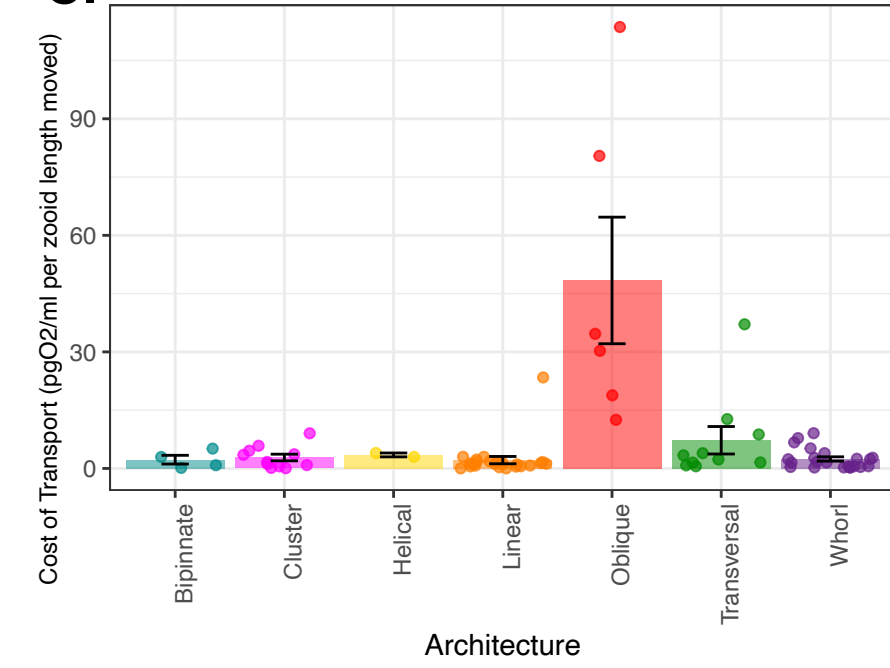
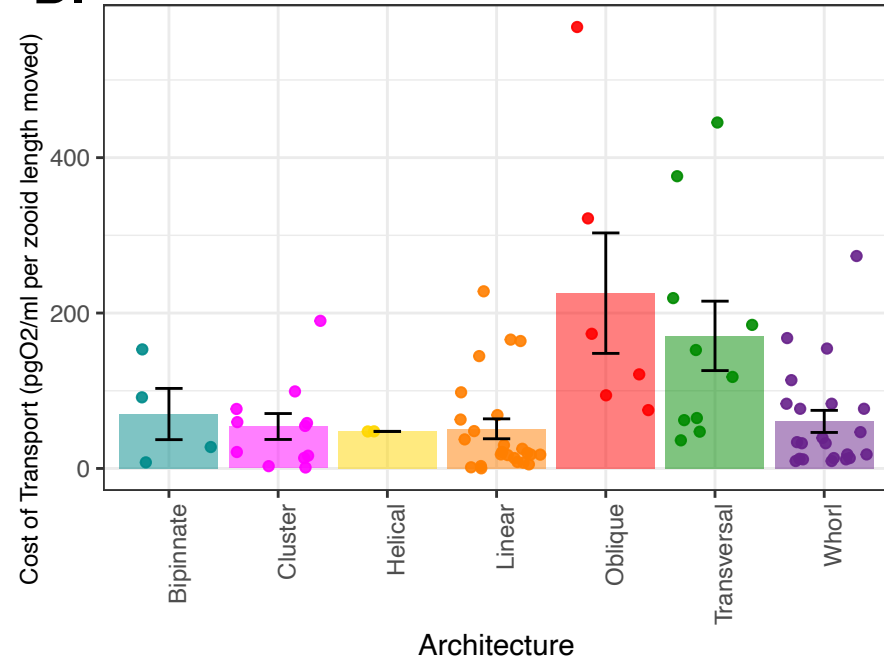
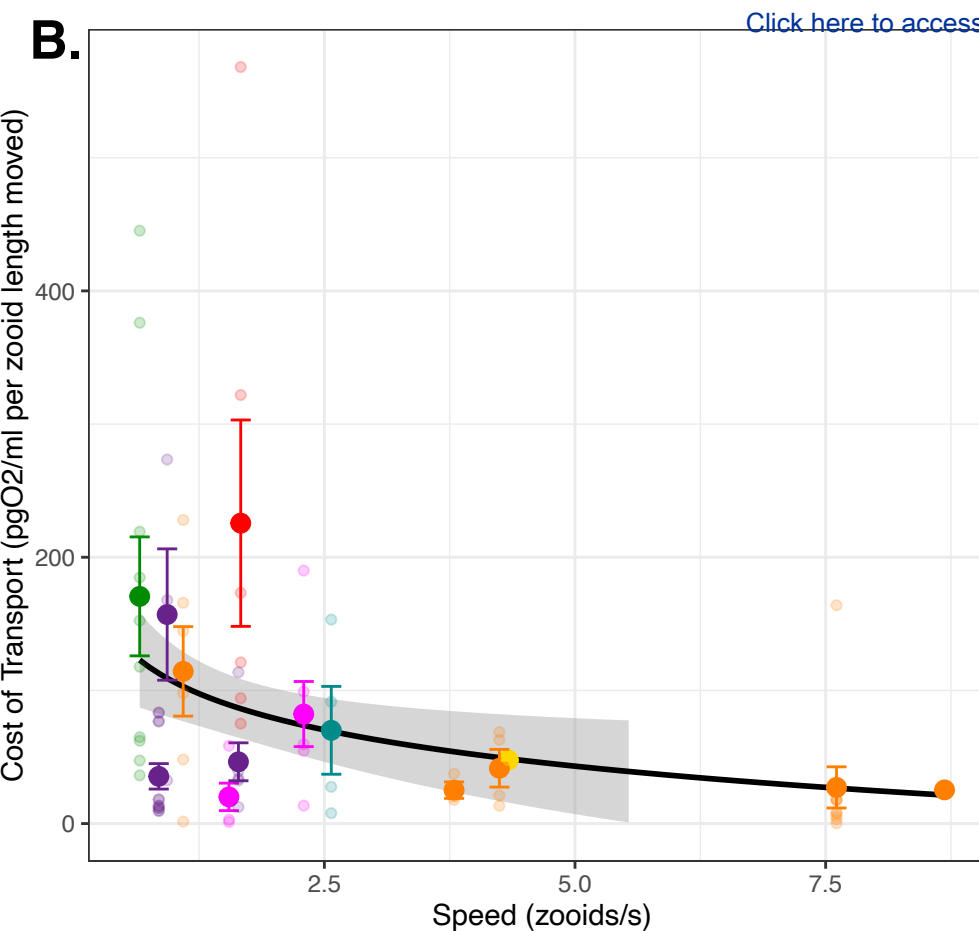
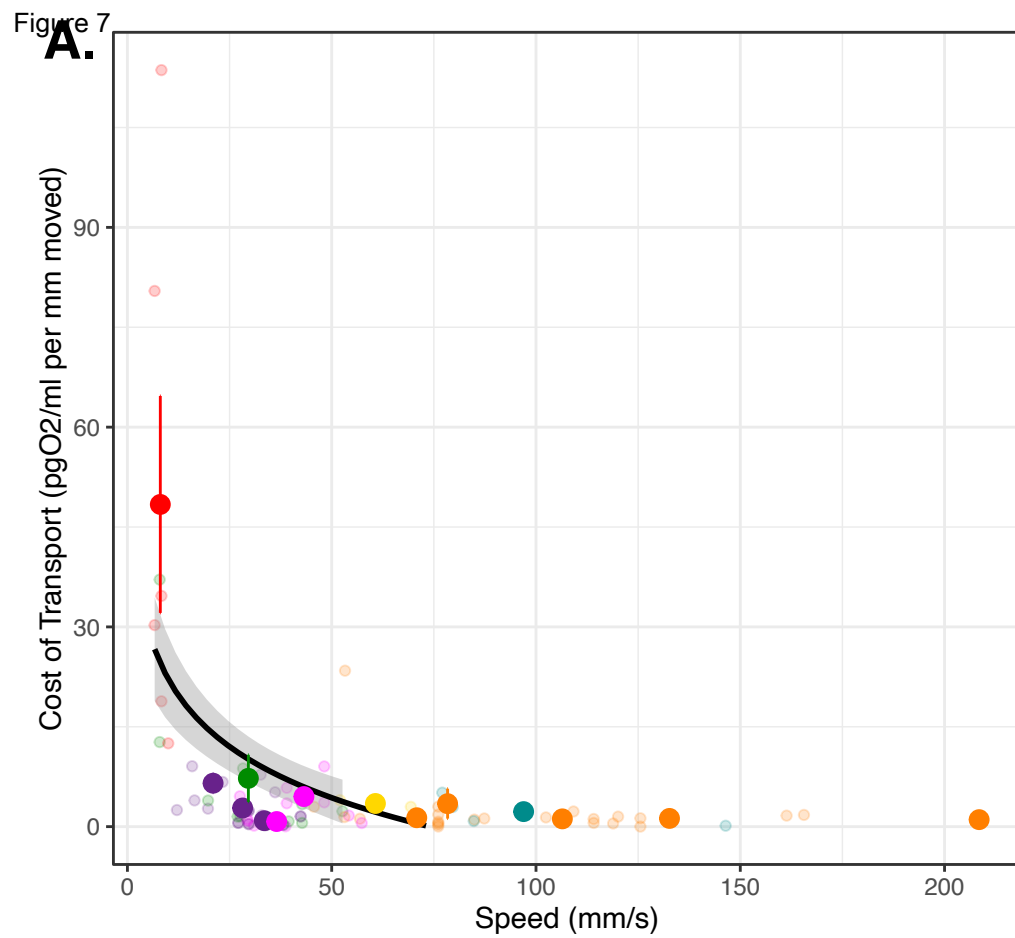
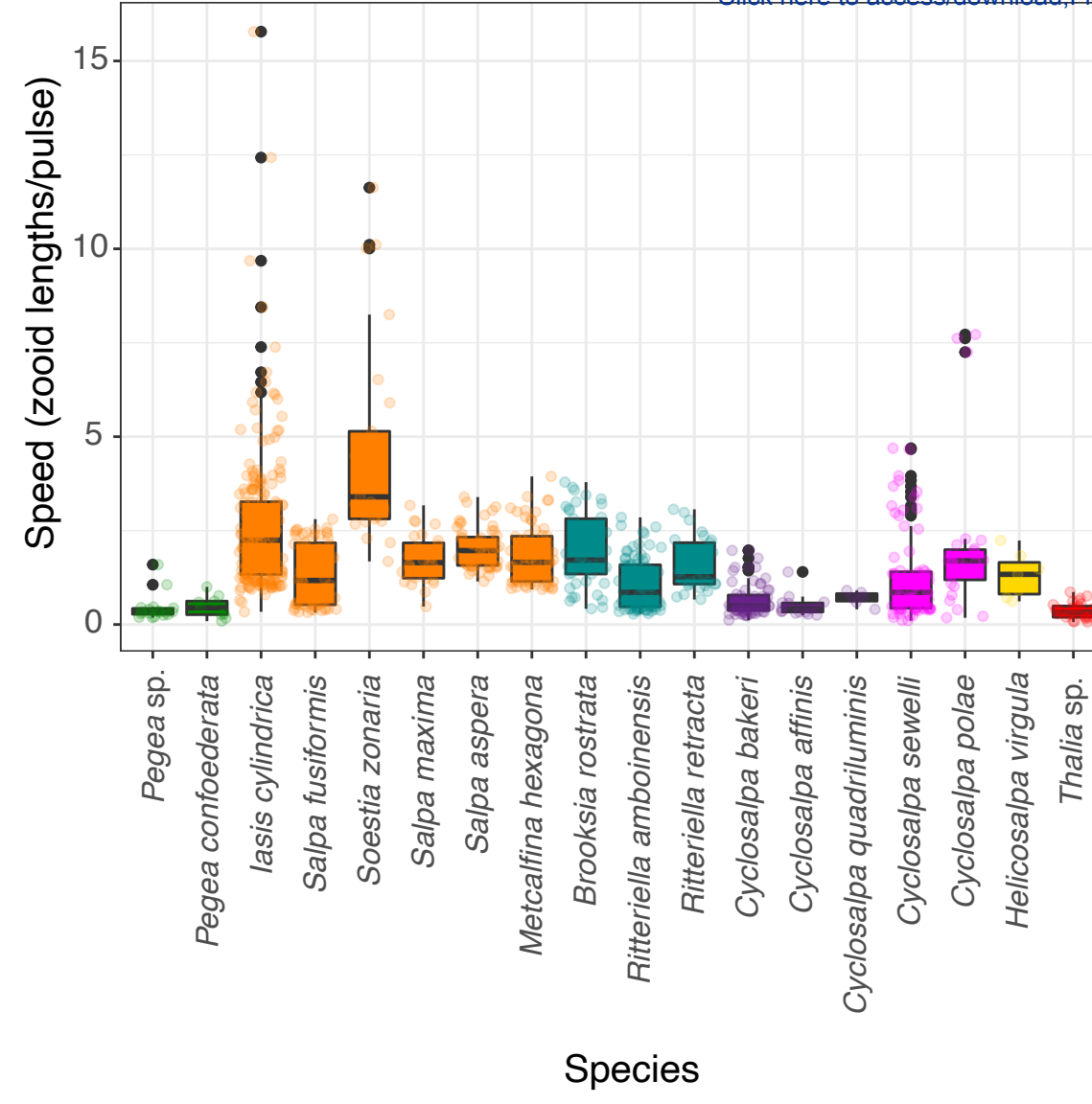
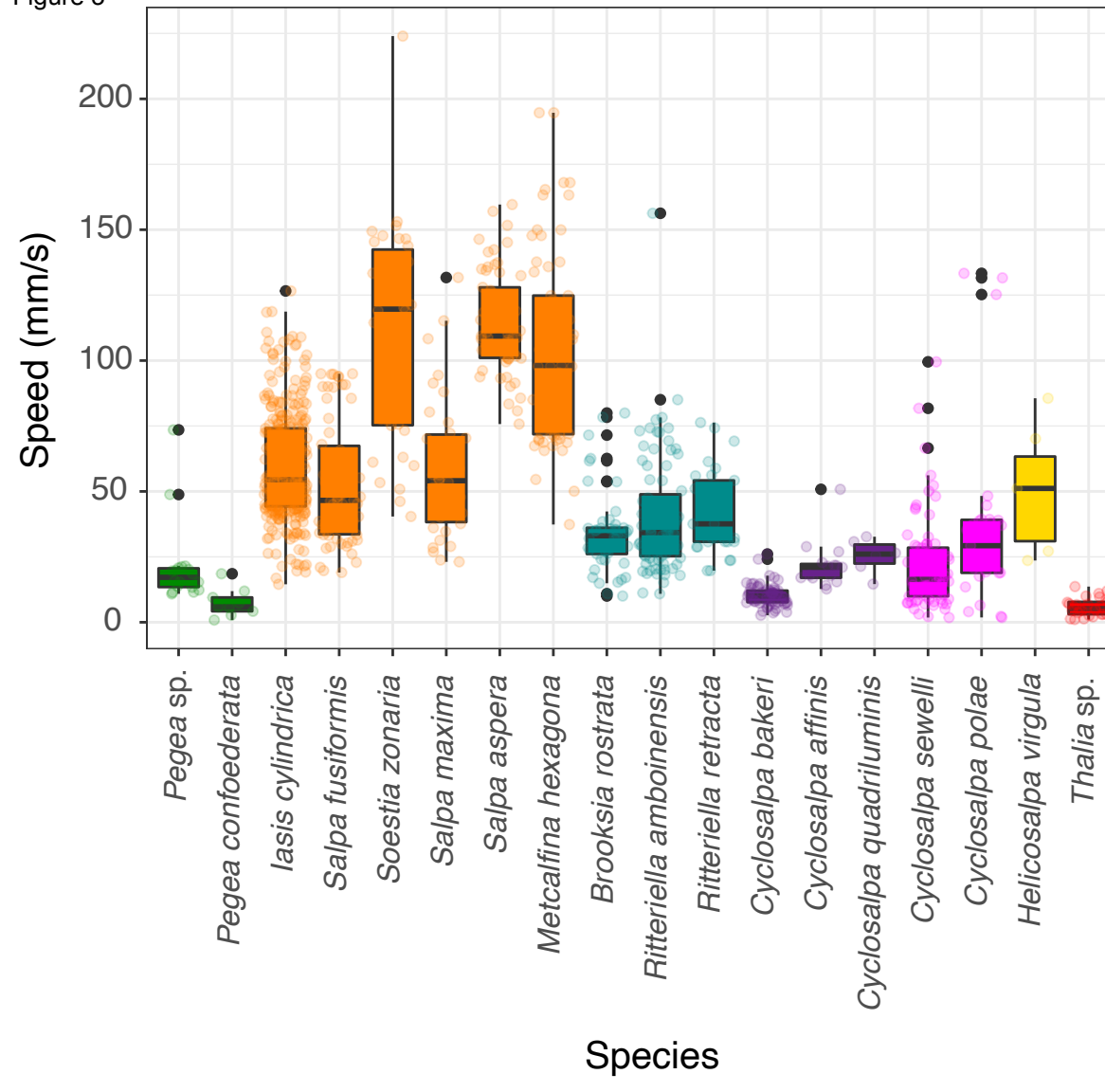
C.**D.**

Figure 7

[Click here to access/download;Figure;F6_points.pdf](#)

- Architecture**
- Transversal ($n = 10, N = 9$)
 - Oblique ($n = 6, N = 4$)
 - Linear ($n = 24, N = 22$)
 - Bipinnate ($n = 4, N = 2$)
 - Helical ($n = 2, N = 2$)
 - Whorl ($n = 15, N = 2$)
 - Cluster ($n = 11, N = 8$)

Figure 3

[Click here to access/download;Figure;F2_jitterplus_compressed.pdf](#)


Architecture

- Transversal (n = 27, N = 4)
- Oblique (n = 28, N = 1)
- Linear (n = 443, N = 52)
- Bipinnate (n = 157, N = 18)
- Helical (n = 7, N = 1)
- Whorl (n = 84, N = 10)
- Cluster (n = 102, N = 14)

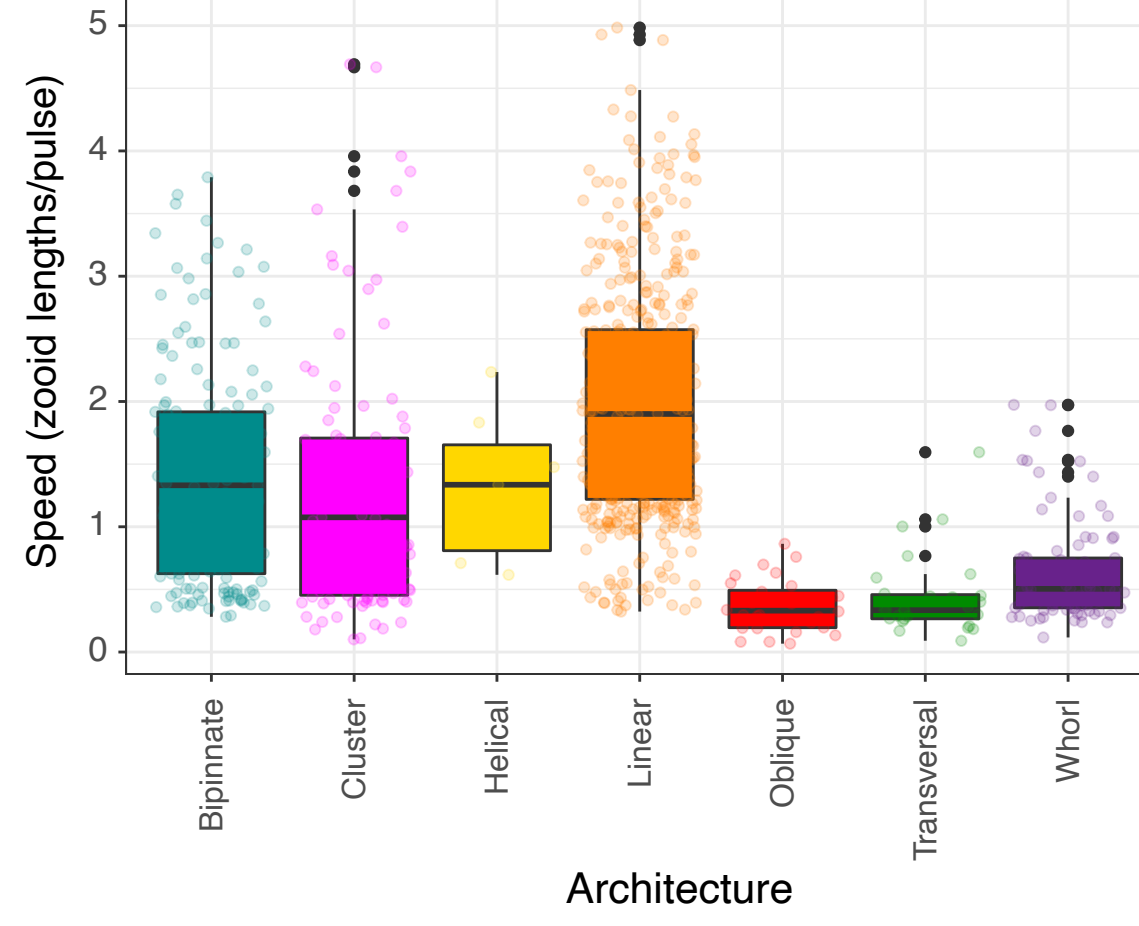
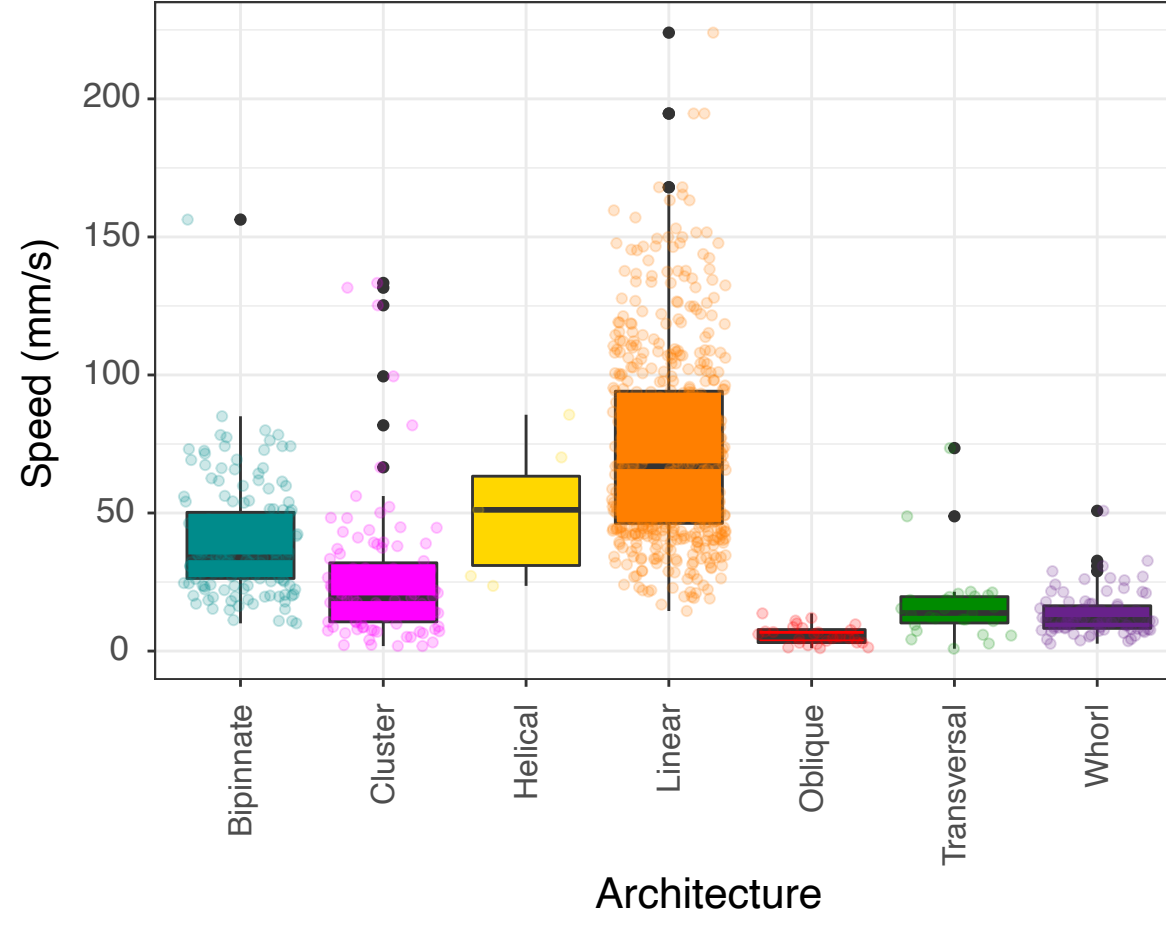


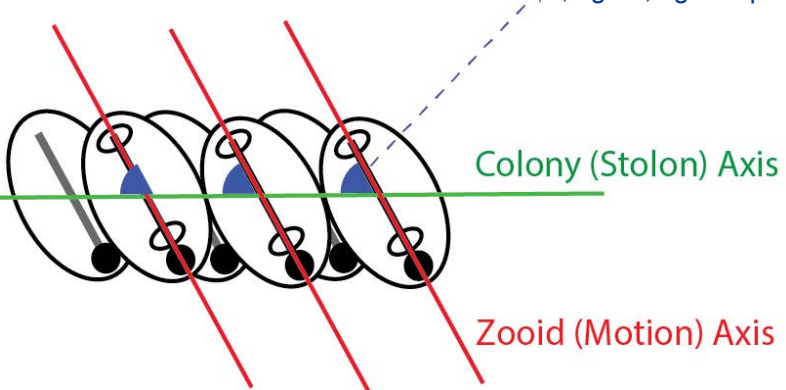
Figure 1

[Click here to access/download;Figure;Fig1.pdf](#)

	Transversal	Whorl	Cluster	Helical	Oblique	Linear	Bipinnate
Architecture							
Frontal area 4 zooids							
Frontal area 8 zooids							
Scaling	2	2	2	1	$1 < x < 2$	1	1

 **Figure 2** Dorsal View

[Click here to access/download Figure 2.pdf](#)



1
2
3
4 1 **Title: Colonial Architecture Modulates the Speed and**
5 2 **Efficiency of Multi-Jet Swimming in Salp Colonies**

6 3
7 4 **Authors:** Alejandro Damian-Serrano¹, Kai A. Walton¹, Anneliese Bishop-Perdue¹, Sophie
8 5 Bagoye¹, Kevin T. Du Clos², Bradford J. Gemmell³, Sean P. Colin^{4,5}, John H. Costello⁶, Kelly R.
9 6 Sutherland¹

10 7
11 8 **Author Affiliations:**

12 9
13 10 (1) Institute of Ecology and Evolution, Department of Biology, University of Oregon. 473 Onyx
14 11 Bridge, 5289 University of Oregon, Eugene, OR 97403-5289, USA.

15 12 (2) Louisiana Universities Marine Consortium, 8124 Highway 56, Chauvin, LA 70344, USA.

16 13 (3) Department of Integrative Biology, University of South Florida, 4202 East Fowler Avenue,
17 14 Tampa, FL 33620, USA.

18 15 (4) Marine Biology and Environmental Science, Roger Williams University, Bristol, RI 02809, USA.

19 16 (5) Whitman Center, Marine Biological Laboratory, Woods Hole, MA 02543, USA.

20 17 (6) Biology Department, Providence College, Providence, RI 02918, USA.

21 19 **Running title:** Architecture Modulates Salp Swimming

22 20
23 21 **Summary Statement (30 words)**

24 22 Linear arrangements in multi-jet propelled marine colonial invertebrates are faster than less
25 23 streamlined architectures without incurring in higher costs of transport, offering insights for
26 24 bioinspired underwater vehicle design.

1
2
3
4 34 **Abstract**
5 35

6 36 Salps are marine pelagic tunicates with a complex life cycle including a solitary and colonial stage.
7 37 Salp colonies are composed of asexually budded individuals that coordinate their swimming by
8 38 multi-jet propulsion. Colonies develop into species-specific architectures with distinct zooid
9 39 orientations. These distinct colonial architectures vary in how frontal area scales with the number
10 40 of zooids in the colony. Here, we address how differences in frontal area drive differences in
11 41 swimming speed and the relationship between swimming speed and cost of transport in salps.
12 42 We (1) compare swimming speed across salp species and architectures, (2) evaluate how
13 43 swimming speed scales with the number of zooids across colony in architectures, and (3)
14 44 compare the metabolic cost of transport across species and how it scales with swimming speed.
15 45 To measure swimming speeds, we recorded swimming salp colonies using in situ videography
16 46 while SCUBA diving in the open ocean. To estimate the cost of transport, we measured the
17 47 respiration rates of swimming and anesthetized salps collected in situ using jars equipped with
18 48 non-invasive oxygen sensors. We found that linear colonies swim faster, which supports idea that
19 49 their differential advantage in frontal area scales with an increasing number of zooids. We also
20 50 found that higher swimming speeds predict lower costs of transport in salps. These findings
21 51 underscore the importance of considering propeller arrangement to optimize speed and energy
22 52 efficiency in bioinspired underwater vehicle design, leveraging lessons learned from the diverse
23 53 natural laboratory provided by salp diversity.

24 54
25 55 **Keywords:** salps, colonial architecture, multi-jet propulsion, swimming, cost of transport
26 56

27 57 **Introduction**

28 58 Salps (Tunicata: Thaliacea: Salpida) are planktonic invertebrates that have a two-phase
29 59 life cycle comprised of a solitary oozooid that asexually buds colonies of sexually reproducing
30 60 blastozooids. Salp colonies are composed of up to hundreds of genetically identical, physically
31 61 and neurophysiologically integrated pulsatile zooids (Bone et al. 1980, Mackie 1986). Zooids in
32 62 the colony feed and propel themselves by drawing water in through the oral siphon, using muscle
33 63 contraction to compress their pharyngeal chamber, and ejecting a jet of water from their atrial
34 64 siphon (Bone & Trueman 1983). While solitary oozooids move using single-jet propulsion, salp
35 65 blastozooid colonies integrate multiple propelling jets, which increases their thrust and reduces
36 66 the drag that results from periodical acceleration and deceleration via asynchronous swimming
37 67 (Sutherland & Weihs 2017).

1
2
3
4 68 Currently, there are 48 described species of salps (WoRMS, 2024) and while salps are
5 69 widely distributed, most species are restricted to open ocean environments, far from the coast,
6 70 which poses unique challenges to accessing them for direct study in their environment (Hamner
7 et al 1975, Haddock 2004). Moreover, salps cannot be maintained alive in containers beyond a
8 72 few hours since they are extremely fragile and sensitive to the presence of solid walls. Therefore,
9 73 many morphological, ecological, and functional aspects of salp diversity, such as swimming
10 74 speeds and metabolic demands, have remained unexplored. One such aspect is colonial
11 75 architecture or the way that the zooids are arranged relative to each other in the colony. Salp
12 76 colonies develop into species-specific architectures with distinct zooid orientations, including
13 77 transversal, oblique, linear, helical, and bipinnate chains; as well as whorls, and clusters (Damian-
14 78 Serrano & Sutherland, 2023). These architectures likely drive aspects of swimming performance
15 79 (Madin 1990, Damian-Serrano et al. 2023).

24 80 Linear salp chains have been described as more efficient swimmers due to the reduction
25 81 of drag associated with a more streamlined form (Bone & Trueman 1983). In a multi-jet system,
26 82 having a larger number of propellers can improve the hydrodynamic and inertial benefits granted
27 83 by asynchronous multijet propulsion, in addition to providing additional thrust to the colony (Madin
28 84 1990, Sutherland & Weihs 2017). The effect of varying numbers of propeller zooids on swimming
29 85 speed has never been investigated in salps, nor how this relationship may vary across their
30 86 diverse colonial architectures. Salp colonial architectures differ in how the number of zooids in
31 87 the colony scales with their frontal area relative to motion (Madin 1990). Some architectures
32 88 (linear, bipinnate, and helical) have a constant frontal area, regardless of zooid number. These
33 89 architectures may benefit from increased thrust delivered by larger numbers of zooids while
34 90 maintaining a constant frontal area. However, the rest of the architectures (oblique, transversal,
35 91 whorl, and cluster) have an increasing (directly proportional) frontal area as the number of zooids
36 92 increases (Fig. 1). Therefore, we expect the latter architectures to not only obtain more thrust, but
37 93 to also experience more frontal water resistance as zooid number increases. As a result, we
38 94 anticipate that swimming speed will be greater in colonies that bear a larger number of zooids,
39 95 but only (or more so) for species with architectures that have a constant frontal area.

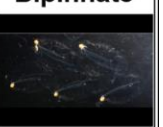
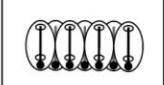
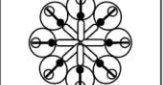
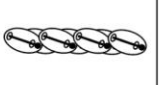
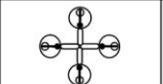
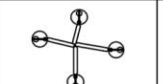
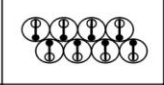
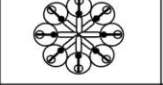
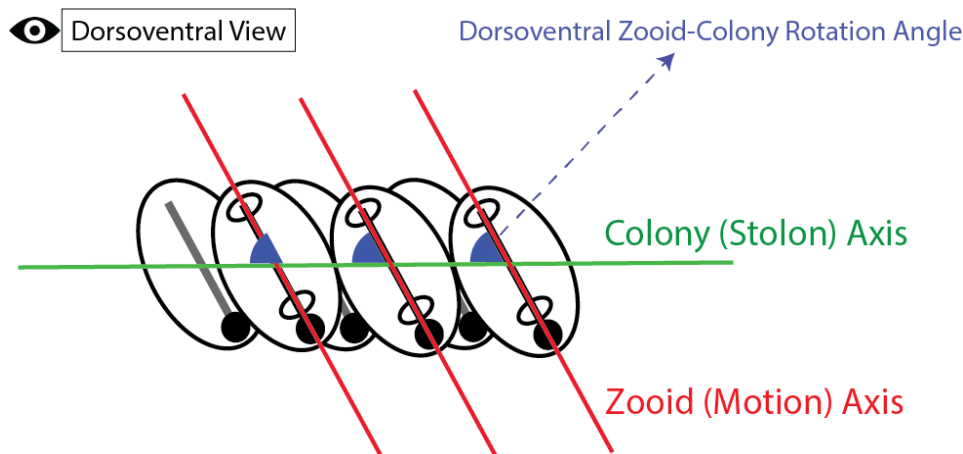
	Transversal	Whorl	Cluster	Helical	Oblique	Linear	Bipinnate
Architecture							
							
Frontal area 4 zooids							
Frontal area 8 zooids							
Scaling	2	2	2	1	1×2	1	1

Figure 1. Salp colonial architectures with representative species photos (*Pegea* sp. for transversal, *Cyclosalpa affinis* for whorl, *Cyclosalpa sewelli* for cluster, *Helicosalpa virgula* for helical, *Thalia cicatricosa* for oblique, *Soestia zonaria* for linear, and *Ritteriella retracta* for bipinnate) and diagrams showing the distinct zooid orientations. The subsequent rows show the frontal view of colonies with four and eight zooids, with the final row indicating the expected frontal area increase factor between the four and the eight zooid colonies. Full black circles in the diagrams represent viscerae (guts) while the open circle represent siphons. Black straight lines inside the zooids indicate gill bars while gray straight lines represent endostyles.

Linearity of colonies, as well as zooid size and pulsation rates, are additional factors that could influence swimming performance. The degree of linearity in a colony can be expressed as the degree of parallelism between the zooids and the elongation axis of the colony (Fig. 2). This angle is determined by the degree of developmental dorsoventral zooid rotation, which can span from 90°, in transversal chains with no rotation, to 0° (perfect linearity), in some linear chains such as those from the species *Soestia zonaria* (Damian-Serrano & Sutherland, 2023). Strong reductions in the dorsoventral zooid rotation angle toward linear forms have evolved multiple times independently (Damian-Serrano et al. 2023), possibly due to adaptive advantages related to their swimming efficiency. Body size predicts swimming velocity in many animals (Andersen et al. 2016), however colonies with multiple swimming units may circumvent this size-speed relationship by having multiple propellers. Pulsation rates may also influence swimming speed as has been shown in solitary salps (Madin 1990). Pulsation by salps serves the dual role of locomotion and filter feeding. The relationship between pulsation and speed might therefore be particularly relevant for species that undergo diel vertical migration (Madin et al. 1996) and in other species pulsation may serve to maximize filtration rates. Considering the tradeoffs between

1
2
3
4 121 swimming and filtering, the eco-evolutionary relevance of swimming speed, and the hydrodynamic
5 efficiency likely varies between species (Damian-Serrano et al. 2023).
6
7 123
8
9 124



10
11
12
13
14
15
16
17
18
19
20
21
22
23
24
25 125 Figure 2. Schematic of an oblique chain from the dorsoventral perspective showing the zooid and
26
27
28
29
30
31
32
33
34
35
36
37
38
39
40
41
42
43
44
45
46
47
48
49
50
51
52
53
54
55
56
57
58
59
60
61
62
63
64
65

126 The energetic costs of salp locomotion from mechanically estimated propulsive efficiency
127 suggest that like other jet-propelled swimmers, salps are hydrodynamically efficient (Sutherland
128 & Madin 2010, Gemmell et al. 2021, Trueman et al. 1984). The few metabolic measurements of
129 swimming salps show that more active species-- in terms of swimming speed and pulsation rates--
130 have the highest respiration rates (Cetta et al. 1986) and that salps have higher respiration rates
131 than other gelatinous taxa (Biggs 1977, Schneider 1992, Mayzaud et al. 2005, Trueblood 2019).
132 However, the specific costs incurred by their swimming activity and their relationship to swimming
133 speed have never been examined across the diversity of salp species.
134

135 In this study, we compare swimming speeds across 17 salp species and energetic costs
136 of swimming across 15 species, encompassing all seven known salp colony architectures (Fig. 1,
137 Table S1). In addition, we investigate how swimming speed varies with the number of propeller
138 zooids and differences in frontal area scaling between colonial architectures. Finally, we compare
139 cost of transport (COT) across salp species and assess how COT scales with swimming speed
140 and pulsation effort.
141
142

144 Materials and Methods

1
2
3
4 145 *Fieldwork* – We observed salps via 48 bluewater SCUBA dives (Haddock & Heine, 2005)
5 from a small vessel off the coast of Kailua-Kona (Hawai'i Big Island, 19°42'38.7" N 156°06'15.8"
6 W), over 2000 m of offshore water during September 2021, April 2022, September 2022 and May
7 147 2023. We spent a total of 42.2 hours (84.4 person hours: ADS & KRS) collecting and imaging
8 148 salp colonies. Some dives were diurnal, where we collected most of the specimens of *Iasis*
9 149 *cylindrica*, *Cyclosalpa affinis*, *Cyclosalpa sewelli*, and *Brooksia rostrata*. We observed and
10 150 collected most specimens of other species during night dives (blackwater diving). We recorded in
11 151 situ underwater videos of salp colonies swimming using a variety of cameras including primarily
12 152 a dark field stereovideography system (Sutherland et al. 2024), as well as a lightweight dual
13 153 GoPro stereo system, a brightfield single-camera system (Colin et al. 2022), and a darkfield
14 154 single-camera system. The primary stereovideography system was comprised of two
15 155 synchronized high-resolution cameras (Z Cam E2, Nan Shan, Shenzhen, China and Sync Cable;
16 156 4K at 60 or 120 fps) with 17mm f/1.8 lenses (Olympus M.Zuiko Digital) housed in custom
17 157 aluminum housings (Sexton Company, Salem, OR, USA). Each field of view was 23 x 42 mm and
18 158 in-focus depth was 20-25 mm. The image from the right-hand camera was viewed using an
19 159 external monitor (Aquatica Digital, Montreal, Quebec, Canada), and illumination was provided
20 160 with two 10,000-lumen lights (Keldan, Bruegg, Switzerland). An L-shaped plastic framer helped
21 161 the videographer position colonies in the field of view of both cameras. Before diving, the stereo
22 162 system was calibrated in a swimming pool using a cube with reflective landmarks. Calibration
23 163 images were processed using the CAL software package (SeaGIS measurement science,
24 164 Bacchus Marsh, Victoria, Australia). Over the course of the study, we observed 241 salp colonies
25 165 (N) from 18 species and recorded 1,946 measurements (n) (Dataset1A, Table S1). Throughout
26 166 the manuscript, we refer to the number of specimens as N and the number of measurements as
27 167 n.
28 168

44 169 *Measuring salp colony swimming speed* – For most species, we collected and analyzed
45 170 footage from multiple specimens (Dataset1A, Table S1). We analyzed the swimming behavior of
46 171 salp colonies arranged in linear (six species, 64 specimens), bipinnate (three species, 17
47 172 specimens), whorl (three species, 10 specimens), cluster (two species, eight specimens), and
48 173 transversal (one species, two specimens) architectures, with oblique and helical architectures
49 174 represented by a single specimen. We used a combination of spatially calibrated stereo video
50 175 and 2D videos with a reference scale in the frame. From the stereo videos, we manually selected
51 176 and measured the relative XYZ positions of salp colony zooids in EventMeasure (SeaGIS). We
52 177 implemented a cutoff in the RMS (root mean squared) point error estimate of < 2 mm.
53
54
55
56
57
58
59
60
61
62
63
64
65

1
2
3
4 178 We complemented gaps in taxon sampling with archived 2D videos in the lab from
5 previous expeditions to West Palm Beach (FL, USA) and the Pacific coast of Panama. These two-
6 dimensional single-camera videos were collected using a Sony FDR-AX700 4K Camcorder
7 (3840x2160 pixels, 60-120 fps) with a Gates Underwater Housing (Poway, CA, USA) using
8 brightfield illumination (Colin et al 2022) or darkfield illumination. For these 2D videos, we used
9 the FFmpeg plugin in ImageJ to manually select and measure the relative XY positions of salp
10 zooids in sequences where the colony was swimming horizontally within the focal plane. The
11 colonies were assumed to be in the same plane as the scale bar so at same distance from the
12 camera. However, in videos with a broad focal depth, this may not always had been the case,
13 thus potentially introducing some measurement error.
14

15 188 We tracked and manually selected the position of the first zooid's viscera (using a contrast-
16 based centering macro to mark the center point) as well as the position of a reference particle in
17 the water (methods described in Sutherland et al. 2024) in 10-30 frames across 50-500 frame
18 windows spanning 2-4s of swimming on the synchronized left and right videos in EventMeasure.
19 The reference particle was a non-swimming organism (such as a foraminiferan or radiolarian) or
20 a non-living particle. In addition, we recorded the pulsation rates of the specimens measured by
21 counting the number of times the atrial siphon contracted in a known period. For each analyzed
22 frame, we calculated the horizontal x, vertical y, and depth z (in the case of the stereo video
23 measurement files) components of the relative positions of the frontal zooid to the reference
24 particle as shown in Eq. 1.
25

26 198
27 199 $x_n = x_{n\ animal} - x_{n\ particle}$
28 200 $y_n = y_{n\ animal} - y_{n\ particle}$ Eq. 1
29 201 $z_n = z_{n\ animal} - z_{n\ particle}$
30

31 203 Then we calculated the instantaneous relative speeds of the frontal zooid using Eq. 2
32 (without the z component in the case of the 2D videos) given the known frame rate of each video.
33

34 205
35 206 $U = \frac{\sqrt{(x_2-x_1)^2 + (y_2-y_1)^2 + (z_2-z_1)^2}}{t_2-t_1}$ Eq. 2
36

37 208 *Salp colonial architecture* – To examine the relationships between locomotory variables
38 209 and colonial architecture, we adopted the species-specific architecture characterizations and
39 210 dorsoventral zooid rotation angle measurements for each species from Damian-Serrano et al.
40

1
2
3
4 211 (2023). Using stills from the underwater videos, we measured zooid length, zooid width, and
5 number of zooids in ImageJ manually selecting the point coordinates. These measurements were
6 repeated in at least three locations from each colony. When a distinct zooid size gradient was
7 observed, we measured zooids in locations from the proximal, middle, and distal regions to
8 capture the full range of variation in the specimen.
9
10

11 215
12 216 *Respiration measurements* – We collected healthy, adult blastozooid (aggregate stage)
13 colonies across 18 salp species (Dataset S1B) during blue- and black-water SCUBA dives off the
14 coast of Kona (Hawaii, USA) between September 2021 and May 2023. We analyzed the
15 respiration rates of salp colonies arranged in linear (seven species, N = 46), bipinnate (three
16 species, N = 29), whorl (three species, N = 23), cluster (two species, N = 18), and transversal
17 (one species, N = 13) architectures, oblique chains (*Thalia* sp., N = 7), and helical architectures
18 represented by *Helicosalpa virgula* (N = 2). Specimens were sealed *in situ* with their surrounding
19 water in plastic jars equipped with a PreSens oxygen sensor spot (Regensburg, Germany) and a
20 self-healing rubber port to allow for the injection of solutions without the introduction of air bubbles.
21
22 We removed as many symbiotic animals from the salps as possible before closing the lid without
23 damaging the colony. The same method was applied to one or more seawater controls to account
24 for the oxygen demand of the local seawater's microbiome. Several collection events occurred
25 during each 20-60 min long SCUBA dive. Jars with larger animals were opened during the safety
26 stop to allow them to re-oxygenate. Upon the divers' return to the boat, we measured the initial
27 oxygen concentration (mg/l) and temperature, and then repeated the measurements at intervals
28 between 15min and 3h, for total periods ranging between 2h and 5h, depending on logistic
29 constraints in the field and the rate of oxygen depletion. The exact interval time for each
30 measurement was variable but recorded (Dataset S1B).
31
32

33 233
34 234 To estimate the energetic expenditure of different salp species while actively swimming,
35 we recorded the oxygen consumption of intact specimens while swimming inside the jar. To obtain
36 a baseline of basal respiration rate (while not swimming), we anesthetized some specimens
37 before the start of the first oxygen measurement time. A few specimens were used for paired
38 experiments, where their swimming respiration was recorded for a few hours, then inoculated with
39 the anesthetic, and recorded anesthetized for another set of hours. To anesthetize salps, we
40 injected their jars with small volumes of concentrated (50 g/l) bicarbonate-buffered MS-222
41 through the rubber ports on the lids. We tailored the injection volume to the jar size aiming for a
42 final concentration of 0.2g/l, following the methods in Trueman et al. (1984). We also injected
43 some seawater control jars to evaluate the effect of MS-222 on oxygen concentration in seawater
44 and found no effect.
45
46
47
48
49
50
51
52
53
54
55
56
57
58
59
60
61
62
63
64
65

1
2
3
4 245 When multiple seawater controls were collected using jars of different sizes, we paired
5 each jar with the control that had the most similar volume. If among multiple controls only some
6 were jars injected with anesthetic, we paired the anesthetized specimen jars with the injected
7 controls and the intact specimen jars with the intact controls. In experiment 26 (see Dataset S1B
8 for experiment numbers), the control jar was lost due to an encounter with an oceanic white tip
9 shark, thus we paired those measurements with the nearest relative time points from the control
10 jar in experiment 25, collected the same day hours earlier. At the end of each experiment, we
11 identified the salp specimens used in the experiments to the species level, counted the number
12 of zooids, measured the zooid length (total length including projections), and measured the
13 biovolume of the colony using a graduated cylinder. For those specimens where colony or zooid
14 volume was not measured directly, we estimated the colony volume from their zooid length and
15 the number of zooids using a Generalized Additive Model with the measured specimens.
16 256

17 257 We estimated the oxygen consumption rate for each specimen by fitting a linear
18 regression of consumed oxygen mass (concentration by container volume) against the duration
19 of the measurement series. We subtracted the slope calculated for the relevant control jar to the
20 estimated slope of the animal jar. Since our seawater controls were not filtered, some experiments
21 had abnormally high estimated background respiration rates, leading to negative values. We
22 removed these data points before the analysis. To estimate biovolume-specific rates, we divided
23 the rates by the colony volumes. We then compared the biovolume-specific respiration rates of
24 active (swimming) and anesthetized specimens within each species, calculating the difference as
25 a measure of biovolume-specific swimming cost respiration rate. Biovolume was used instead of
26 dry mass to normalize measurements due to the inherent difficulties of accurately measuring dry
27 mass of these fragile gelatinous organisms in the field. Biovolume provides a consistent and
28 reliable measure of the live size of the colony, which is directly relevant to the volume of water
29 being displaced during swimming. We also calculated the relative investment in swimming as the
30 proportion of biovolume-specific respiration rate comprised by the swimming-specific rate. To
31 capture variability within species, we calculated the mean respiration rate of anesthetized
32 specimens for each species and subtracted it from each intact specimen's total respiration rate to
33 get multiple swimming-specific rate values within each species. We noticed that some species
34 had higher average respiration rates among the anesthetized specimens than among the
35 swimming specimens, leading to negative swimming-specific respiration estimates. We
36 interpreted this anomaly as a systematic error due to the extremely low respiration rates of some
37 species that fall within the effective detection limit of our experimental setup given the random
38 variation range of respiration rates in seawater both in experimental jars and in control jars. Small
39 278

40
41
42
43
44
45
46
47
48
49
50
51
52
53
54
55
56
57
58
59
60
61
62
63
64
65

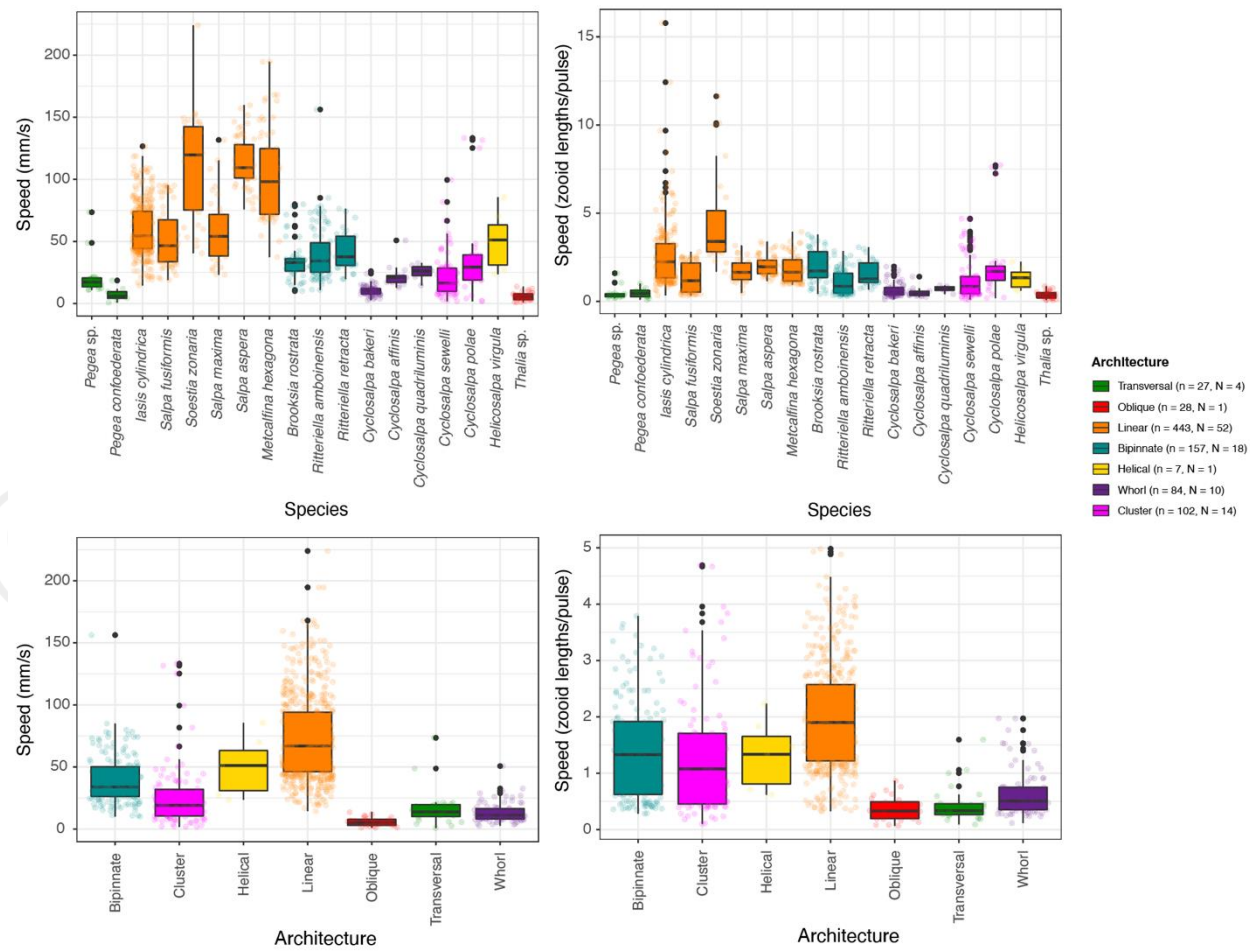
absolute negative values get amplified into large relative values, especially in small animals with a minuscule biovolume denominator. Therefore, we removed the swimming specimens that had lower respiration rates than the mean anesthetized respiration rate for their species. We also removed two respirometry outliers of *Thalia* sp. which had extremely high swimming respiration rates (>7500 pgO₂/ml/min, whereas all other measurements across species including other *Thalia* sp. were limited to 0-1700 pgO₂/ml/min), which were likely due to amplification of experimental error (presence of organic matter or symbionts, underestimation of colony volume due to loss of tiny zooids in the sieves) with the small biovolume denominators in this species.

Estimating costs of transport – We define the cost of transport (COT) as the amount of oxygen consumed per tissue volume per distance traveled by the colony. To estimate the COT, we divided the swimming-specific respiration rates by the mean swimming speed for each species measured from the stereo and 2D video data. Since the specimens used for speed measurements in the videos and those used in the respirometry experiments had different zooid sizes, we used the mean zooid-lengths per second speeds from the video measurements and then multiplied them by the actual zooid lengths of the respirometry specimens to estimate their absolute (mm/s) speeds. Pulsation rate estimates were taken from species averages from the video specimens. We also calculated the size-specific COT by transforming the swimming distances into zooid lengths measured from the respirometry specimens.

Statistical Analyses – All data wrangling and statistics were carried out in R 3.6.3 (R Core Team 2021). To test for differences between architectures, we used ANOVAs with Tukey's post-hoc pairwise contrasts, reporting the difference magnitude and the adjusted p-value in supplementary tables S2A and S2B. To test the relationships between pairs of continuous variables across architectures (e.g. swimming speed vs. number of zooids), we used linear regressions. We evaluated the significance of the slope parameter when compared against a flat slope (one-tailed t-test) to test whether changes in the independent variable (e.g. number of zooids) were associated with changes in the dependent variable (e.g. swimming speed). Owing to the patchiness of some species despite 80+ hours spent underwater (Table S1), we used replicate measurements (n) from each specimen (N) in swimming speed ANOVAs and regressions. We used an exponential regression to test the relationship between speed and COT. Specimen means (N) were used for all COT comparisons and regressions. Individual measurements (n) were used up to determine oxygen consumption rates. To evaluate the relative contribution of zooid size, pulsation rate, zooid number, and architecture type on swimming speed, we fitted a generalized linear model and evaluated the significance and proportion of variance explained by each factor using their partial R².

1
2
3
4 313
5
6 **Results**

7
8
9
10
11
12
13
14
15
16
17
18
19
20 314
Salp colony swimming speeds, pulsation rates, and respiration rates varied within and across species and colony architectures. When considering speed in terms of mm/s, we found a relationship between pulsation rate (effort) and absolute speed ($n = 947$, $N = 111$, 18 species, Speed mm/s = $0.41 \times$ Pulsation rate + 52.14, $p < 0.0001$, Fig. S1A), as well as with zoid-size corrected swimming speed ($n = 848$, $N = 100$, 18 species, Speed zoid lengths/s = $0.96 \times$ Pulsation rate + 1.73, adjusted $R^2 = 0.18$, $p < 0.0001$, Fig. S1B). Normalized swimming speeds (zoid lengths per pulse) allow for a more direct comparison of swimming speed across colonial architectures.



52 323
53 324 Figure 3. Boxplots showing the absolute (A) and corrected for body size and pulsation rate (B)
54 325 swimming speeds recorded for each salp species and architecture (C, D) respectively. Colors
55 326 correspond to colonial architecture types. Sample sizes are included in the legend and Tukey's
56
57
58
59
60
61
62
63
64
65

1
2
3
4 327 post-hoc pairwise comparisons across architecture types are listed in Dataset 1A and Table S2A,
5
6 328 respectively.
7
8 329

9 330 *Swimming speeds across salp architectures*
10

11 331 Swimming speed varied significantly (5 architectures, 16 species, N = 109, n = 913,
12
13 332 ANOVA F > 38, p < 0.001) between colonial architecture types (Fig. 3C, D, Table S2A). Speeds
14
15 333 measured with 2D methods were slightly slower than those measured with 3D methods within the
16
17 334 species in which they overlapped. This is to be expected since 2D methods cannot account for
18
19 335 the z (depth) component of the speed vector. Measurements of helical and oblique chains were
20
21 336 limited to a single specimen, so they were excluded from the analysis. In terms of absolute speed
22
23 337 (mm/s), linear architectures were significantly faster than every other architecture (Tukey's p <
24
25 338 0.001). While bipinnate chains were significantly slower than linear chains, they were significantly
26
27 339 faster than transversal chains, clusters, and whorls (Tukey's p < 0.002). Clusters were not
28
29 340 significantly faster than transversal chains nor whorls. Transversal chains were on par to whorls,
30
31 341 with no significant differences between them.

32
33 342 In terms of relative speed (zooid lengths/pulse), linear architectures were significantly
34
35 343 faster than every other architecture (Tukey's p < 0.001). Bipinnate chains were significantly faster
36
37 344 than whorls and transversal chains (Tukey's p < 0.01), but not significantly different from clusters.
38
39 345 Clusters were significantly faster than whorls (Tukey's p < 0.001) in relative speed. Whorls and
40
41 346 transversal chains presented similar relative swimming speeds with no significant differences.
42

43
44 347 Since linear architectures had the fastest mean swimming speeds (Fig. 3C, D), we
45
46 348 investigated the relationship between swimming speeds with the dorsoventral zooid rotation
47
48 349 angle, which represents the degree of linearity of the colony (Fig. 4). Species with more parallel
49
50
51
52
53
54
55
56
57
58
59
60
61
62
63
64
65 (lower angles) dorsoventral zooid rotation presented faster absolute speeds (n = 910, N = 107,
16 species, Speed mm/s = -0.78*DV Zooid angle + 81.25, adjusted R² = 0.33, p < 0.0001) and
faster size-and-effort corrected swimming speeds (n = 810, N = 96, 16 species, Speed
zooids/pulse = -0.016*DV Zooid angle + 2.37, adjusted R² = 0.09, p < 0.0001).

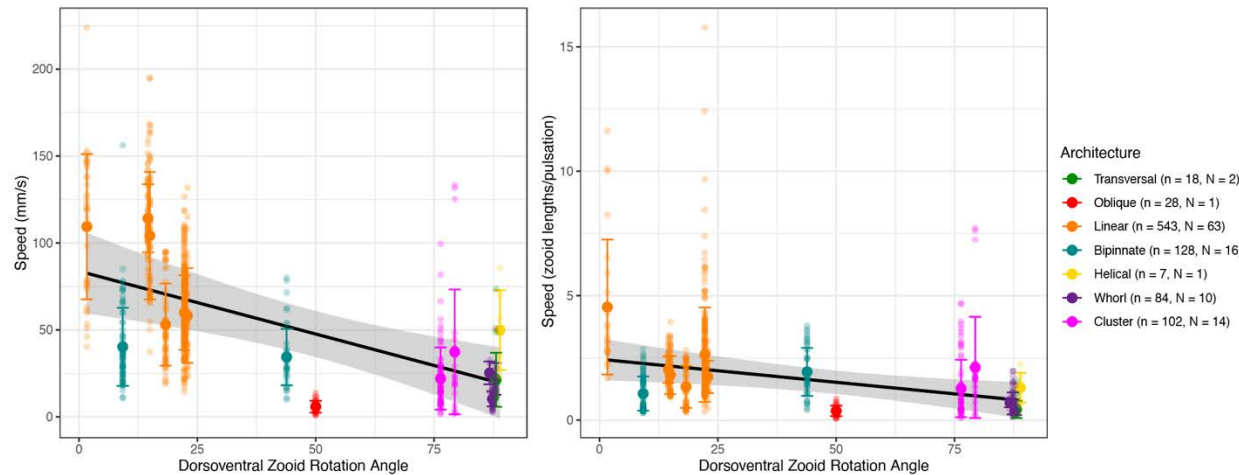
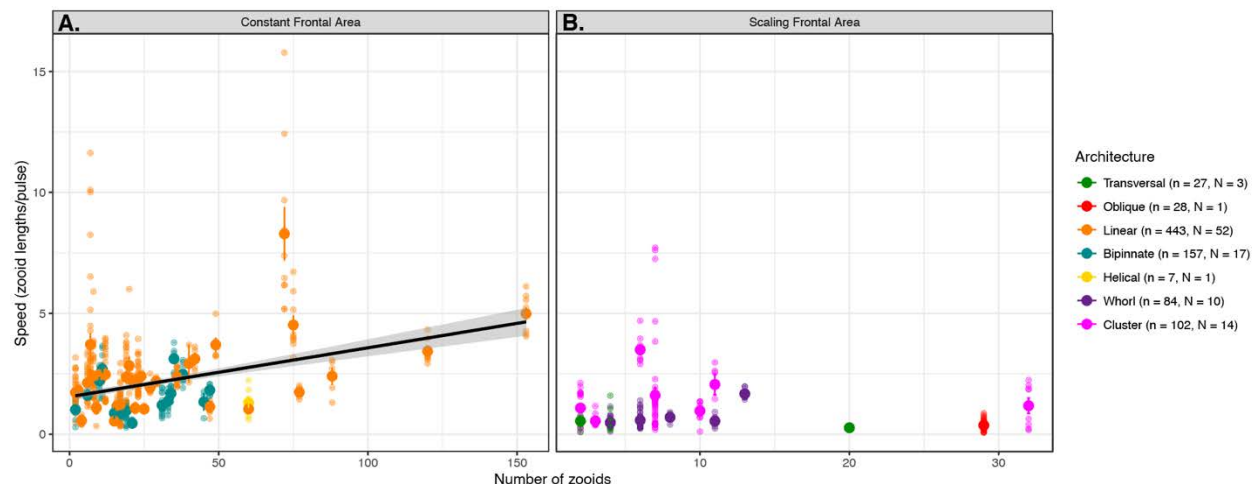


Figure 4. Absolute (A) and relative (B) colony swimming speed (specimen mean with standard errors, total n=103) for each salp species across their degree of dorsoventral zooid rotation. Error bars indicate standard error. The color indicates colonial architecture. Gray areas indicate the 95% confidence interval of the linear regression (black line).

We compared how swimming speeds scale with the number of zooids in the colony and found differences between colonial architectures. Swimming speed in whorls increased with number of zooids ($n = 84$, $N = 10$, 3 species, Speed mm/s = $0.08 \times \text{Number of zooids} + 0.12$, adjusted $R^2 = 0.3$, $p < 0.0001$), though the data for this architecture was limited to small numbers of zooids (4 to 13) and relatively slow speeds (under 51 mm/s). Linear chain architectures did increase in relative speed with the number of zooids ($n = 443$, $N = 52$, 6 species, Speed mm/s = $0.02 \times \text{Number of zooids} + 1.77$, adjusted $R^2 = 0.14$, $p < 0.001$), as did bipinnate chains ($n = 157$, $N = 18$, 3 species, Speed mm/s = $0.015 \times \text{Number of zooids} + 1.05$, adjusted $R^2 = 0.04$, $p < 0.02$). This relationship was not significant for any of the other architectures.

We pooled the data from multiple architectures into scaling modes to evaluate the overall relationship in colonies with a constant frontal area (linear, bipinnate, and helical species) and in colonies with scaling frontal area (transversal, whorl, cluster, and oblique species) with linear regressions (Fig. 1). This aggregation allowed the inclusion of data from architectures for which we only have one specimen (helical and oblique). When pooled by scaling mode (Fig. 5), the regression on colonies with a constant frontal area had a higher intercept on the swimming speed axis than in those with a scaling frontal area (1.54 and 1.09 zoid lengths/pulse, respectively), reflecting the generally higher swimming speed of the former. Moreover, the regression on colonies with constant frontal area had a significant positive slope ($n = 607$, $N = 71$, 10 species, Speed mm/s = $0.02 \times \text{Number of zooids} + 1.55$, adjusted $R^2 = 0.12$, $p < 0.001$), while the regression



382
 383 Figure 5. Linear relationships between relative swimming speed (zoid lengths per pulsation,
 384 specimen mean with standard errors) and number of zooids in the colony for constant (A) and
 385 scaling ($N=71$) (B) frontal motion-orthogonal frontal area ($N=29$) scaling modes. Gray areas
 386 represent the 95% confidence intervals of the regressions.
 387

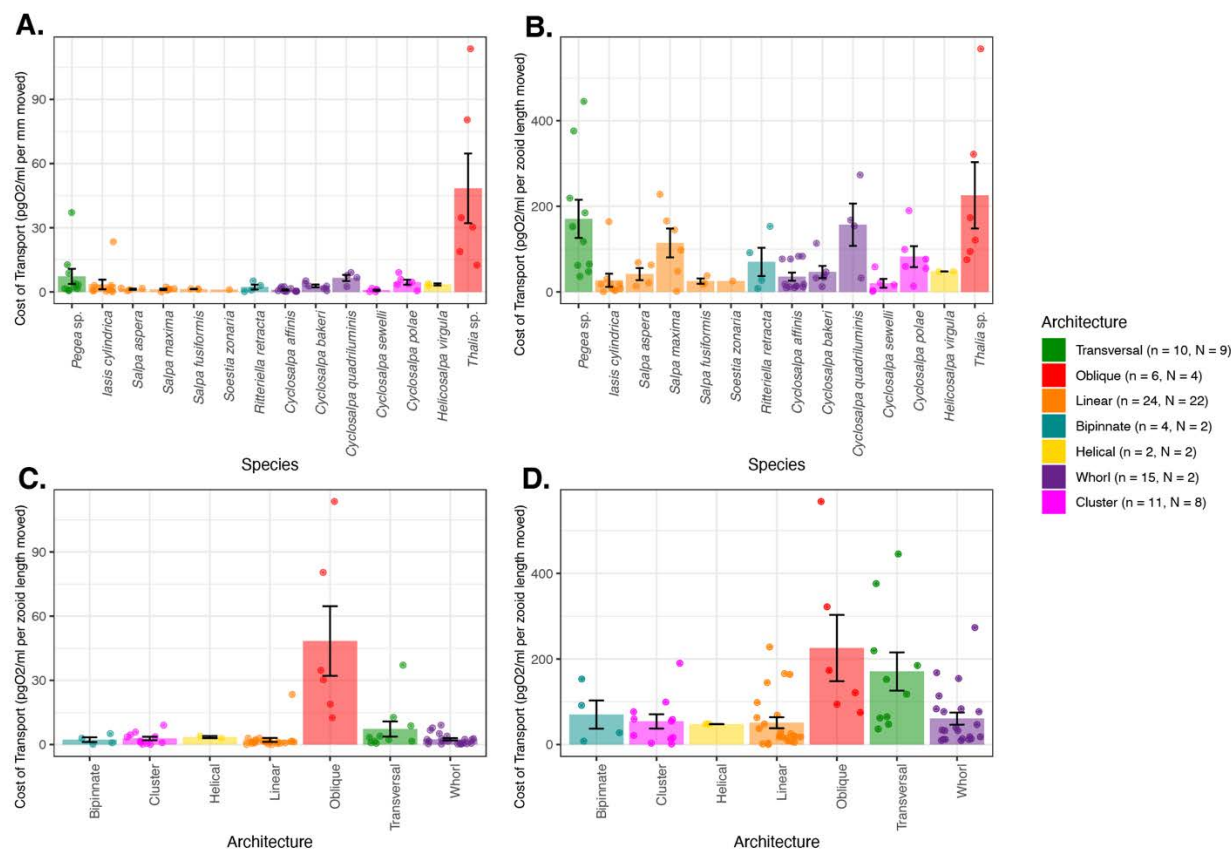
388 Putting together all the different organismal factors that we analyzed in this study, we
 389 calculated a generalized linear regression model to predict absolute salp swimming speed (U)
 390 from zooid length (L), pulsation rate (P), number of zooids (Z), and colonial architecture
 391 represented as frontal area scaling mode (A) as expressed in Eq. 3. While our results suggest
 392 that the effect of Z depends on A , we favored this simpler regression formula because it had a
 393 significantly lower ($\Delta > 70$) AIC score than those with interaction terms between Z and A .
 394 $U \sim L + P + Z + A$ Eq. 3

395 In this global model, we found significant effects on swimming speed (848 measurements,
 396 100 videos, 18 species, $U = 0.29L - 0.60P - 0.2Z - 50.34A$, $\text{pseudo-}R^2 = 0.37$, $p < 0.001$) for L ,
 397 Z , and A . We found that our global regression explains 36.8% of the variance in our swimming
 398 speed data: 5.8% is explained by zooid size, 3.5% by pulsation rate, 0.8% from zooid number,
 399 and 26.6% by the frontal scaling mode.
 400

401 *Respiration rates and cost of transport (COT)*

402 The respiration rates of swimming and anesthetized salps revealed broad differences
 403 between species (Fig. 6, S2A). After estimating COT, we found a few significant differences
 404
 405

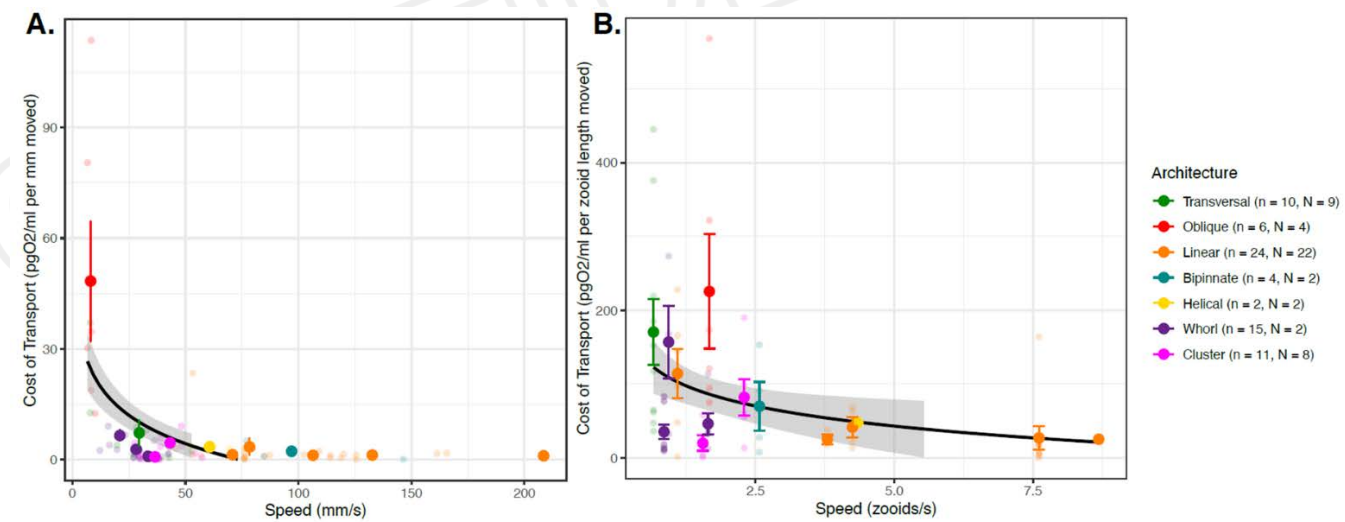
1
 2
 3
 4 404 between architectures (Fig. 6, ANOVA $F > 5.9$, $p < 0.001$, Table S2B). In terms of absolute COT
 5 per mm traveled, all architectures except oblique chains had similar high transport efficiencies
 6 under 13 pgO₂/ml. Every one of these architectures was significantly more efficient per mm
 7 traveled than oblique architectures (Tukey's $p < 0.001$). In terms of relative COT per zooid length
 8 traveled, linear chains, clusters, and whorls had similar transport efficiencies that are significantly
 9 faster than transversal and oblique chains (Tukey's $p < 0.05$). Some of the differences between
 10 COT per mm and COT per zooid length are likely due to scaling with body size, as can be
 11 observed with the relative shift in the minuscule *Thalia* sp. (5.2 mm zooids) and the massive *Salpa*
 12 *maxima* (93.4 mm zooids).



413
 414 Figure 6. Mean cost-of-transport per mm (A) and per zooid length (B) moved for each salp
 415 species, and for each colonial architecture (C, D) with standard errors. Bar colors indicate colonial
 416 architecture. Sample sizes and Tukey's post-hoc pairwise comparisons across architecture types
 417 are listed in Dataset 1B and Table S2B, respectively.

418
 419 When comparing the proportion of investment of metabolic costs into swimming
 420 (compared to the species mean baseline) across salp species (Fig. S2B), eight species had
 421 locomotion budgets under 50%, and the other seven have budgets above 50%. We then

1
 2
 3
 4 422 compared the proportion of energetic investment in swimming to the COT values across species
 5 423 (Fig. S3A,B). We found no relationship with absolute COT ($N = 74$, 14 species, $p = 0.24$). We
 6 424 found a positive relationship with zooid-length scaled COT ($N = 74$, 14 species, Swimming % =
 7 425 $0.11 \times \text{COT per zooid length} + 34.4$, adjusted $R^2 = 0.22$, $p < 0.001$), indicating that species with
 8 426 more costly locomotion per zooid length invest a larger proportion of their energy budget in
 9 427 swimming. Finally, we compared the proportion of energetic investment in swimming with speed
 10 428 (Fig. S3C,D). We found no relationship (neither in mm/s nor in zooids/s), indicating that faster
 11 429 swimmers do not invest more of their energy budget into their locomotion efforts. We found that
 12 430 regardless of whether we consider transport in terms of absolute distances (Fig. 7A, $N = 64$, 14
 13 431 species, linear regression: COT per mm = $-0.12 \times \text{Speed mm/s} + 13.46$, adjusted $R^2 = 0.09$, $p <$
 14 432 0.005 ; exponential regression: $\log\text{COT per mm} = -0.015 \times \text{Speed mm/s} + 1.39$, adjusted $R^2 = 0.14$,
 15 433 $p < 0.001$) or relative to body lengths (Fig. 7B, 64 specimens, 14 species, linear regression COT
 16 434 per zooid length = $-12.9 \times \text{Speed zooid lengths/s} + 116.1$, adjusted $R^2 = 0.07$, $p < 0.01$, exponential
 17 435 regression $\log\text{COT per zooid length} = -0.24 \times \text{Speed zooid lengths/s} + 4.28$, adjusted $R^2 = 0.14$ p
 18 436 < 0.001), the COT decreases in species with faster swimming speeds.
 19 437
 20 438



1
2
3
4 446 We compared the swimming speeds and costs of transport of salp colonies across the
5 most comprehensive representation of salp species diversity. Our results show a wide range of
6 colonial swimming speeds across salp species and architectures with linear species swimming
7 fastest (Fig. 3). Moreover, this study shows for the first time how salp colonial swimming speed
8 scales with the number of zooids in the colony (Fig. 5), suggesting that incremental propulsive
9 power from additional zooids does can produce higher swimming speeds for species with a
10 constant frontal area. Across species, salps have a low COT (Fig. 6) and as speed increases,
11 COT decreases (Fig. 7), which may be a unique advantage of multi-jet swimmers.
12
13 451
14 452
15 453
16 454
17 455
18 456
19 457
20 458
21 459
22 460
23 461
24 462
25 463
26 464
27 465
28 466
29 467
30 468
31 469
32 470
33 471
34 472
35 473
36 474
37 475
38 476
39 477
40 478
41 479
42
43
44
45
46
47
48
49
50
51
52
53
54
55
56
57
58
59
60
61
62
63
64
65

We compared the swimming speeds and costs of transport of salp colonies across the most comprehensive representation of salp species diversity. Our results show a wide range of colonial swimming speeds across salp species and architectures with linear species swimming fastest (Fig. 3). Moreover, this study shows for the first time how salp colonial swimming speed scales with the number of zooids in the colony (Fig. 5), suggesting that incremental propulsive power from additional zooids does can produce higher swimming speeds for species with a constant frontal area. Across species, salps have a low COT (Fig. 6) and as speed increases, COT decreases (Fig. 7), which may be a unique advantage of multi-jet swimmers.

Architectural determinants of salp swimming speed

Colonial architecture was the strongest predictor of swimming speed, though there is a large amount of unexplained variation which may relate to species-specific differences, behavioral, or environmental factors (see global GLM results). We expected that swimming speed in colonial salps would be predicted by pulsation rate as a measure of swimming effort. Our results indicate that this relationship only exists when accounting for zooid size (Fig. S1B), suggesting an underlying relationship between pulsation rate and zooid length that may be masking its predictive power over absolute speeds. This is consistent with the distribution of our data and our observations in the field where larger salps pulsate at a slower rate than smaller ones. We find a significant increase in speed with larger zooid sizes (Fig. S1C,D), consistent with previous findings of jet propelled invertebrates (Gemmell et al 2021; Bone and Trueman 1983) and more broadly across aquatic swimmers (Andersen et al. 2016).

The relationship between the number of zooids and speed in linear chains is complicated by shifts in zooid orientation during development. Salp colonies start their free-living phase when the developing buds detach from the solitary oozooid. The newly released colony has the maximum number of zooids since the zooid number only gets reduced as the colony splits or loses zooids to turbulence, disease, or predation. Therefore, colonies with higher numbers of zooids are typically composed of smaller, younger zooids. In linear architectures, these younger colonies could still be developing their dorsoventral rotation (Damian-Serrano & Sutherland 2023), thus effectively being more like oblique architecture. A less acute dorsoventral rotation angle would explain why these more numerous linear chains are not as fast as we would expect, given that our results support a significant relationship between this angle and swimming speed (Fig. 4). Finding a strong relationship between zooid number and speed in whorls was surprising given their less streamlined configuration (Fig. 5). This could be due to the smaller range of slow speeds and few zooids in the data we obtained for these species. Our regression results on pooled architectures, as well as finding a significant relationship between number of zooids and speed

1
2
3
4 480 for linear and bipinnate chains but not for clusters nor transversal chains, support our primary
5 hypothesis that the different frontal area scaling relationships across architectures has an impact
6 on swimming speed.
7
8

9 483 Linear chains swam faster than all other architectures, including those that share a
10 constant frontal area feature like bipinnate chains (Fig. 3, Table S2). One potential explanation
11 for this difference could come from the relative thrust provided by the jets. Linear chains eject
12 their jet plumes at very small angles (near parallel) to the axis of locomotion (Sutherland et al.
13 16 486 2024), just wide enough to avoid interaction between jet plumes (Sutherland & Weihs 2017).
17 487 Bipinnate and helical chains (both with constant frontal area) have the atrial siphons (point of jet
18 488 ejection) of their constituent blastozooids oriented at a wider angle (Madin 1990), which may lead
19 489 to wider angles of their jets relative to the axis of locomotion. This in turn would result in a larger
20 490 proportion of the force exerted by the jet to be applied as torque rather than thrust onto the colony.
21 491 This hypothesis could be tested by measuring the 3D angles of the actual jets instead of the
22 492 angles of the zooids since salps can use their atrial muscles and siphon morphology to direct the
23 493 angle of their jets.
24 494

25 495 Finding that clusters can swim at speeds comparable to those of bipinnate and helical
26 496 chains, even faster than whorls, defies our intuitive understanding of the mechanical properties
27 497 of these colonies and thus warrants further investigation into how these species coordinate their
28 498 jets to produce forward thrust. While oblique chains are architectural intermediates between
29 499 transversal and linear chains (Damian-Serrano & Sutherland 2023), our data indicate that oblique
30 500 chains may be the slowest swimmers among salps. This incongruence may be explained by the
31 501 fact that we only had speed data from one oblique specimen (of *Thalia* sp.) with very small zooid
32 502 sizes. Small salps might operate at notably lower Reynolds numbers than large ones, which may
33 503 require a non-linear size correction for meaningful speed comparisons. Swimming speed data
34 504 from the much larger oblique chains of *Thetys vagina* may provide a more comparable example
35 505 of the locomotory performance of this oblique colonial configuration.
36

37 506 The questions addressed in this study focus on the effect of frontal area of colonial
38 507 architectures on swimming speed. This effect may be associated with form and pressure drag
39 508 differences between more and less streamlined colony shapes. To test whether these are the
40 509 forces responsible for differences in swimming speed, drag would have to be measured or
41 510 calculated, which is beyond the scope of this study. Other unaccounted forces may be significant
42 511 energetic contributors to the system that explain the remainder of the observed variation. Chain
43 512 length for the streamlined forms (helical, linear, and bipinnate chains) could have negative effects
44 513 on swimming speeds that may partially counteract the positive effect of increased propeller thrust.
45
46
47
48
49
50
51
52
53
54
55
56
57
58
59
60
61
62
63
64
65

1
2
3
4 514 For example, skin drag increases proportionally to the surface area of the system, and the
5 smoothness of the chain may increase pressure drag through vortex shredding (Vogel 1981).
6 515 While added (virtual) mass could also be an issue, asynchronously swimming colonies do not
7 suffer as much from these acceleration-related costs, since their speed is maintained near
8 constant while cruising (Bone & Trueman 1983). Chain length could also lead to reduced stability
9 and efficiency, though some linear species capitalize on this by swimming in corkscrew orbital
10 spirals (Sutherland et al. 2024). However, if friction drag, chain stability, or vortex shredding were
11 indeed more important contributors than frontal form drag, we would predict that linear chains
12 would appear slower than other more stable and compact architectures. Future studies may
13 unravel these potential confounding effects on the biomechanics of colonial salp swimming.
14 521
15 522
16 523
17 524 *Salp swimming speed and diel vertical migration*
18 525
19 526
20 527
21 528
22 529
23 530
24 531
25 532
26 533
27 534
28 535
29 536
30
31
32
33
34
35
36
37
38
39
40
41
42
43
44
45
46
47
48
49
50
51
52
53
54
55
56
57
58
59
60
61
62
63
64
65

Salps are important players in the oceanic carbon cycle, grazing upon both phytoplankton and bacteria (Henschke et al. 2016). Their carcasses and fecal pellets export large quantities of fixed carbon into the deep sea, accelerating carbon sequestration in the biological carbon pump (Wiebe et al. 1979, Décima et al. 2023). Part of this process is enhanced by the diel vertical migrations by some salp species though the distribution of this behavior across species diversity is poorly known. Off Bermuda, Madin et al. (1996) reported *Pegea* spp., *B. rostrata*, and *C. polae* as non-migratory, all of which we found to have slow swimming speeds. Other slow-swimmer species like *C. affinis* were found to only migrate a few meters through the diel cycle. The species *S. aspera*, *S. fusiformis*, *S. zonaria*, *I. punctata*, and *R. retracta* have been observed vertically migrating off Bermuda (Madin et al 1996, Stone & Steinberg 2014), which is congruent with our observations during fieldwork. These species all have constant frontal area and fast swimming speeds.

Vertical migrators need to be fast enough to follow the dark isolumes as they shift during dawn and dusk in time to maximize their exploitation of the food resources near the surface. Thus, absolute speed is important to the autoecology of these animals. Other *Salpa* species have also been reported as strong vertical migrators throughout the literature (Henschke et al. 2021, Madin et al. 2006, Pascual et al. 2017). A species that does not fit this pattern is *I. cylindrica*, a fast-swimming non-migratory species that spends night and day near the surface (Madin et al 1996; and pers. obs.). However, other studies do report moderate diel vertical migration for this species (Stone & Steinberg 2014), so it may be adapted for facultative vertical migration under specific oceanographic conditions. Some migratory species, such as *S. aspera*, are known to travel distances of over 800m at dawn and dusk, at rates predicted to require 5-10 m/min (83-166 mm/s)

1
2
3
4 547 based on MOCNESS trawl intervals (Wiebe et al. 1979). These predictions are consistent with
5
6 548 the speeds we recorded for this species (88-145 mm/s) and similar congeners.
7
8 549 *Ecophysiological implications*

9 550 While the importance of a few well-studied linear chain salp species in the biological
10
11 551 carbon pump has been delineated, the question of whether this ecological role is generalizable to
12
13 552 other salp species remains unanswered. In addition to vertical migration behavior, another likely
14
15 553 important factor in their carbon flow is their respiration rate. The higher their respiration rate, the
16
17 554 larger the proportion of assimilated carbon that will be released back into the water as dissolved
18
19 555 carbon dioxide. This study provides the broadest taxonomic perspective on respiration rates (18
20
21 556 species, Fig. S2A) and swimming cost of transport (14 species), finding 17-fold differences in their
22
23 557 respiration rates and over 77-fold differences in their mean COT. Except for a few species with
24
25 558 extremely high and low values, most respiration rates are centered between 0.2 and 1
26
27 559 $\mu\text{mol/g/hour}$, assuming a salp tissue density of 1.025 g/ml. In general, the respiration rates we
28
29 560 estimated for salps are within the range of those reported in the literature (Trueblood 2019, Iguchi
30
31 561 and Ikeda 2004). Compared to the metabolic rates estimated for the broader diversity of marine
32
33 562 pelagic animals (Seibel & Drazen 2007), the rates that we measured for salps are in a similar
34
35 563 range to those measured for *Salpa thompsoni* (Iguchi and Ikeda 2004). Our values are also similar
36
37 564 to those measured by Seibel & Drazen (2007) in nemerteans, chaetognaths, and most fishes (0.1-
38
39 565 1 $\mu\text{molO}_2/\text{g/h}$), which are generally higher than other gelatinous animals like ctenophores or
40
41 566 scyphomedusae (0.01-0.1 $\mu\text{molO}_2/\text{g/h}$), but generally lower than those of cephalopods,
42
43 567 crustaceans, or large fish (1-10 $\mu\text{molO}_2/\text{g/h}$). Salp species known to have strong vertical migration
44
45 568 behaviors (*Salpa* spp., *S. zonaria*, *I. punctata*, and *R. retracta*) have low basal metabolic rates
46
47 569 (Fig. S2A) and low costs of transport. These results indicate that many non-migratory species,
48
49 570 while likely still being important players in the biological carbon pump via their fecal pellet
50
51 571 production, are releasing more of the consumed carbon as carbon dioxide near the surface than
52
53 572 their more metabolically efficient relatives. The ultimate ecological outcome of each species
54
55 573 needs to be assessed holistically, considering their microbial filtration and pellet deposition rate
56
57 574 as well as their relative abundance in the water column.

58
59 575 Our metabolically calculated costs of transport range between 5-50 J/kg/m when
60
61 576 converting the mg of oxygen to J via aerobic respiration free energy equations at 23°C. These
62
63 577 values are higher than the highly efficient 1-2 J/kg/m reported for salps in the literature (Bone &
64
65 578 Trueman 1983, Gemmell et al. 2021), and approach the less-efficient values found in single jet-
propelled invertebrates like scallops or squids. We suspect that COT calculated from mechanical
parameters such as the displacement of water mass is not directly comparable to the COT

1
2
3
4 581 calculated from respiration rates. Furthermore, the standard aerobic respiration free-energy
5 equation based on glucose may not fully represent the metabolic energy-conversion processes
6 in salps, which could rely on a combination of sugars and fatty acids derived from their
7
8
9
10

11 585 While COT increases with swimming speed fishes (Rubio-Gracia et al. 2020) and jet-
12 propelled squid (Bi & Zhu 2019), multi-jet swimmers may circumvent this tradeoff by having
13 multiple swimming units. In colonial siphonophores, as zooid number increases swimming speed
14 increases together with a decrease in COT (Du Clos et al. 2022). Our results show that faster
15 swimming species have lower COT (Fig. 6), which suggests that faster speeds and higher
16 locomotory efficiency have a common cause, where both speed and efficiency depend on frontal
17 area which may partly drive form and pressure drag forces. However, this hypothesis is not
18 supported by the distribution of COT across architectures (Fig 6C, D), where except for oblique
19 and transversal chains, all architectures present similarly efficient COT values. Perhaps there are
20 other underlying explanatory factors linking swimming speed and swimming efficiency, such as
21 shared ancestry, muscle content, jet coordination, or jetting angles (thrust-to-torque ratios).
22
23

24 596 *Evolutionary implications*
25
26

27 597 Across the evolutionary history of salps, linear chains have evolved multiple times
28 independently from oblique ancestors (Damian-Serrano et al. 2023), suggesting the adaptive role
29 of this architecture as a functional trait. Linear chain architectures evolved independently in *M.*
30 *hexagona*, *S. zonaria*, *I. punctata*, and before the common ancestor of *Iasis* and *Salpa*. Our results
31 show that going from an oblique form to a linear one may confer significant advantages in
32 locomotory speed and energetic efficiency. However, multiple colonial architectures, which we
33 find to be slower swimmers (such as transversal chains, helical chains, whorls, and clusters in
34 the genus *Pegea* and the Cyclosalpidae family) had also evolved from oblique and linear
35 ancestors. This is incongruent with a scenario where natural selection strongly favors locomotion
36 efficiency across all ecological niches of salps. Therefore, the evolution of colonial architecture
37 may be driven by ecological trade-offs with other non-locomotory functions. Alternatively, in some
38 of these lineages, locomotion at the colonial stage may not be important enough for selection to
39 maintain these highly streamlined forms, allowing for neutral evolutionary processes to produce
40 a diversity of non-adaptive forms. In the current study, we did not use phylogenetic comparative
41 methods in our analysis because like other investigators comparing biomechanical properties
42 across species (e.g. Dabiri et al. 2010, DiSanto et al. 2021) we were interested in inherent
43 mechanical relationships dictated by the colony architectures. For instance, a linear arrangement
44 of zooids inherently reduces drag due to a cluster arrangement, leading to faster swimming
45
46
47
48
49
50
51
52
53
54
55
56
57
58
59
60
61
62
63
64
65

1
2
3
4 615 speeds and potentially higher efficiency regardless of phylogenetic history. In other words, any
5 phylogenetic inertia is irrelevant in instantaneous relationships between traits (Felsenstein 1985).
6 616 Moreover, independence of data is often incorrectly assumed to be an assumption of standard
7 (nonphylogenetic) regressions (Uyeda et al. 2018), when in reality the assumptions relate to the
8 independence and distribution of the error terms. Thus, when all the phylogenetic signal is present
9 in the predictor, as it is in the case with colonial architecture (Damian-Serrano et al. 2022) and its
10 associated characteristics, there is no need for any “phylogenetic correction” (Uyeda et al. 2018).
11 619
12 620 However, there may be unaccounted factors explaining the residual variation in our analyses that
13 may bear phylogenetic signal. For example, tunic stiffness, tunic smoothness, muscle band
14 number, muscle fiber density, swimming behavior, as well as metabolic and physiological
15 baselines may be more similar between more closely related species, potentially erasing some of
16 the architecture-specific signal. Future studies could address the role of phylogeny and heritable
17 factors in salp swimming speed and cost of transport using phylogenetic comparative methods.
18 621 These analyses could reveal whether these factors have co-evolved with each other and/or with
19 respiration rate or colonial architecture.

20 622
21 623
22 624
23 625
24 626
25 627
26 628
27 629
28 630 *Insights for bioinspired underwater vehicle design*

29 631 Pulsatile jet propulsion is a promising avenue for bioinspired aquatic vehicles and robots
30 (Mohensi 2006, Gohardini 2014, Yue et al. 2015). Multijet propulsion systems with multiple
31 632 propellers akin to salp colonies have been explored in an engineering context (Chao et al. 2017,
32 633 Costello et al. 2015) with direct inspiration from gelatinous animals (Marut 2014, Krummel 2019,
33 634 Bi et al 2022, Du Clos et al. 2022). Salp diversity provides a natural laboratory to explore the
34 635 hydrodynamic implications of different multijet arrangement designs. Our findings underscore the
35 636 importance of considering the scaling hydrodynamic properties of propeller arrangements to
36 637 optimize speed and energy efficiency in bioinspired underwater vehicle design. While linear chain
37 638 arrangements were the fastest and among the most energy efficient, robot (or vehicle)
38 639 configurations such as a cluster form may confer unique object manipulation or maneuverability
39 640 advantages. Our results show that these seemingly inefficient propeller configurations do not
40 641 impose large disadvantages in terms of speed and fuel efficiency.

41 642
42 643 **Acknowledgments:**

43 644 We are grateful to the crew of Aquatic Life Divers, Kona Honu Divers for their assistance
44 645 and support in hosting our offshore diving operations. We also wish to thank Marc Hughes, Jeff
45 646 Milisen, Rebecca Gordon, Matt Connelly, Clint Collins, Paul Richardson, and Anne Thompson for
46 647 their assistance during diving, collections, and filming operations in the field. We would like to
47
48
49
50
51
52
53
54
55
56
57
58
59
60
61
62
63
64
65

1
2
3
4 648 thank Tiffany Bachtel for her valuable advice on the respirometry experiment design. We thank
5
6 649 the associate editor and two anonymous reviewers for their helpful comments.
7
8 650

9 651 **Funding**

10 652 This research was supported by the Gordon and Betty Moore Foundation [grant number
11 653 8835] and the Office of Naval Research [grant number N00014-23-1-2171].
12
13 654

14 655 **Data availability**

15 656 Data used to generate the results presented in this paper are available in the supplementary
16 657 information. Any other datasets used directly or indirectly for this study are available from the
17 658 authors upon reasonable request.
18

19 659 **Competing interests**

20 660 No competing interests declared.
21

22 661 **Literature cited**

23 662 Alexander, A. J. (1968). Forward Speed Effects on Annular Jet Cushions. *The Aeronautical
24 663 Journal*, 72(689), 438-441.
25

26 664 Andersen, K. H., Berge, T., Gonçalves, R. J., Hartvig, M., Heuschele, J., Hylander, S., ... &
27 665 Kiørboe, T. (2016). Characteristic sizes of life in the oceans, from bacteria to whales.
28 666 *Annual review of marine science*, 8(1), 217-241.
29

30 667 Bi, X., & Zhu, Q. (2019). Dynamics of a squid-inspired swimmer in free swimming. *Bioinspiration
31 668 & Biomimetics*, 15(1), 016005.
32

33 669 Bi, X., Tang, H., & Zhu, Q., 2022. Feasibility of hydrodynamically activated valves for 416 salp-
34 670 like propulsion. *Physics of Fluids*, 34(10), 101903.
35

36 671 Biggs, D. C. (1977). Respiration and ammonium excretion by open ocean gelatinous zooplankton
37 672 1. *Limnology and Oceanography*, 22(1), 108-117.
38

39 673 Bone, Q., Anderson, P. A. V., & Pulsford, A. (1980). Morphology of salp chain communication.
40 674 *Proceedings of the Royal Society of London. Series B. Biological Sciences*, 210(1181),
41 675 549-558.
42

43 676 Bone, Q., & Trueman, E. R. (1983). Jet propulsion in salps (Tunicata: Thaliacea). *Journal of
44 677 Zoology*, 201(4), 481-506.
45

46 678 Cetta, C. M., Madin, L. P., & Kremer, P. (1986). Respiration and excretion by oceanic salps.
47 679 *Marine Biology*, 91, 529-537.
48

49 680 Chao, S., Guan, G., & Hong, G. S., 2017, September. Design of a finless torpedo-shaped micro
50 681 AUV with high maneuverability. In OCEANS 2017-Anchorage (pp. 425 1-6). IEEE.
51

52 682 Colin, S. P., Gemmell, B. J., Costello, J. H., & Sutherland, K. R. (2022). In situ high-speed
53 683 brightfield imaging for studies of aquatic organisms. *Protocols.io*.
54

- 1
2
3
- 4 682 Costello, J. H., Colin, S. P., Gemmell, B. J., Dabiri, J. O., & Sutherland, K. R., 2015. 429 Multi-jet
5
6 683 propulsion organized by clonal development in a colonial siphonophore. 430 *Nature*
7
8 684 communications, 6(1), 8158.
- 9 685 Dabiri, J. O., Colin, S. P., Katija, K., & Costello, J. H. (2010). A wake-based correlate of
10
11 686 swimming performance and foraging behavior in seven co-occurring jellyfish species.
12
13 687 *Journal of experimental biology*, 213(8), 1217-1225.
- 14 688 Damian-Serrano, A., & Sutherland, K. R. (2023). A developmental ontology for the colonial
15
16 689 architecture of salps. *The Biological Bulletin*, 245(1), 9-18..
- 17 690 Damian-Serrano, A., Hughes, M., & Sutherland, K. R. (2023). A new molecular phylogeny of salps
18
19 691 (Tunicata: thalicea: salpida) and the evolutionary history of their colonial architecture.
20
21 692 *Integrative Organismal Biology*, 5(1), obad037.
- 22 693 Décima, M., Stukel, M. R., Nodder, S. D., Gutiérrez-Rodríguez, A., Selph, K. E., Dos Santos, A.
23
24 694 L., ... & Pinkerton, M. (2023). Salp blooms drive strong increases in passive carbon export
25
26 695 in the Southern Ocean. *Nature communications*, 14(1), 425.
- 27 696 Di Santo, V., Goerig, E., Wainwright, D. K., Akanyeti, O., Liao, J. C., Castro-Santos, T., & Lauder,
28
29 697 G. V. (2021). Convergence of undulatory swimming kinematics across a diversity of fishes.
30
31 698 *Proceedings of the National Academy of Sciences*, 118(49), e2113206118.
- 32 699 Du Clos, K. T., Gemmell, B. J., Colin, S. P., Costello, J. H., Dabiri, J. O., and Sutherland, K. R.
33
34 700 2022. Distributed propulsion enables fast and efficient swimming modes in physonect
35
36 701 siphonophores. *Proceedings of the National Academy of Sciences*. 119:e2202494119.
- 37 702 Felsenstein, J. (1985). Phylogenies and the comparative method. *The American
38
39 703 Naturalist*, 125(1), 1-15.
- 40
41 704 Gemmell, B. J., Dabiri, J. O., Colin, S. P., Costello, J. H., Townsend, J. P., & Sutherland, K. R.
42
43 705 (2021). Cool your jets: biological jet propulsion in marine invertebrates. *Journal of
44
45 706 Experimental Biology*, 224(12), jeb222083.
- 46 707 Gohardani, A. S. *Distributed Propulsion Technology* Nova Science Publishers (2014).
- 47
48 708 Haddock, S. H. (2004). A golden age of gelata: past and future research on planktonic
49
50 709 ctenophores and cnidarians. *Hydrobiologia*, 530, 549-556.
- 51 710 Haddock, S. H., & Heine, J. N. (2005). Scientific blue-water diving.
- 52
53 711 Hamner, W. M., Madin, L. P., Alldredge, A. L., Gilmer, R. W., & Hamner, P. P. (1975). Underwater
54
55 712 observations of gelatinous zooplankton: Sampling problems, feeding biology, and
56
57 behavior 1. *Limnology and Oceanography*, 20(6), 907-917.
- 58
59
60
61
62
63
64
65

- 1
2
3
- 4 714 Henschke, N., Cherel, Y., Cotté, C., Espinasse, B., Hunt, B.P. and Pakhomov, E.A., 2021. Size
5 and stage specific patterns in *Salpa thompsoni* vertical migration. *Journal of Marine*
6 Systems, 222, p.103587.
- 7 716
8 717 Krummel, G. M. (2019). Locomotion and Control of Cnidarian-Inspired Robots (Doctoral
9 dissertation, Virginia Tech).
- 10 718
11 719 Mackie, G. O. (1986). From aggregates to integrates: physiological aspects of modularity in
12 colonial animals. *Philosophical Transactions of the Royal Society of London. B, Biological*
13 Sciences, 313(1159), 175-196.
- 14 720
15 721
16 722 Madin, L. P. (1990). Aspects of jet propulsion in salps. *Canadian Journal of Zoology*, 68(4), 765-
17 723 777.
- 18 724 Madin, L. P., & Deibel, D. (1998). Feeding and energetics of Thaliacea. *The biology of pelagic*
19 725 *tunicates*, 81-104.
- 20 726 Madin, L. P., Kremer, P., & Hacker, S. (1996). Distribution and vertical migration of salps
21 (Tunicata, Thaliacea) near Bermuda. *Journal of Plankton Research*, 18(5), 747-755.
- 22 727
23 728 Madin, L.P., Kremer, P., Wiebe, P.H., Purcell, J.E., Horgan, E.H. and Nemazie, D.A., 2006.
24 729 Periodic swarms of the salp *Salpa aspera* in the Slope Water off the NE United States:
25 Biovolume, vertical migration, grazing, and vertical flux. *Deep Sea Research Part I:*
26 730 Oceanographic Research Papers, 53(5), pp.804-819.
- 27 731
28 732 Marut, K. J. (2014). Underwater Robotic Propulsors Inspired by Jetting Jellyfish (Doctoral
29 dissertation, Virginia Tech).
- 30 733
31 734 Mayzaud, P., Boutoute, M., Gasparini, S., Mousseau, L., & Lefevre, D. (2005). Respiration in
32 marine zooplankton—the other side of the coin: CO₂ production. *Limnology and*
33 *Oceanography*, 50(1), 291-298.
- 34 735
35 736 Mohensi, K., 2006. Pulsatile vortex generators for low-speed maneuvering of small
36 482 underwater vehicles. *Ocean Eng.* 33, 2209–2223.
- 37 737
38 738 Pascual, M., Acuña, J.L., Sabatés, A., Raya, V. and Fuentes, V., 2017. Contrasting diel vertical
39 739 migration patterns in *Salpa fusiformis* populations. *Journal of Plankton Research*, 39(5),
40 740 pp.836-842.
- 41 741
42 742 R Core Team, R. (2021). R: A language and environment for statistical computing.
- 43 743 Rubio-Gracia, F., García-Berthou, E., Guasch, H., Zamora, L., & Vila-Gispert, A. (2020). Size-
44 744 related effects and the influence of metabolic traits and morphology on swimming
45 performance in fish. *Current Zoology*, 66(5), 493-503.
- 46 745
47
48
49
50
51
52
53
54
55
56
57
58
59
60
61
62
63
64
65

- 1
2
3
4 746 Schneider, G. (1992). A comparison of carbon-specific respiration rates in gelatinous and non-
5
6 747 gelatinous zooplankton: a search for general rules in zooplankton metabolism.
7
8 748 *Helgoländer Meeresuntersuchungen*, 46, 377-388.
9
10 749 Seibel, B. A., & Drazen, J. C. (2007). The rate of metabolism in marine animals: environmental
11
12 750 constraints, ecological demands and energetic opportunities. *Philosophical Transactions of the Royal Society B: Biological Sciences*, 362(1487), 2061-2078.
13
14 752 Stone, J. P., & Steinberg, D. K. (2014). Long-term time-series study of salp population dynamics
15
16 753 in the Sargasso Sea. *Marine Ecology Progress Series*, 510, 111-127.
17
18 754 Sutherland, K. R., & Weihs, D. (2017). Hydrodynamic advantages of swimming by salp chains.
19
20 755 *Journal of The Royal Society Interface*, 14(133), 20170298.
21
22 756 Sutherland, K. R., Damian-Serrano, A., Du Clos, K. T., Gemmell, B. J., Colin, S. P., Costello, J.
23
24 757 H. (2024). Spinning and corkscrewing of oceanic macroplankton revealed through in situ
25
imaging. *Science Advances* 10(20).
26
27 759 Sutherland, K. R., & Madin, L. P. (2010). Comparative jet wake structure and swimming
28
29 760 performance of salps. *Journal of Experimental Biology*, 213(17), 2967-2975.
30
31 761 Trueblood, L. A. (2019). Salp metabolism: temperature and oxygen partial pressure effect on the
32
33 762 physiology of *Salpa fusiformis* from the California Current. *Journal of Plankton Research*,
41(3), 281-291.
34
35 764 Trueman, E. R., Bone, Q., & Braconnor, J. C. (1984). Oxygen consumption in swimming salps
36
37 765 (Tunicata: Thaliacea). *Journal of Experimental Biology*, 110(1), 323-327.
38
39 766 Uyeda, J. C., Zenil-Ferguson, R., & Pennell, M. W. (2018). Rethinking phylogenetic comparative
40
methods. *Systematic Biology*, 67(6), 1091-1109.
41
42 768 Vogel, S. (1981). Life in moving fluids. *Princeton University Press*, Princeton, NJ.
43
44 769 Vogel, S. (2008). Modes and scaling in aquatic locomotion. *Integrative and Comparative Biology*,
45
46 770 48(6), 702-712.
47
48 771 Wiebe, P. H., Madin, L. P., Haury, L. R., Harbison, G. R., & Philbin, L. M. (1979). Diel vertical
49
50 772 migration by *Salpa aspera* and its potential for large-scale particulate organic matter
51
52 773 transport to the deep-sea. *Marine Biology*, 53, 249-255.
53
54 774 World Register of Marine Species (WoRMS). (2024). WoRMS Editorial Board. Accessed January
55
56 776 Yue, C. et al., 2015. Mechantronic system and experiments of a spherical underwater 510 robot:
57
58 SUR-II. *J. Intell. Robot Syst.* Doi:10.1007/s10846-015-0177-3.
59
60
61
62
63
64
65

Supplementary Material

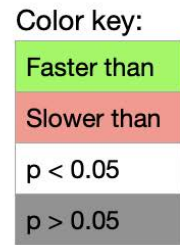
Dataset S1. (A) Salp video specimens analyzed with video specifications, as well as mean morphological and kinematic attributes. (B) Salp specimens used in the respirometry experiments with mean physiological attributes. (Please see attached file.)

Table S1. Summary of numbers of specimens (N), number of measurements (n), and descriptive variable averages per species including both the video speed data and the respiration experiments data.

Species	Architecture	Speed Measurements from Videos						Respiration Measurements from Experiments				
		Mean Number of zooids	Mean zoid length (mm)	Mean Pulsation rate (pulses/s)	Mean swimming speed (mm/s)	N	n	Mean Number of zooids	Mean zoid length (mm)	Mean Colony volume (ml)	N	n
<i>Brookia rostrata</i>	Bipinnate	26	7.4	2.6	34.4	5	45	20.3	6.5	3.7	16	130
<i>Ritterellia amboinensis</i>	Bipinnate	18	25.6	1.9	42.5	9	77	12.7	22.1	8.0	7	44
<i>Ritterellia sp.</i>	Bipinnate	33	21.3	1.3	43.1	3	49	18.7	34.5	22.5	6	42
<i>Cyclosalpa polae</i>	Cluster	5	17.2	1.2	47.6	2	19	7.0	20.0	4.3	7	55
<i>Cyclosalpa sewelli</i>	Cluster	7	15.0	1.4	26.8	6	52	6.2	19.4	7.2	11	88
<i>Helicosalpa virgula</i>	Helical	60	11.5	3.3	49.9	1	7	66.0	14.0	14.8	2	13
<i>Iasis cylindrica</i>	Linear	43	8.9	3.6	61.1	32	308	26.8	10.5	6.5	15	103
<i>Ihlea punctata</i>	Linear	NA	NA	NA	NA	0	0	68	12	3.7	1	7
<i>Metcalflina hexagona</i>	Linear	18	26.8	2.4	109.6	9	105	16.0	28.0	22.0	1	7
<i>Salpa aspera</i>	Linear	9	28.3	2.1	114.3	7	57	16.2	32.0	9.1	6	42
<i>Salpa fusiformis</i>	Linear	16	17.2	3.0	57.2	8	74	13.0	17.7	2.1	7	47
<i>Salpa maxima</i>	Linear	2	61.6	0.7	55.9	4	34	3.6	87.8	27.8	8	52
<i>Soestia zonaria</i>	Linear	11	13.7	1.9	109.2	4	34	9.1	19.6	4.6	8	23
<i>Thalia sp.</i>	Oblique	29	3.5	4.5	5.8	1	28	18.6	5.9	0.3	7	53
<i>Pegaea sp.</i>	Transversal	12	31.0	1.7	20.3	2	18	13.1	43.2	29.2	13	91
<i>Cyclosalpa affinis</i>	Whorl	5	33.0	1.4	24.5	2	15	6.7	37.9	23.4	10	65
<i>Cyclosalpa bakeri</i>	Whorl	7	7.0	2.6	10.4	7	63	6.9	14.6	3.0	7	57
<i>Cyclosalpa quadriluminis</i>	Whorl	8	27.1	1.3	25.3	1	6	8.3	24.5	12.7	6	36

Table S2. Tukey's post-hoc pairwise comparisons from an ANOVA on (A) swimming speed and (B) COT across different colonial architectures reporting magnitude of difference and adjusted p-values.

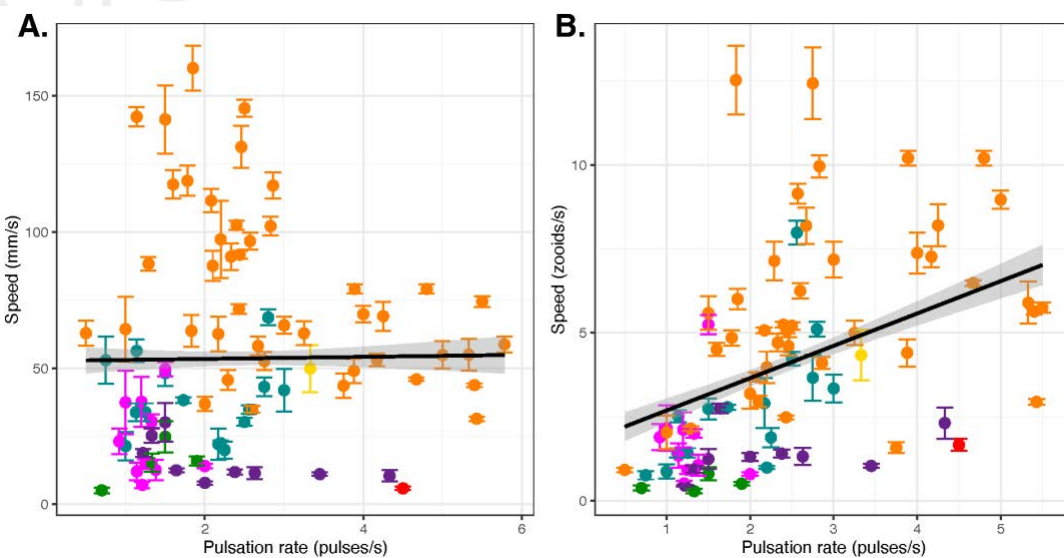
A.		Speed (mm/s)		Speed (zooids/pulse)	
Architecture		Difference	p-value adj.	Difference	p-value adj.
Cluster	Bipinnate	-12.900	0.005	0.082	0.991
Linear	Bipinnate	33.971	0.000	0.896	0.000
Transversal	Bipinnate	-22.314	0.002	-0.969	0.009
Whorl	Bipinnate	-25.559	0.000	-0.774	0.001
Linear	Cluster	46.871	0.000	0.814	0.000
Transversal	Cluster	-9.415	0.570	-1.050	0.006
Whorl	Cluster	-12.659	0.028	-0.856	0.000
Transversal	Linear	-56.286	0.000	-1.864	0.000
Whorl	Linear	-59.530	0.000	-1.670	0.000
Whorl	Transversal	-3.245	0.987	0.195	0.972



B.		COT per mm		COT per zooid length	
Architecture		Difference	p-value adj.	Difference	p-value adj.
Cluster	Bipinnate	0.558	1.000	-16.055	1.000
Linear	Bipinnate	-0.109	1.000	-19.013	0.999
Oblique	Bipinnate	46.132	0.000	155.555	0.099
Transversal	Bipinnate	4.999	0.979	100.580	0.429
Whorl	Bipinnate	0.180	1.000	-9.487	1.000
Linear	Cluster	-0.667	1.000	-2.958	1.000
Oblique	Cluster	45.574	0.000	171.610	0.005
Transversal	Cluster	4.441	0.954	116.636	0.049
Whorl	Cluster	-0.378	1.000	6.568	1.000
Oblique	Linear	46.241	0.000	174.567	0.001
Transversal	Linear	5.108	0.857	119.593	0.010
Whorl	Linear	0.289	1.000	9.526	0.999
Transversal	Oblique	-41.134	0.000	-54.974	0.849
Whorl	Oblique	-45.952	0.000	-165.042	0.003
Whorl	Transversal	-4.819	0.890	-110.067	0.026

Color key:

More efficient than
Less efficient than
p < 0.05
p > 0.05



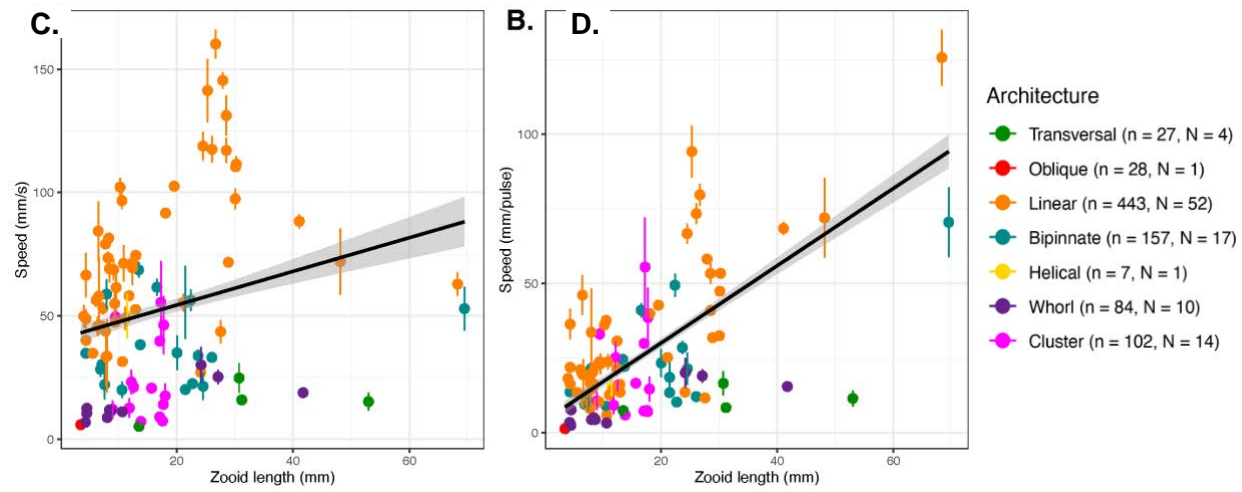
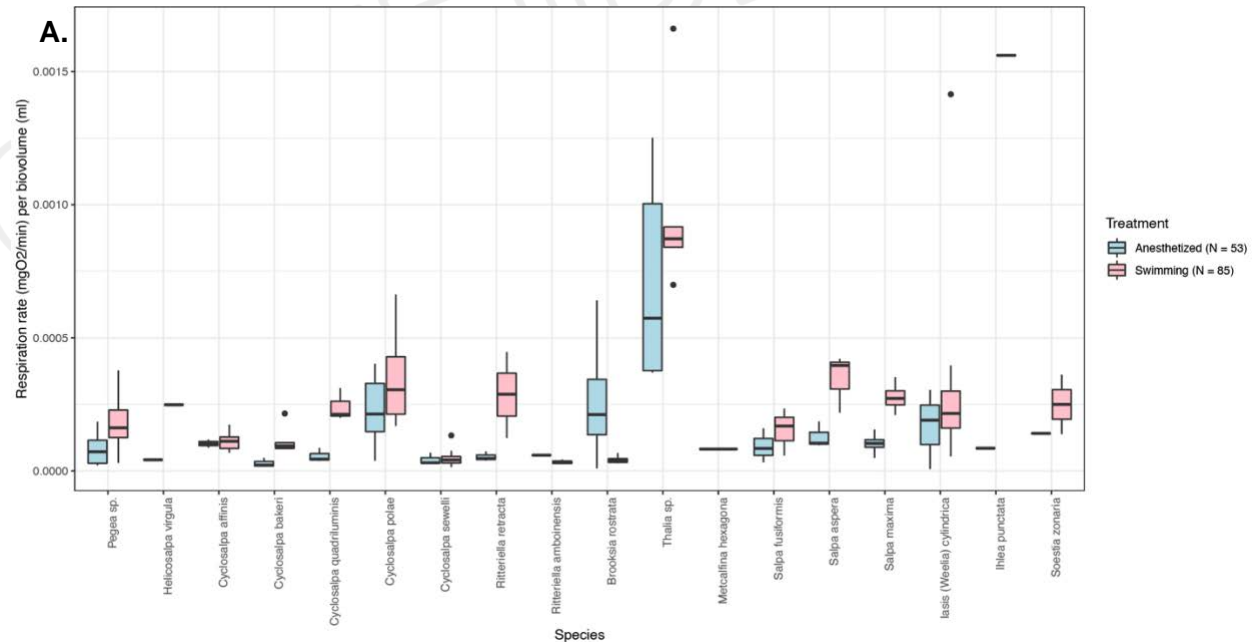


Figure S1. Salp swimming speeds. Distribution of salp colony absolute (A) and zooid size-corrected (B) swimming speed across pulsation rates. Distribution of salp colony absolute (C) and pulsation rate-corrected (D) swimming speed (specimen means with standard errors) across zooid sizes. Lines represent linear regressions with a 95% confidence interval shaded in grey.



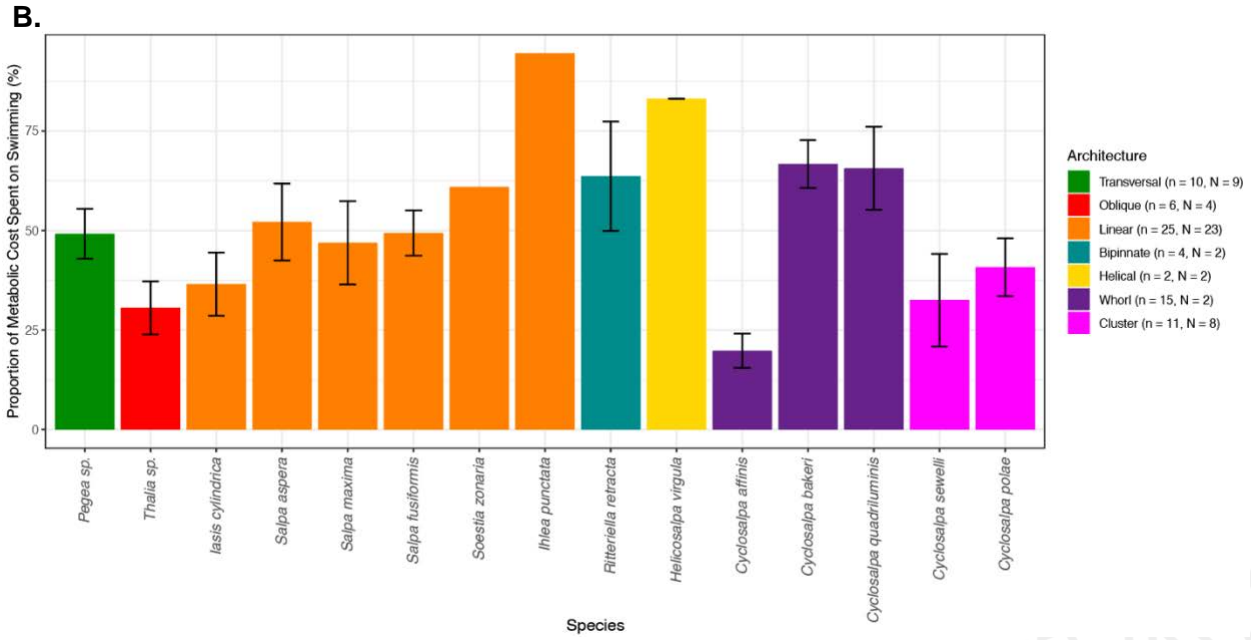
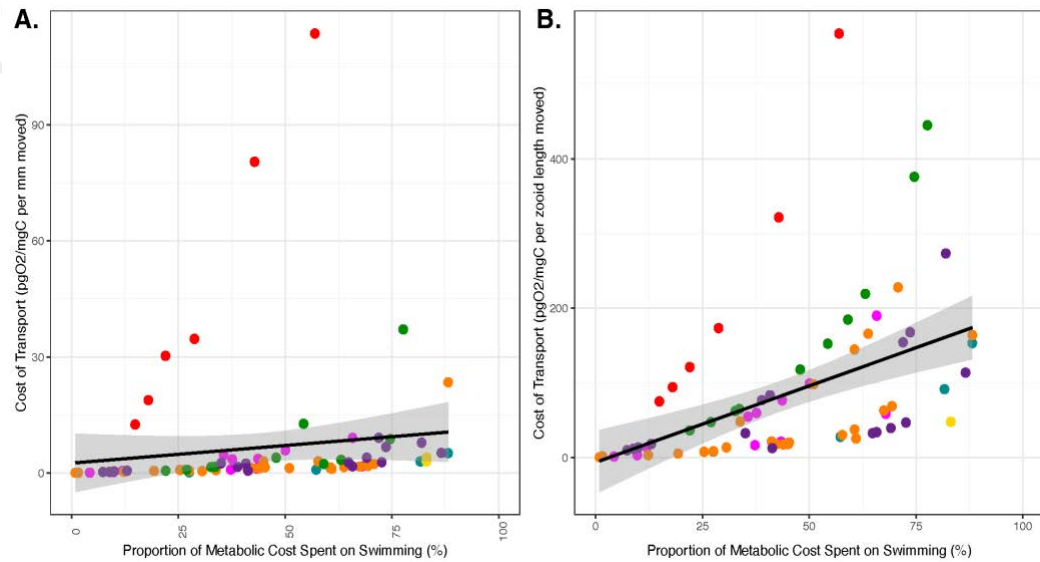


Figure S2. Respiration rates across salp species. (A) Biovolume-normalized respiration rates of swimming (red) and anesthetized (blue) salp colonies across different species. (B) Percentage of the swimming respiration rates matched by the mean anesthetized respiration rate for each salp species. Bars represent species means with black lines representing standard errors. Colors indicate colonial architecture.



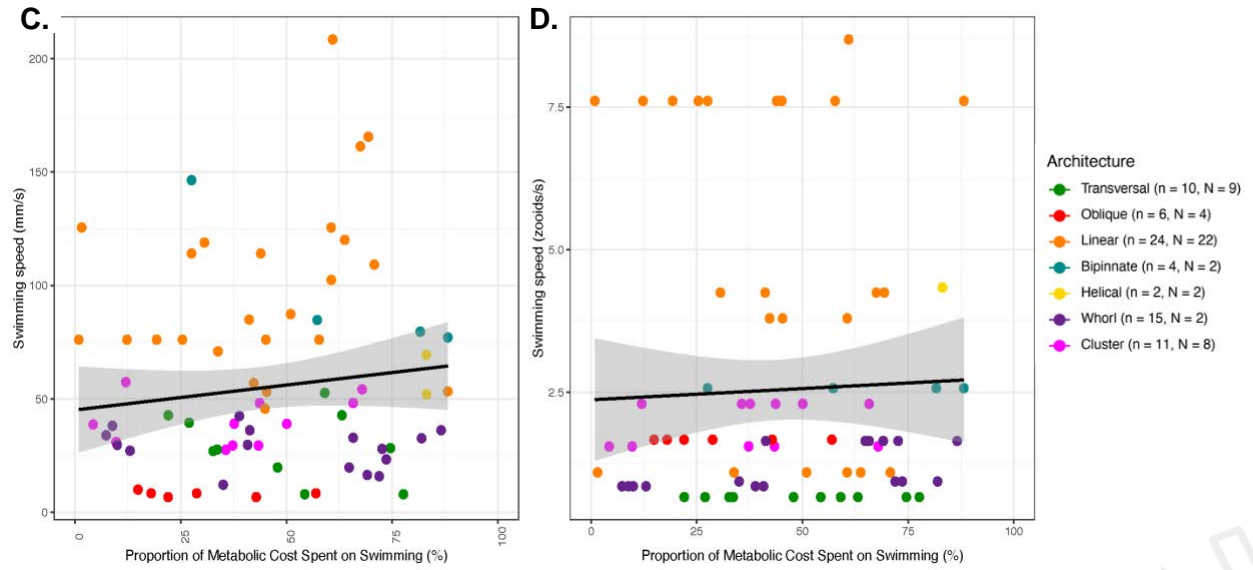


Figure S3. Proportion of metabolic cost spent on swimming. (A and B) Cost of transport (per mm in A, per zooid length in B) for each salp species across their percent swimming respiration rate matched by the species' mean anesthetized respiration rate. (C and D) Swimming speed (in mm/s in A, and zooids/s in B) for each salp species across their percent swimming respiration rate matched by the species mean anesthetized respiration rate. Point color indicates colonial architecture.

[Click here to access/download](#)

Supplementary Movies, Audio and Datasets
Dataset S1A.csv

[Click here to access/download](#)

Supplementary Movies, Audio and Datasets
Dataset S1B.csv

1 **Title: Colonial Architecture Modulates the Speed and
2 Efficiency of Multi-Jet Swimming in Salp Colonies**

3
4 **Authors:** Alejandro Damian-Serrano¹, Kai A. Walton¹, Anneliese Bishop-Perdue¹, Sophie
5 Bagoye¹, Kevin T. Du Clos², Bradford J. Gemmell³, Sean P. Colin^{4,5}, John H. Costello⁶, Kelly R.
6 Sutherland¹

7
8 **Author Affiliations:**
9
10 (1) Institute of Ecology and Evolution, Department of Biology, University of Oregon. 473 Onyx
11 Bridge, 5289 University of Oregon, Eugene, OR 97403-5289, USA.
12 (2) Louisiana Universities Marine Consortium, 8124 Highway 56, Chauvin, LA 70344, USA.
13 (3) Department of Integrative Biology, University of South Florida, 4202 East Fowler Avenue,
14 Tampa, FL 33620, USA.
15 (4) Marine Biology and Environmental Science, Roger Williams University, Bristol, RI 02809, USA.
16 (5) Whitman Center, Marine Biological Laboratory, Woods Hole, MA 02543, USA.
17 (6) Biology Department, Providence College, Providence, RI 02918, USA.

18
19 **Running title:** Architecture Modulates Salp Swimming

20
21 **Summary Statement (30 words)**

22
23 Linear arrangements in multi-jet propelled marine colonial invertebrates are faster than less
24 streamlined architectures without incurring in higher costs of transport, offering insights for
25 bioinspired underwater vehicle design.

26
27
28
29
30
31
32
33

34 **Abstract**

35

36 Salps are marine pelagic tunicates with a complex life cycle including a solitary and colonial stage.
37 Salp colonies are composed of asexually budded individuals that coordinate their swimming by
38 multi-jet propulsion. Colonies develop into species-specific architectures with distinct zooid
39 orientations. These distinct colonial architectures vary in how frontal area scales with the number
40 of zooids in the colony. Here, we address how differences in frontal area drive differences in
41 swimming speed and the relationship between swimming speed and cost of transport in salps.
42 We (1) compare swimming speed across salp species and architectures, (2) evaluate how
43 swimming speed scales with the number of zooids across colony in architectures, and (3)
44 compare the metabolic cost of transport across species and how it scales with swimming speed.
45 To measure swimming speeds, we recorded swimming salp colonies using in situ videography
46 while SCUBA diving in the open ocean. To estimate the cost of transport, we measured the
47 respiration rates of swimming and anesthetized salps collected in situ using jars equipped with
48 non-invasive oxygen sensors. We found that linear colonies swim faster, which supports idea that
49 their differential advantage in frontal area scales with an increasing number of zooids. We also
50 found that higher swimming speeds predict lower costs of transport in salps. These findings
51 underscore the importance of considering propeller arrangement to optimize speed and energy
52 efficiency in bioinspired underwater vehicle design, leveraging lessons learned from the diverse
53 natural laboratory provided by salp diversity.

54

55 **Keywords:** salps, colonial architecture, multi-jet propulsion, swimming, cost of transport

56

57 **Introduction**

58 Salps (Tunicata: Thaliacea: Salpida) are planktonic invertebrates that have a two-phase
59 life cycle comprised of a solitary oozooid that asexually buds colonies of sexually reproducing
60 blastozooids. Salp colonies are composed of up to hundreds of genetically identical, physically
61 and neurophysiologically integrated pulsatile zooids (Bone et al. 1980, Mackie 1986). Zooids in
62 the colony feed and propel themselves by drawing water in through the oral siphon, using muscle
63 contraction to compress their pharyngeal chamber, and ejecting a jet of water from their atrial
64 siphon (Bone & Trueman 1983). While solitary oozooids move using single-jet propulsion, salp
65 blastozooid colonies integrate multiple propelling jets, which increases their thrust and reduces
66 the drag that results from periodical acceleration and deceleration via asynchronous swimming
67 (Sutherland & Weihs 2017).

68 Currently, there are 48 described species of salps (WoRMS, 2024) and while salps are
69 widely distributed, most species are restricted to open ocean environments, far from the coast,
70 which poses unique challenges to accessing them for direct study in their environment (Hamner
71 et al 1975, Haddock 2004). Moreover, salps cannot be maintained alive in containers beyond a
72 few hours since they are extremely fragile and sensitive to the presence of solid walls. Therefore,
73 many morphological, ecological, and functional aspects of salp diversity, such as swimming
74 speeds and metabolic demands, have remained unexplored. One such aspect is colonial
75 architecture or the way that the zooids are arranged relative to each other in the colony. Salp
76 colonies develop into species-specific architectures with distinct zooid orientations, including
77 transversal, oblique, linear, helical, and bipinnate chains; as well as whorls, and clusters (Damian-
78 Serrano & Sutherland, 2023). These architectures likely drive aspects of swimming performance
79 (Madin 1990, Damian-Serrano et al. 2023).

80 Linear salp chains have been described as more efficient swimmers due to the reduction
81 of drag associated with a more streamlined form (Bone & Trueman 1983). In a multi-jet system,
82 having a larger number of propellers can improve the hydrodynamic and inertial benefits granted
83 by asynchronous multijet propulsion, in addition to providing additional thrust to the colony (Madin
84 1990, Sutherland & Weihs 2017). The effect of varying numbers of propeller zooids on swimming
85 speed has never been investigated in salps, nor how this relationship may vary across their
86 diverse colonial architectures. Salp colonial architectures differ in how the number of zooids in
87 the colony scales with their frontal area relative to motion (Madin 1990). Some architectures
88 (linear, bipinnate, and helical) have a constant frontal area, regardless of zooid number. These
89 architectures may benefit from increased thrust delivered by larger numbers of zooids while
90 maintaining a constant frontal area. However, the rest of the architectures (oblique, transversal,
91 whorl, and cluster) have an increasing (directly proportional) frontal area as the number of zooids
92 increases (Fig. 1). Therefore, we expect the latter architectures to not only obtain more thrust, but
93 to also experience more frontal water resistance as zooid number increases. As a result, we
94 anticipate that swimming speed will be greater in colonies that bear a larger number of zooids,
95 but only (or more so) for species with architectures that have a constant frontal area.

96

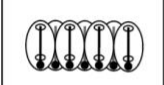
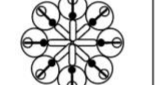
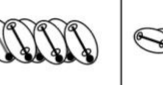
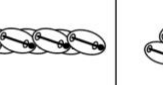
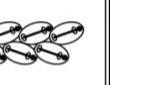
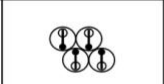
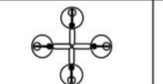
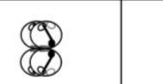
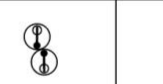
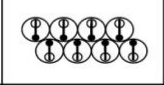
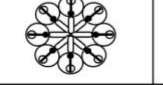
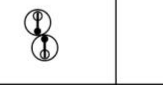
	Transversal	Whorl	Cluster	Helical	Oblique	Linear	Bipinnate
Architecture							
							
Frontal area 4 zooids							
Frontal area 8 zooids							
Scaling	2	2	2	1	1<<2	1	1

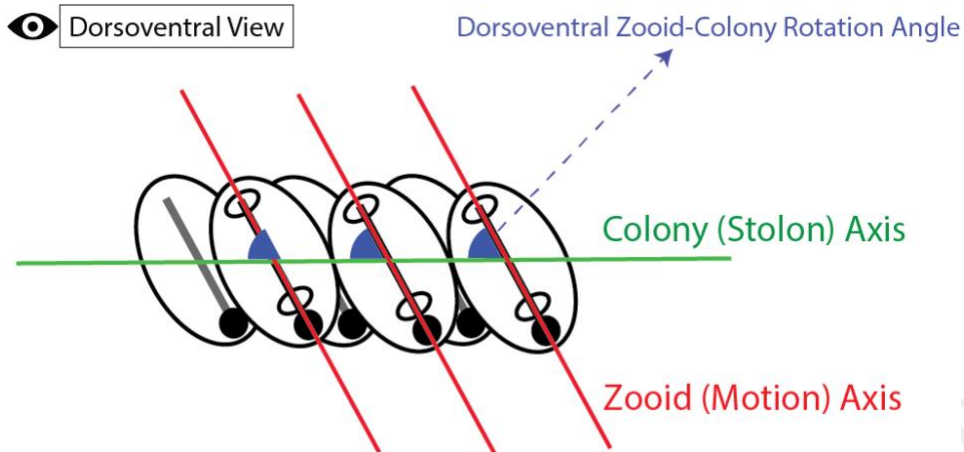
Figure 1. Salp colonial architectures with representative species photos (*Pegea* sp. for transversal, *Cyclosalpa affinis* for whorl, *Cyclosalpa sewelli* for cluster, *Helicosalpa virgula* for helical, *Thalia cicatricosa* for oblique, *Soestia zonaria* for linear, and *Ritterella retracta* for bipinnate) and diagrams showing the distinct zooid orientations. The subsequent rows show the frontal view of colonies with four and eight zooids, with the final row indicating the expected frontal area increase factor between the four and the eight zooid colonies. Full black circles in the diagrams represent viscerae (guts) while the open circle represent siphons. Black straight lines inside the zooids indicate gill bars while gray straight lines represent endostyles.

Linearity of colonies, as well as zooid size and pulsation rates, are additional factors that could influence swimming performance. The degree of linearity in a colony can be expressed as the degree of parallelism between the zooids and the elongation axis of the colony (Fig. 2). This angle is determined by the degree of developmental dorsoventral zooid rotation, which can span from 90°, in transversal chains with no rotation, to 0° (perfect linearity), in some linear chains such as those from the species *Soestia zonaria* (Damian-Serrano & Sutherland, 2023). Strong reductions in the dorsoventral zooid rotation angle toward linear forms have evolved multiple times independently (Damian-Serrano et al. 2023), possibly due to adaptive advantages related to their swimming efficiency. Body size predicts swimming velocity in many animals (Andersen et al. 2016), however colonies with multiple swimming units may circumvent this size-speed relationship by having multiple propellers. Pulsation rates may also influence swimming speed as has been shown in solitary salps (Madin 1990). Pulsation by salps serves the dual role of locomotion and filter feeding. The relationship between pulsation and speed might therefore be particularly relevant for species that undergo diel vertical migration (Madin et al. 1996) and in other species pulsation may serve to maximize filtration rates. Considering the tradeoffs between

121 swimming and filtering, the eco-evolutionary relevance of swimming speed, and the hydrodynamic
122 efficiency likely varies between species (Damian-Serrano et al. 2023).

123

124



125
126 Figure 2. Schematic of an oblique chain from the dorsoventral perspective showing the zooid and
127 stolon axes and the zooid rotation angle (degree of linearity) relative to those axes. Black lines
128 indicate gill bars (mostly occluded by zooid axis) while gray lines represent endostyles.

129 The energetic costs of salp locomotion from mechanically estimated propulsive efficiency
130 suggest that like other jet-propelled swimmers, salps are hydrodynamically efficient (Sutherland
131 & Madin 2010, Gemmell et al. 2021, Trueman et al. 1984). The few metabolic measurements of
132 swimming salps show that more active species-- in terms of swimming speed and pulsation rates--
133 have the highest respiration rates (Cetta et al. 1986) and that salps have higher respiration rates
134 than other gelatinous taxa (Biggs 1977, Schneider 1992, Mayzaud et al. 2005, Trueblood 2019).
135 However, the specific costs incurred by their swimming activity and their relationship to swimming
136 speed have never been examined across the diversity of salp species.

137 In this study, we compare swimming speeds across 17 salp species and energetic costs
138 of swimming across 15 species, encompassing all seven known salp colony architectures (Fig. 1,
139 Table S1). In addition, we investigate how swimming speed varies with the number of propeller
140 zooids and differences in frontal area scaling between colonial architectures. Finally, we compare
141 cost of transport (COT) across salp species and assess how COT scales with swimming speed
142 and pulsation effort.

143

144 Materials and Methods

145 *Fieldwork* – We observed salps via 48 bluewater SCUBA dives (Haddock & Heine, 2005)
146 from a small vessel off the coast of Kailua-Kona (Hawai'i Big Island, 19°42'38.7" N 156°06'15.8"
147 W), over 2000 m of offshore water during September 2021, April 2022, September 2022 and May
148 2023. We spent a total of 42.2 hours (84.4 person hours: ADS & KRS) collecting and imaging
149 salp colonies. Some dives were diurnal, where we collected most of the specimens of *Iasis*
150 *cylindrica*, *Cyclosalpa affinis*, *Cyclosalpa sewelli*, and *Brooksia rostrata*. We observed and
151 collected most specimens of other species during night dives (blackwater diving). We recorded in
152 situ underwater videos of salp colonies swimming using a variety of cameras including primarily
153 a dark field stereovideography system (Sutherland et al. 2024), as well as a lightweight dual
154 GoPro stereo system, a brightfield single-camera system (Colin et al. 2022), and a darkfield
155 single-camera system. The primary stereovideography system was comprised of two
156 synchronized high-resolution cameras (Z Cam E2, Nan Shan, Shenzhen, China and Sync Cable;
157 4K at 60 or 120 fps) with 17mm f/1.8 lenses (Olympus M.Zuiko Digital) housed in custom
158 aluminum housings (Sexton Company, Salem, OR, USA). Each field of view was 23 x 42 mm and
159 in-focus depth was 20-25 mm. The image from the right-hand camera was viewed using an
160 external monitor (Aquatica Digital, Montreal, Quebec, Canada), and illumination was provided
161 with two 10,000-lumen lights (Keldan, Bruegg, Switzerland). An L-shaped plastic framer helped
162 the videographer position colonies in the field of view of both cameras. Before diving, the stereo
163 system was calibrated in a swimming pool using a cube with reflective landmarks. Calibration
164 images were processed using the CAL software package (SeaGIS measurement science,
165 Bacchus Marsh, Victoria, Australia). Over the course of the study, we observed 241 salp colonies
166 (N) from 18 species and recorded 1,946 measurements (n) (Dataset1A, Table S1). Throughout
167 the manuscript, we refer to the number of specimens as N and the number of measurements as
168 n.

169 *Measuring salp colony swimming speed* – For most species, we collected and analyzed
170 footage from multiple specimens (Dataset1A, Table S1). We analyzed the swimming behavior of
171 salp colonies arranged in linear (six species, 64 specimens), bipinnate (three species, 17
172 specimens), whorl (three species, 10 specimens), cluster (two species, eight specimens), and
173 transversal (one species, two specimens) architectures, with oblique and helical architectures
174 represented by a single specimen. We used a combination of spatially calibrated stereo video
175 and 2D videos with a reference scale in the frame. From the stereo videos, we manually selected
176 and measured the relative XYZ positions of salp colony zooids in EventMeasure (SeaGIS). We
177 implemented a cutoff in the RMS (root mean squared) point error estimate of < 2 mm.

178 We complemented gaps in taxon sampling with archived 2D videos in the lab from
179 previous expeditions to West Palm Beach (FL, USA) and the Pacific coast of Panama. These two-
180 dimensional single-camera videos were collected using a Sony FDR-AX700 4K Camcorder
181 (3840x2160 pixels, 60-120 fps) with a Gates Underwater Housing (Poway, CA, USA) using
182 brightfield illumination (Colin et al 2022) or darkfield illumination. For these 2D videos, we used
183 the FFmpeg plugin in ImageJ to manually select and measure the relative XY positions of salp
184 zooids in sequences where the colony was swimming horizontally within the focal plane. The
185 colonies were assumed to be in the same plane as the scale bar so at same distance from the
186 camera. However, in videos with a broad focal depth, this may not always had been the case,
187 thus potentially introducing some measurement error.

188 We tracked and manually selected the position of the first zooid's viscera (using a contrast-
189 based centering macro to mark the center point) as well as the position of a reference particle in
190 the water (methods described in Sutherland et al. 2024) in 10-30 frames across 50-500 frame
191 windows spanning 2-4s of swimming on the synchronized left and right videos in EventMeasure.
192 The reference particle was a non-swimming organism (such as a foraminiferan or radiolarian) or
193 a non-living particle. In addition, we recorded the pulsation rates of the specimens measured by
194 counting the number of times the atrial siphon contracted in a known period. For each analyzed
195 frame, we calculated the horizontal x, vertical y, and depth z (in the case of the stereo video
196 measurement files) components of the relative positions of the frontal zooid to the reference
197 particle as shown in Eq. 1.

$$\begin{aligned} x &= n_{animal} - n_{particle} \\ y &= n_{animal} - n_{particle} \quad \text{Eq. 1} \\ z &= n_{animal} - n_{particle} \end{aligned}$$

203 Then we calculated the instantaneous relative speeds of the frontal zooid using Eq. 2
204 (without the z component in the case of the 2D videos) given the known frame rate of each video.
205

$$U = \frac{\sqrt{(x_2 - x_1)^2 + (y_2 - y_1)^2 + (z_2 - z_1)^2}}{t_2 - t_1} \quad \text{Eq. 2}$$

207
208 *Salp colonial architecture* – To examine the relationships between locomotory variables
209 and colonial architecture, we adopted the species-specific architecture characterizations and
210 dorsoventral zooid rotation angle measurements for each species from Damian-Serrano et al.

211 (2023). Using stills from the underwater videos, we measured zooid length, zooid width, and
212 number of zooids in ImageJ manually selecting the point coordinates. These measurements were
213 repeated in at least three locations from each colony. When a distinct zooid size gradient was
214 observed, we measured zooids in locations from the proximal, middle, and distal regions to
215 capture the full range of variation in the specimen.

216 *Respiration measurements* – We collected healthy, adult blastozooid (aggregate stage)
217 colonies across 18 salp species (Dataset S1B) during blue- and black-water SCUBA dives off the
218 coast of Kona (Hawaii, USA) between September 2021 and May 2023. We analyzed the
219 respiration rates of salp colonies arranged in linear (seven species, N = 46), bipinnate (three
220 species, N = 29), whorl (three species, N = 23), cluster (two species, N = 18), and transversal
221 (one species, N = 13) architectures, oblique chains (*Thalia* sp., N = 7), and helical architectures
222 represented by *Helicosalpa virgula* (N = 2). Specimens were sealed *in situ* with their surrounding
223 water in plastic jars equipped with a PreSens oxygen sensor spot (Regensburg, Germany) and a
224 self-healing rubber port to allow for the injection of solutions without the introduction of air bubbles.
225 We removed as many symbiotic animals from the salps as possible before closing the lid without
226 damaging the colony. The same method was applied to one or more seawater controls to account
227 for the oxygen demand of the local seawater's microbiome. Several collection events occurred
228 during each 20-60 min long SCUBA dive. Jars with larger animals were opened during the safety
229 stop to allow them to re-oxygenate. Upon the divers' return to the boat, we measured the initial
230 oxygen concentration (mg/l) and temperature, and then repeated the measurements at intervals
231 between 15min and 3h, for total periods ranging between 2h and 5h, depending on logistic
232 constraints in the field and the rate of oxygen depletion. The exact interval time for each
233 measurement was variable but recorded (Dataset S1B).

234 To estimate the energetic expenditure of different salp species while actively swimming,
235 we recorded the oxygen consumption of intact specimens while swimming inside the jar. To obtain
236 a baseline of basal respiration rate (while not swimming), we anesthetized some specimens
237 before the start of the first oxygen measurement time. A few specimens were used for paired
238 experiments, where their swimming respiration was recorded for a few hours, then inoculated with
239 the anesthetic, and recorded anesthetized for another set of hours. To anesthetize salps, we
240 injected their jars with small volumes of concentrated (50 g/l) bicarbonate-buffered MS-222
241 through the rubber ports on the lids. We tailored the injection volume to the jar size aiming for a
242 final concentration of 0.2g/l, following the methods in Trueman et al. (1984). We also injected
243 some seawater control jars to evaluate the effect of MS-222 on oxygen concentration in seawater
244 and found no effect.

When multiple seawater controls were collected using jars of different sizes, we paired each jar with the control that had the most similar volume. If among multiple controls only some were jars injected with anesthetic, we paired the anesthetized specimen jars with the injected controls and the intact specimen jars with the intact controls. In experiment 26 (see Dataset S1B for experiment numbers), the control jar was lost due to an encounter with an oceanic white tip shark, thus we paired those measurements with the nearest relative time points from the control jar in experiment 25, collected the same day hours earlier. At the end of each experiment, we identified the salp specimens used in the experiments to the species level, counted the number of zooids, measured the zooid length (total length including projections), and measured the biovolume of the colony using a graduated cylinder. For those specimens where colony or zooid volume was not measured directly, we estimated the colony volume from their zooid length and the number of zooids using a Generalized Additive Model with the measured specimens.

We estimated the oxygen consumption rate for each specimen by fitting a linear regression of consumed oxygen mass (concentration by container volume) against the duration of the measurement series. We subtracted the slope calculated for the relevant control jar to the estimated slope of the animal jar. Since our seawater controls were not filtered, some experiments had abnormally high estimated background respiration rates, leading to negative values. We removed these data points before the analysis. To estimate biovolume-specific rates, we divided the rates by the colony volumes. We then compared the biovolume-specific respiration rates of active (swimming) and anesthetized specimens within each species, calculating the difference as a measure of biovolume-specific swimming cost respiration rate. Biovolume was used instead of dry mass to normalize measurements due to the inherent difficulties of accurately measuring dry mass of these fragile gelatinous organisms in the field. Biovolume provides a consistent and reliable measure of the live size of the colony, which is directly relevant to the volume of water being displaced during swimming. We also calculated the relative investment in swimming as the proportion of biovolume-specific respiration rate comprised by the swimming-specific rate. To capture variability within species, we calculated the mean respiration rate of anesthetized specimens for each species and subtracted it from each intact specimen's total respiration rate to get multiple swimming-specific rate values within each species. We noticed that some species had higher average respiration rates among the anesthetized specimens than among the swimming specimens, leading to negative swimming-specific respiration estimates. We interpreted this anomaly as a systematic error due to the extremely low respiration rates of some species that fall within the effective detection limit of our experimental setup given the random variation range of respiration rates in seawater both in experimental jars and in control jars. Small

279 absolute negative values get amplified into large relative values, especially in small animals with
280 a minuscule biovolume denominator. Therefore, we removed the swimming specimens that had
281 lower respiration rates than the mean anesthetized respiration rate for their species. We also
282 removed two respirometry outliers of *Thalia* sp. which had extremely high swimming respiration
283 rates (>7500 pgO₂/ml/min, whereas all other measurements across species including other
284 *Thalia* sp. were limited to 0-1700 pgO₂/ml/min), which were likely due to amplification of
285 experimental error (presence of organic matter or symbionts, underestimation of colony volume
286 due to loss of tiny zooids in the sieves) with the small biovolume denominators in this species.

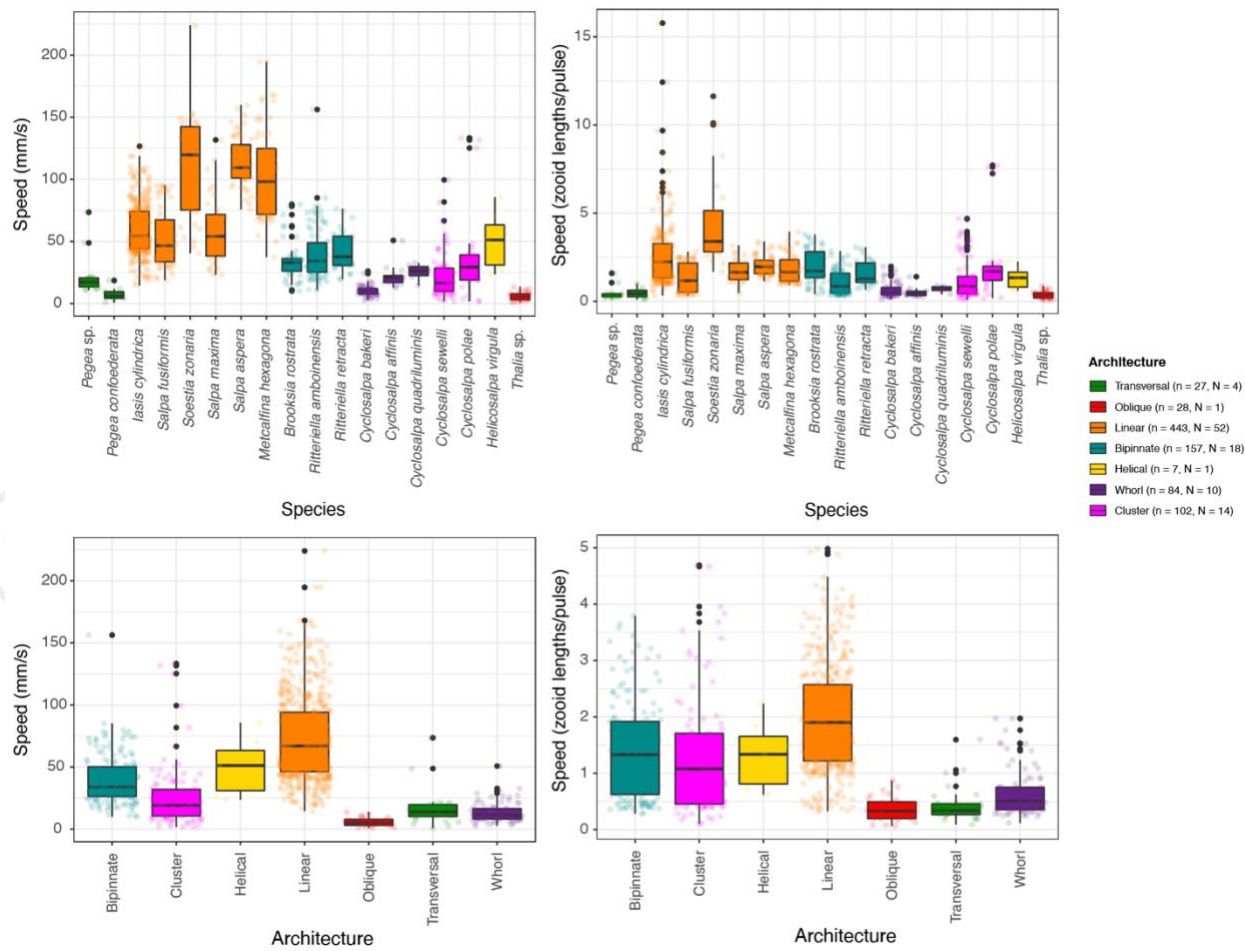
287 *Estimating costs of transport* – We define the cost of transport (COT) as the amount of
288 oxygen consumed per tissue volume per distance traveled by the colony. To estimate the COT,
289 we divided the swimming-specific respiration rates by the mean swimming speed for each species
290 measured from the stereo and 2D video data. Since the specimens used for speed measurements
291 in the videos and those used in the respirometry experiments had different zooid sizes, we used
292 the mean zooid-lengths per second speeds from the video measurements and then multiplied
293 them by the actual zooid lengths of the respirometry specimens to estimate their absolute (mm/s)
294 speeds. Pulsation rate estimates were taken from species averages from the video specimens.
295 We also calculated the size-specific COT by transforming the swimming distances into zooid
296 lengths measured from the respirometry specimens.

297 *Statistical Analyses* – All data wrangling and statistics were carried out in R 3.6.3 (R Core
298 Team 2021). To test for differences between architectures, we used ANOVAs with Tukey's post-
299 hoc pairwise contrasts, reporting the difference magnitude and the adjusted p-value in
300 supplementary tables S2A and S2B. To test the relationships between pairs of continuous
301 variables across architectures (e.g. swimming speed vs. number of zooids), we used linear
302 regressions. We evaluated the significance of the slope parameter when compared against a flat
303 slope (one-tailed t-test) to test whether changes in the independent variable (e.g. number of
304 zooids) were associated with changes in the dependent variable (e.g. swimming speed). Owing
305 to the patchiness of some species despite 80+ hours spent underwater (Table S1), we used
306 replicate measurements (n) from each specimen (N) in swimming speed ANOVAs and
307 regressions. We used an exponential regression to test the relationship between speed and COT.
308 Specimen means (N) were used for all COT comparisons and regressions. Individual
309 measurements (n) were used up to determine oxygen consumption rates. To evaluate the relative
310 contribution of zooid size, pulsation rate, zooid number, and architecture type on swimming
311 speed, we fitted a generalized linear model and evaluated the significance and proportion of
312 variance explained by each factor using their partial R².

313

314 **Results**

315 Salp colony swimming speeds, pulsation rates, and respiration rates varied within and
 316 across species and colony architectures. When considering speed in terms of mm/s, we found
 317 a relationship between pulsation rate (effort) and absolute speed ($n = 947$, $N = 111$, 18
 318 species, Speed mm/s = $0.41 \times$ Pulsation rate + 52.14, $p < 0.0001$, Fig. S1A), as well as with
 319 zoid-size corrected swimming speed ($n = 848$, $N = 100$, 18 species, Speed zoid lengths/s
 320 = $0.96 \times$ Pulsation rate + 1.73, adjusted $R^2 = 0.18$, $p < 0.0001$, Fig. S1B). Normalized swimming
 321 speeds (zoid lengths per pulse) allow for a more direct comparison of swimming speed across
 322 colonial architectures.



323

324 Figure 3. Boxplots showing the absolute (A) and corrected for body size and pulsation rate (B)
 325 swimming speeds recorded for each salp species and architecture (C, D) respectively. Colors
 326 correspond to colonial architecture types. Sample sizes are included in the legend and Tukey's

327 post-hoc pairwise comparisons across architecture types are listed in Dataset 1A and Table S2A,
328 respectively.

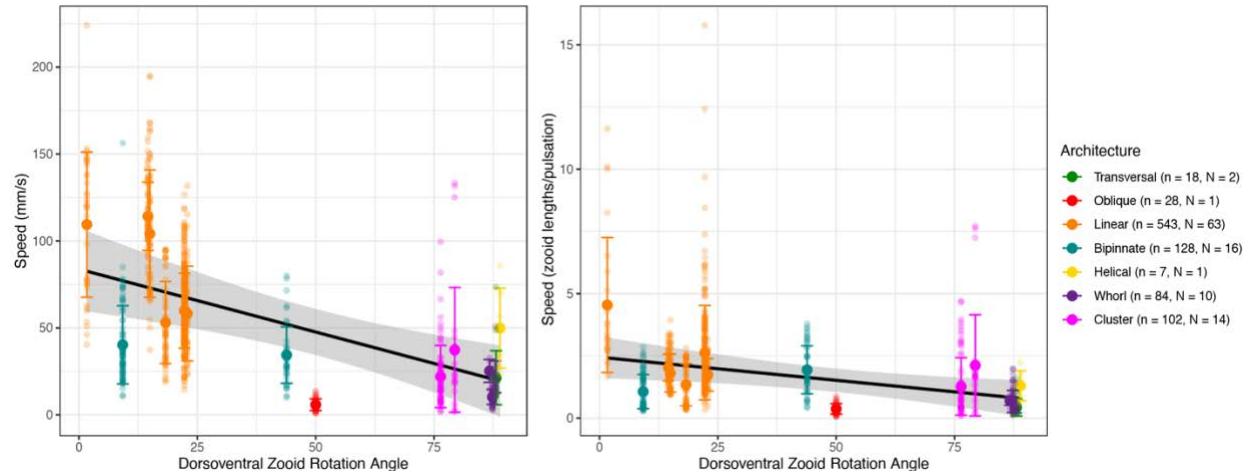
329

330 *Swimming speeds across salp architectures*

331 Swimming speed varied significantly (5 architectures, 16 species, N = 109, n = 913,
332 ANOVA F > 38, p < 0.001) between colonial architecture types (Fig. 3C, D, Table S2A). Speeds
333 measured with 2D methods were slightly slower than those measured with 3D methods within the
334 species in which they overlapped. This is to be expected since 2D methods cannot account for
335 the z (depth) component of the speed vector. Measurements of helical and oblique chains were
336 limited to a single specimen, so they were excluded from the analysis. In terms of absolute speed
337 (mm/s), linear architectures were significantly faster than every other architecture (Tukey's p <
338 0.001). While bipinnate chains were significantly slower than linear chains, they were significantly
339 faster than transversal chains, clusters, and whorls (Tukey's p < 0.002). Clusters were not
340 significantly faster than transversal chains nor whorls. Transversal chains were on par to whorls,
341 with no significant differences between them.

342 In terms of relative speed (zooid lengths/pulse), linear architectures were significantly
343 faster than every other architecture (Tukey's p < 0.001). Bipinnate chains were significantly faster
344 than whorls and transversal chains (Tukey's p < 0.01), but not significantly different from clusters.
345 Clusters were significantly faster than whorls (Tukey's p < 0.001) in relative speed. Whorls and
346 transversal chains presented similar relative swimming speeds with no significant differences.

347 Since linear architectures had the fastest mean swimming speeds (Fig. 3C, D), we
348 investigated the relationship between swimming speeds with the dorsoventral zooid rotation
349 angle, which represents the degree of linearity of the colony (Fig. 4). Species with more parallel
350 (lower angles) dorsoventral zooid rotation presented faster absolute speeds (n = 910, N = 107,
351 16 species, Speed mm/s = -0.78*DV Zooid angle + 81.25, adjusted R² = 0.33, p < 0.0001) and
352 faster size-and-effort corrected swimming speeds (n = 810, N = 96, 16 species, Speed
353 zooids/pulse = -0.016*DV Zooid angle + 2.37, adjusted R² = 0.09, p < 0.0001).

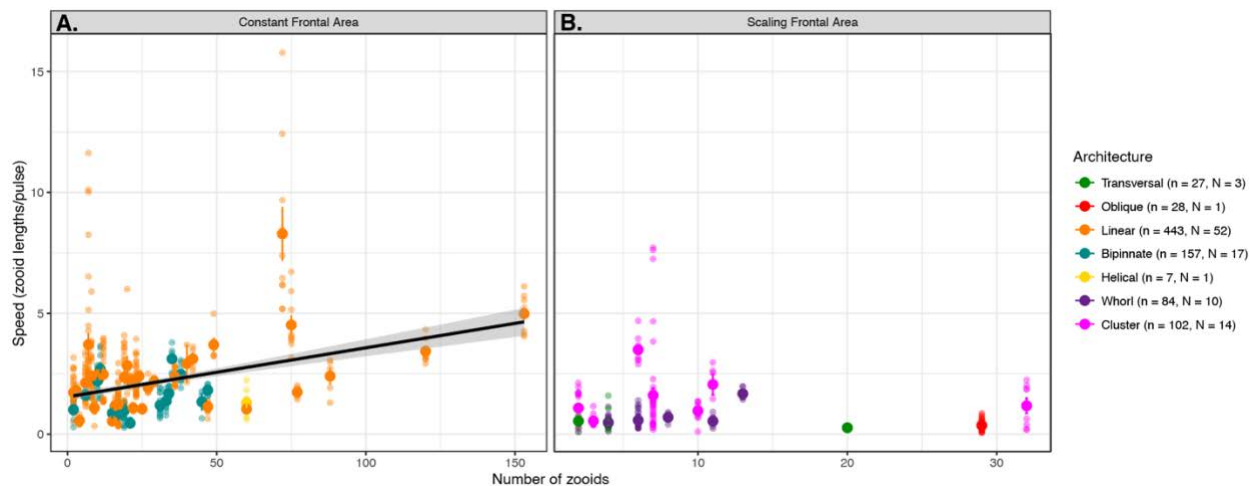


354
355 Figure 4. Absolute (A) and relative (B) colony swimming speed (specimen mean with standard
356 errors, total n=103) for each salp species across their degree of dorsoventral zooid rotation. Error
357 bars indicate standard error. The color indicates colonial architecture. Gray areas indicate the
358 95% confidence interval of the linear regression (black line).

359
360 We compared how swimming speeds scale with the number of zooids in the colony and
361 found differences between colonial architectures. Swimming speed in whorls increased with
362 number of zooids ($n = 84$, $N = 10$, 3 species, Speed mm/s = $0.08 \times \text{Number of zooids} + 0.12$,
363 adjusted $R^2 = 0.3$, $p < 0.0001$), though the data for this architecture was limited to small numbers
364 of zooids (4 to 13) and relatively slow speeds (under 51 mm/s). Linear chain architectures did
365 increase in relative speed with the number of zooids ($n = 443$, $N = 52$, 6 species, Speed mm/s =
366 $0.02 \times \text{Number of zooids} + 1.77$, adjusted $R^2 = 0.14$, $p < 0.001$), as did bipinnate chains ($n = 157$,
367 $N = 18$, 3 species, Speed mm/s = $0.015 \times \text{Number of zooids} + 1.05$, adjusted $R^2 = 0.04$, $p < 0.02$).
368 This relationship was not significant for any of the other architectures.

369 We pooled the data from multiple architectures into scaling modes to evaluate the overall
370 relationship in colonies with a constant frontal area (linear, bipinnate, and helical species) and in
371 colonies with scaling frontal area (transversal, whorl, cluster, and oblique species) with linear
372 regressions (Fig. 1). This aggregation allowed the inclusion of data from architectures for which
373 we only have one specimen (helical and oblique). When pooled by scaling mode (Fig. 5), the
374 regression on colonies with a constant frontal area had a higher intercept on the swimming speed
375 axis than in those with a scaling frontal area (1.54 and 1.09 zoid lengths/pulse, respectively),
376 reflecting the generally higher swimming speed of the former. Moreover, the regression on
377 colonies with constant frontal area had a significant positive slope ($n = 607$, $N = 71$, 10 species,
378 Speed mm/s = $0.02 \times \text{Number of zooids} + 1.55$, adjusted $R^2 = 0.12$, $p < 0.001$), while the regression

379 on those with scaling frontal area was not significant ($n = 241$, $N = 29$, 8 species, $p = 0.073$).
 380 However, the limited sample sizes for helical and oblique chains prevent us from drawing firm
 381 conclusions about these architectures.



382
 383 Figure 5. Linear relationships between relative swimming speed (zoid lengths per pulsation,
 384 specimen mean with standard errors) and number of zooids in the colony for constant (A) and
 385 scaling ($N=71$) (B) frontal motion-orthogonal frontal area ($N=29$) scaling modes. Gray areas
 386 represent the 95% confidence intervals of the regressions.

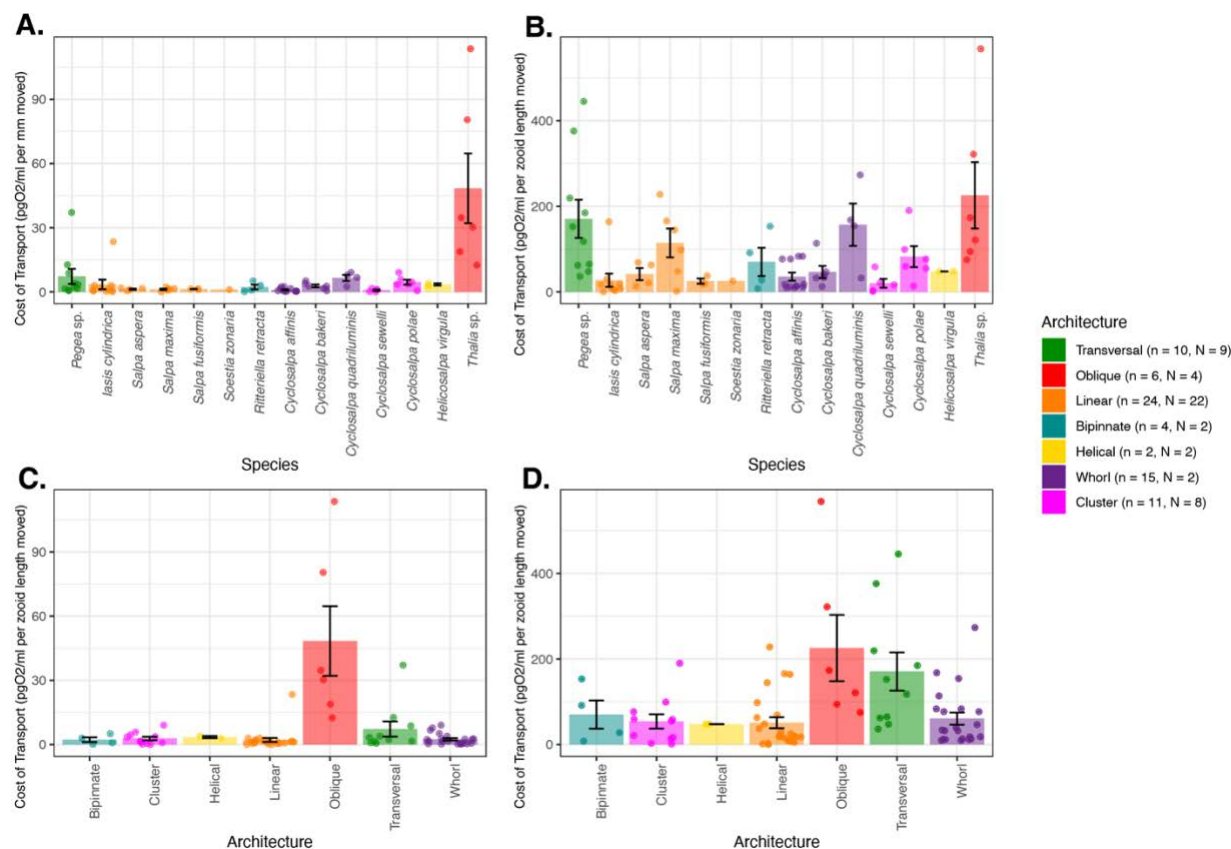
387
 388 Putting together all the different organismal factors that we analyzed in this study, we
 389 calculated a generalized linear regression model to predict absolute salp swimming speed (U)
 390 from zooid length (L), pulsation rate (P), number of zooids (Z), and colonial architecture
 391 represented as frontal area scaling mode (A) as expressed in Eq. 3. While our results suggest
 392 that the effect of Z depends on A , we favored this simpler regression formula because it had a
 393 significantly lower ($\Delta > 70$) AIC score than those with interaction terms between Z and A .

394
$$U \sim L + P + Z + A \quad \text{Eq. 3}$$

395 In this global model, we found significant effects on swimming speed (848 measurements,
 396 100 videos, 18 species, $U = 0.29L - 0.60P - 0.2Z - 50.34A$, $\text{pseudo-}R^2 = 0.37$, $p < 0.001$) for L ,
 397 Z , and A . We found that our global regression explains 36.8% of the variance in our swimming
 398 speed data: 5.8% is explained by zooid size, 3.5% by pulsation rate, 0.8% from zooid number,
 399 and 26.6% by the frontal scaling mode.

400
 401 *Respiration rates and cost of transport (COT)*
 402 The respiration rates of swimming and anesthetized salps revealed broad differences
 403 between species (Fig. 6, S2A). After estimating COT, we found a few significant differences

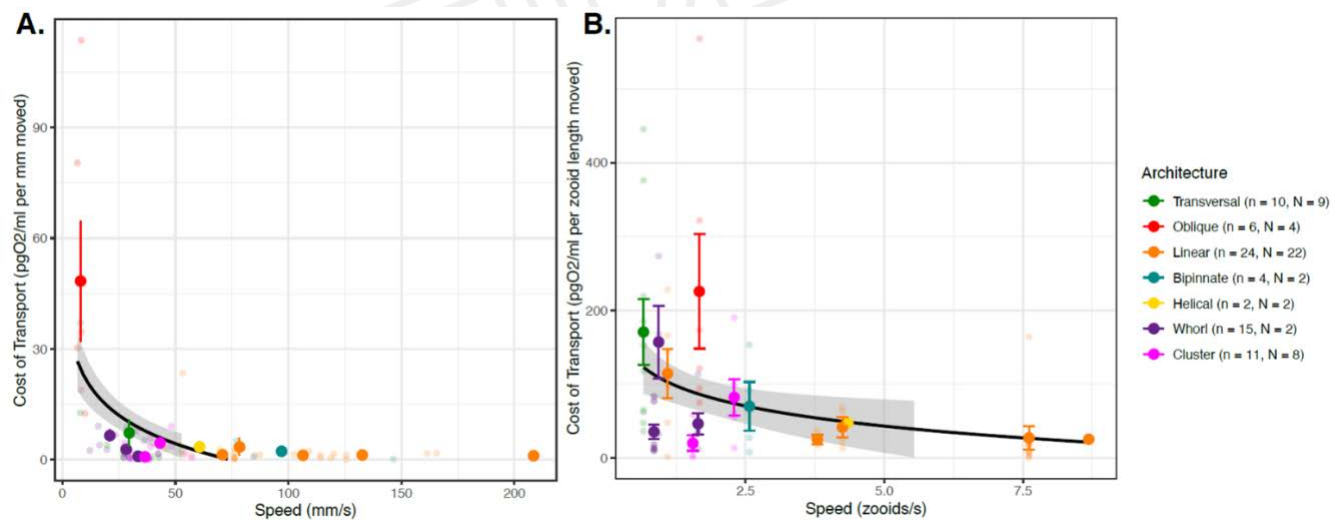
404 between architectures (Fig. 6, ANOVA $F > 5.9$, $p < 0.001$, Table S2B). In terms of absolute COT
 405 per mm traveled, all architectures except oblique chains had similar high transport efficiencies
 406 under 13 pgO₂/ml. Every one of these architectures was significantly more efficient per mm
 407 traveled than oblique architectures (Tukey's $p < 0.001$). In terms of relative COT per zooid length
 408 traveled, linear chains, clusters, and whorls had similar transport efficiencies that are significantly
 409 faster than transversal and oblique chains (Tukey's $p < 0.05$). Some of the differences between
 410 COT per mm and COT per zooid length are likely due to scaling with body size, as can be
 411 observed with the relative shift in the minuscule *Thalia* sp. (5.2 mm zooids) and the massive *Salpa*
 412 *maxima* (93.4 mm zooids).



413
 414 Figure 6. Mean cost-of-transport per mm (A) and per zooid length (B) moved for each salp
 415 species, and for each colonial architecture (C, D) with standard errors. Bar colors indicate colonial
 416 architecture. Sample sizes and Tukey's post-hoc pairwise comparisons across architecture types
 417 are listed in Dataset 1B and Table S2B, respectively.

418
 419 When comparing the proportion of investment of metabolic costs into swimming
 420 (compared to the species mean baseline) across salp species (Fig. S2B), eight species had
 421 locomotion budgets under 50%, and the other seven have budgets above 50%. We then

422 compared the proportion of energetic investment in swimming to the COT values across species
 423 (Fig. S3A,B). We found no relationship with absolute COT ($N = 74$, 14 species, $p = 0.24$). We
 424 found a positive relationship with zooid-length scaled COT ($N = 74$, 14 species, Swimming % =
 425 $0.11 \times \text{COT per zooid length} + 34.4$, adjusted $R^2 = 0.22$, $p < 0.001$), indicating that species with
 426 more costly locomotion per zooid length invest a larger proportion of their energy budget in
 427 swimming. Finally, we compared the proportion of energetic investment in swimming with speed
 428 (Fig. S3C,D). We found no relationship (neither in mm/s nor in zooids/s), indicating that faster
 429 swimmers do not invest more of their energy budget into their locomotion efforts. We found that
 430 regardless of whether we consider transport in terms of absolute distances (Fig. 7A, $N = 64$, 14
 431 species, linear regression: COT per mm = $-0.12 \times \text{Speed mm/s} + 13.46$, adjusted $R^2 = 0.09$, $p <$
 432 0.005; exponential regression: $\log\text{COT per mm} = -0.015 \times \text{Speed mm/s} + 1.39$, adjusted $R^2 = 0.14$,
 433 $p < 0.001$) or relative to body lengths (Fig. 7B, 64 specimens, 14 species, linear regression COT
 434 per zooid length = $-12.9 \times \text{Speed zooid lengths/s} + 116.1$, adjusted $R^2 = 0.07$, $p < 0.01$, exponential
 435 regression $\log\text{COT per zooid length} = -0.24 \times \text{Speed zooid lengths/s} + 4.28$, adjusted $R^2 = 0.14$ p
 436 < 0.001), the COT decreases in species with faster swimming speeds.
 437
 438



439
 440 Figure 7. COT (specimen mean with standard error, $n=75$) per mm (A) and zooid length (B) moved
 441 across the specimen mean absolute (A) or relative (B) swimming speeds. The dot color indicates
 442 colonial architecture. Gray areas represent the 95% confidence intervals of the exponential
 443 regressions (black lines).

444

445 Discussion

446 We compared the swimming speeds and costs of transport of salp colonies across the
447 most comprehensive representation of salp species diversity. Our results show a wide range of
448 colonial swimming speeds across salp species and architectures with linear species swimming
449 fastest (Fig. 3). Moreover, this study shows for the first time how salp colonial swimming speed
450 scales with the number of zooids in the colony (Fig. 5), suggesting that incremental propulsive
451 power from additional zooids does can produce higher swimming speeds for species with a
452 constant frontal area. Across species, salps have a low COT (Fig. 6) and as speed increases,
453 COT decreases (Fig. 7), which may be a unique advantage of multi-jet swimmers.

454 *Architectural determinants of salp swimming speed*

455 Colonial architecture was the strongest predictor of swimming speed, though there is a
456 large amount of unexplained variation which may relate to species-specific differences,
457 behavioral, or environmental factors (see global GLM results). We expected that swimming speed
458 in colonial salps would be predicted by pulsation rate as a measure of swimming effort. Our results
459 indicate that this relationship only exists when accounting for zooid size (Fig. S1B), suggesting
460 an underlying relationship between pulsation rate and zooid length that may be masking its
461 predictive power over absolute speeds. This is consistent with the distribution of our data and our
462 observations in the field where larger salps pulsate at a slower rate than smaller ones. We find a
463 significant increase in speed with larger zooid sizes (Fig. S1C,D), consistent with previous findings
464 of jet propelled invertebrates (Gemmell et al 2021; Bone and Trueman 1983) and more broadly
465 across aquatic swimmers (Andersen et al. 2016).

466 The relationship between the number of zooids and speed in linear chains is complicated
467 by shifts in zooid orientation during development. Salp colonies start their free-living phase when
468 the developing buds detach from the solitary oozooid. The newly released colony has the
469 maximum number of zooids since the zooid number only gets reduced as the colony splits or
470 loses zooids to turbulence, disease, or predation. Therefore, colonies with higher numbers of
471 zooids are typically composed of smaller, younger zooids. In linear architectures, these younger
472 colonies could still be developing their dorsoventral rotation (Damian-Serrano & Sutherland 2023),
473 thus effectively being more like oblique architecture. A less acute dorsoventral rotation angle
474 would explain why these more numerous linear chains are not as fast as we would expect, given
475 that our results support a significant relationship between this angle and swimming speed (Fig.
476 4). Finding a strong relationship between zooid number and speed in whorls was surprising given
477 their less streamlined configuration (Fig. 5). This could be due to the smaller range of slow speeds
478 and few zooids in the data we obtained for these species. Our regression results on pooled
479 architectures, as well as finding a significant relationship between number of zooids and speed

480 for linear and bipinnate chains but not for clusters nor transversal chains, support our primary
481 hypothesis that the different frontal area scaling relationships across architectures has an impact
482 on swimming speed.

483 Linear chains swam faster than all other architectures, including those that share a
484 constant frontal area feature like bipinnate chains (Fig. 3, Table S2). One potential explanation
485 for this difference could come from the relative thrust provided by the jets. Linear chains eject
486 their jet plumes at very small angles (near parallel) to the axis of locomotion (Sutherland et al.
487 2024), just wide enough to avoid interaction between jet plumes (Sutherland & Weihs 2017).
488 Bipinnate and helical chains (both with constant frontal area) have the atrial siphons (point of jet
489 ejection) of their constituent blastozooids oriented at a wider angle (Madin 1990), which may lead
490 to wider angles of their jets relative to the axis of locomotion. This in turn would result in a larger
491 proportion of the force exerted by the jet to be applied as torque rather than thrust onto the colony.
492 This hypothesis could be tested by measuring the 3D angles of the actual jets instead of the
493 angles of the zooids since salps can use their atrial muscles and siphon morphology to direct the
494 angle of their jets.

495 Finding that clusters can swim at speeds comparable to those of bipinnate and helical
496 chains, even faster than whorls, defies our intuitive understanding of the mechanical properties
497 of these colonies and thus warrants further investigation into how these species coordinate their
498 jets to produce forward thrust. While oblique chains are architectural intermediates between
499 transversal and linear chains (Damian-Serrano & Sutherland 2023), our data indicate that oblique
500 chains may be the slowest swimmers among salps. This incongruence may be explained by the
501 fact that we only had speed data from one oblique specimen (of *Thalia* sp.) with very small zooid
502 sizes. Small salps might operate at notably lower Reynolds numbers than large ones, which may
503 require a non-linear size correction for meaningful speed comparisons. Swimming speed data
504 from the much larger oblique chains of *Thetys vagina* may provide a more comparable example
505 of the locomotory performance of this oblique colonial configuration.

506 The questions addressed in this study focus on the effect of frontal area of colonial
507 architectures on swimming speed. This effect may be associated with form and pressure drag
508 differences between more and less streamlined colony shapes. To test whether these are the
509 forces responsible for differences in swimming speed, drag would have to be measured or
510 calculated, which is beyond the scope of this study. Other unaccounted forces may be significant
511 energetic contributors to the system that explain the remainder of the observed variation. Chain
512 length for the streamlined forms (helical, linear, and bipinnate chains) could have negative effects
513 on swimming speeds that may partially counteract the positive effect of increased propeller thrust.

514 For example, skin drag increases proportionally to the surface area of the system, and the
515 smoothness of the chain may increase pressure drag through vortex shredding (Vogel 1981).
516 While added (virtual) mass could also be an issue, asynchronously swimming colonies do not
517 suffer as much from these acceleration-related costs, since their speed is maintained near
518 constant while cruising (Bone & Trueman 1983). Chain length could also lead to reduced stability
519 and efficiency, though some linear species capitalize on this by swimming in corkscrew orbital
520 spirals (Sutherland et al. 2024). However, if friction drag, chain stability, or vortex shredding were
521 indeed more important contributors than frontal form drag, we would predict that linear chains
522 would appear slower than other more stable and compact architectures. Future studies may
523 unravel these potential confounding effects on the biomechanics of colonial salp swimming.

524 *Salp swimming speed and diel vertical migration*

525 Salps are important players in the oceanic carbon cycle, grazing upon both phytoplankton
526 and bacteria (Henschke et al. 2016). Their carcasses and fecal pellets export large quantities of
527 fixed carbon into the deep sea, accelerating carbon sequestration in the biological carbon pump
528 (Wiebe et al. 1979, Décima et al. 2023). Part of this process is enhanced by the diel vertical
529 migrations by some salp species though the distribution of this behavior across species diversity
530 is poorly known. Off Bermuda, Madin et al. (1996) reported *Pegea* spp., *B. rostrata*, and *C. polae*
531 as non-migratory, all of which we found to have slow swimming speeds. Other slow-swimmer
532 species like *C. affinis* were found to only migrate a few meters through the diel cycle. The species
533 *S. aspera*, *S. fusiformis*, *S. zonaria*, *I. punctata*, and *R. retracta* have been observed vertically
534 migrating off Bermuda (Madin et al 1996, Stone & Steinberg 2014), which is congruent with our
535 observations during fieldwork. These species all have constant frontal area and fast swimming
536 speeds.

537 Vertical migrators need to be fast enough to follow the dark isolumes as they shift during
538 dawn and dusk in time to maximize their exploitation of the food resources near the surface. Thus,
539 absolute speed is important to the autoecology of these animals. Other *Salpa* species have also
540 been reported as strong vertical migrators throughout the literature (Henschke et al. 2021, Madin
541 et al. 2006, Pascual et al. 2017). A species that does not fit this pattern is *I. cylindrica*, a fast-
542 swimming non-migratory species that spends night and day near the surface (Madin et al 1996;
543 and pers. obs.). However, other studies do report moderate diel vertical migration for this species
544 (Stone & Steinberg 2014), so it may be adapted for facultative vertical migration under specific
545 oceanographic conditions. Some migratory species, such as *S. aspera*, are known to travel
546 distances of over 800m at dawn and dusk, at rates predicted to require 5-10 m/min (83-166 mm/s)

547 based on MOCNESS trawl intervals (Wiebe et al. 1979). These predictions are consistent with
548 the speeds we recorded for this species (88-145 mm/s) and similar congeners.

549 *Ecophysiological implications*

550 While the importance of a few well-studied linear chain salp species in the biological
551 carbon pump has been delineated, the question of whether this ecological role is generalizable to
552 other salp species remains unanswered. In addition to vertical migration behavior, another likely
553 important factor in their carbon flow is their respiration rate. The higher their respiration rate, the
554 larger the proportion of assimilated carbon that will be released back into the water as dissolved
555 carbon dioxide. This study provides the broadest taxonomic perspective on respiration rates (18
556 species, Fig. S2A) and swimming cost of transport (14 species), finding 17-fold differences in their
557 respiration rates and over 77-fold differences in their mean COT. Except for a few species with
558 extremely high and low values, most respiration rates are centered between 0.2 and 1
559 $\mu\text{mol/g/hour}$, assuming a salp tissue density of 1.025 g/ml. In general, the respiration rates we
560 estimated for salps are within the range of those reported in the literature (Trueblood 2019, Iguchi
561 and Ikeda 2004). Compared to the metabolic rates estimated for the broader diversity of marine
562 pelagic animals (Seibel & Drazen 2007), the rates that we measured for salps are in a similar
563 range to those measured for *Salpa thompsoni* (Iguchi and Ikeda 2004). Our values are also similar
564 to those measured by Seibel & Drazen (2007) in nemerteans, chaetognaths, and most fishes (0.1-
565 1 $\mu\text{molO}_2/\text{g/h}$), which are generally higher than other gelatinous animals like ctenophores or
566 scyphomedusae (0.01-0.1 $\mu\text{molO}_2/\text{g/h}$), but generally lower than those of cephalopods,
567 crustaceans, or large fish (1-10 $\mu\text{molO}_2/\text{g/h}$). Salp species known to have strong vertical migration
568 behaviors (*Salpa* spp., *S. zonaria*, *I. punctata*, and *R. retracta*) have low basal metabolic rates
569 (Fig. S2A) and low costs of transport. These results indicate that many non-migratory species,
570 while likely still being important players in the biological carbon pump via their fecal pellet
571 production, are releasing more of the consumed carbon as carbon dioxide near the surface than
572 their more metabolically efficient relatives. The ultimate ecological outcome of each species
573 needs to be assessed holistically, considering their microbial filtration and pellet deposition rate
574 as well as their relative abundance in the water column.

575 Our metabolically calculated costs of transport range between 5-50 J/kg/m when
576 converting the mg of oxygen to J via aerobic respiration free energy equations at 23°C. These
577 values are higher than the highly efficient 1-2 J/kg/m reported for salps in the literature (Bone &
578 Trueman 1983, Gemmell et al. 2021), and approach the less-efficient values found in single jet-
579 propelled invertebrates like scallops or squids. We suspect that COT calculated from mechanical
580 parameters such as the displacement of water mass is not directly comparable to the COT

581 calculated from respiration rates. Furthermore, the standard aerobic respiration free-energy
582 equation based on glucose may not fully represent the metabolic energy-conversion processes
583 in salps, which could rely on a combination of sugars and fatty acids derived from their
584 microscopic prey.

585 While COT increases with swimming speed fishes (Rubio-Gracia et al. 2020) and jet-
586 propelled squid (Bi & Zhu 2019), multi-jet swimmers may circumvent this tradeoff by having
587 multiple swimming units. In colonial siphonophores, as zooid number increases swimming speed
588 increases together with a decrease in COT (Du Clos et al. 2022). Our results show that faster
589 swimming species have lower COT (Fig. 6), which suggests that faster speeds and higher
590 locomotory efficiency have a common cause, where both speed and efficiency depend on frontal
591 area which may partly drive form and pressure drag forces. However, this hypothesis is not
592 supported by the distribution of COT across architectures (Fig 6C, D), where except for oblique
593 and transversal chains, all architectures present similarly efficient COT values. Perhaps there are
594 other underlying explanatory factors linking swimming speed and swimming efficiency, such as
595 shared ancestry, muscle content, jet coordination, or jetting angles (thrust-to-torque ratios).

596 *Evolutionary implications*

597 Across the evolutionary history of salps, linear chains have evolved multiple times
598 independently from oblique ancestors (Damian-Serrano et al. 2023), suggesting the adaptive role
599 of this architecture as a functional trait. Linear chain architectures evolved independently in *M.*
600 *hexagona*, *S. zonaria*, *I. punctata*, and before the common ancestor of *Iasis* and *Salpa*. Our results
601 show that going from an oblique form to a linear one may confer significant advantages in
602 locomotory speed and energetic efficiency. However, multiple colonial architectures, which we
603 find to be slower swimmers (such as transversal chains, helical chains, whorls, and clusters in
604 the genus *Pegea* and the Cyclosalpidae family) had also evolved from oblique and linear
605 ancestors. This is incongruent with a scenario where natural selection strongly favors locomotion
606 efficiency across all ecological niches of salps. Therefore, the evolution of colonial architecture
607 may be driven by ecological trade-offs with other non-locomotory functions. Alternatively, in some
608 of these lineages, locomotion at the colonial stage may not be important enough for selection to
609 maintain these highly streamlined forms, allowing for neutral evolutionary processes to produce
610 a diversity of non-adaptive forms. In the current study, we did not use phylogenetic comparative
611 methods in our analysis because like other investigators comparing biomechanical properties
612 across species (e.g. Dabiri et al. 2010, DiSanto et al. 2021) we were interested in inherent
613 mechanical relationships dictated by the colony architectures. For instance, a linear arrangement
614 of zooids inherently reduces drag due to a cluster arrangement, leading to faster swimming

615 speeds and potentially higher efficiency regardless of phylogenetic history. In other words, any
616 phylogenetic inertia is irrelevant in instantaneous relationships between traits (Felsenstein 1985).
617 Moreover, independence of data is often incorrectly assumed to be an assumption of standard
618 (nonphylogenetic) regressions (Uyeda et al. 2018), when in reality the assumptions relate to the
619 independence and distribution of the error terms. Thus, when all the phylogenetic signal is present
620 in the predictor, as it is in the case with colonial architecture (Damian-Serrano et al. 2022) and its
621 associated characteristics, there is no need for any “phylogenetic correction” (Uyeda et al. 2018).
622 However, there may be unaccounted factors explaining the residual variation in our analyses that
623 may bear phylogenetic signal. For example, tunic stiffness, tunic smoothness, muscle band
624 number, muscle fiber density, swimming behavior, as well as metabolic and physiological
625 baselines may be more similar between more closely related species, potentially erasing some of
626 the architecture-specific signal. Future studies could address the role of phylogeny and heritable
627 factors in salp swimming speed and cost of transport using phylogenetic comparative methods.
628 These analyses could reveal whether these factors have co-evolved with each other and/or with
629 respiration rate or colonial architecture.

630 *Insights for bioinspired underwater vehicle design*

631 Pulsatile jet propulsion is a promising avenue for bioinspired aquatic vehicles and robots
632 (Mohensi 2006, Gohardini 2014, Yue et al. 2015). Multijet propulsion systems with multiple
633 propellers akin to salp colonies have been explored in an engineering context (Chao et al. 2017,
634 Costello et al. 2015) with direct inspiration from gelatinous animals (Marut 2014, Krummel 2019,
635 Bi et al 2022, Du Clos et al. 2022). Salp diversity provides a natural laboratory to explore the
636 hydrodynamic implications of different multijet arrangement designs. Our findings underscore the
637 importance of considering the scaling hydrodynamic properties of propeller arrangements to
638 optimize speed and energy efficiency in bioinspired underwater vehicle design. While linear chain
639 arrangements were the fastest and among the most energy efficient, robot (or vehicle)
640 configurations such as a cluster form may confer unique object manipulation or maneuverability
641 advantages. Our results show that these seemingly inefficient propeller configurations do not
642 impose large disadvantages in terms of speed and fuel efficiency.

643 **Acknowledgments:**

644 We are grateful to the crew of Aquatic Life Divers, Kona Honu Divers for their assistance
645 and support in hosting our offshore diving operations. We also wish to thank Marc Hughes, Jeff
646 Milisen, Rebecca Gordon, Matt Connelly, Clint Collins, Paul Richardson, and Anne Thompson for
647 their assistance during diving, collections, and filming operations in the field. We would like to

648 thank Tiffany Bachtel for her valuable advice on the respirometry experiment design. We thank
649 the associate editor and two anonymous reviewers for their helpful comments.

650 **Funding**

651 This research was supported by the Gordon and Betty Moore Foundation [grant number
652 8835] and the Office of Naval Research [grant number N00014-23-1-2171].

653 **Data availability**

654 Data used to generate the results presented in this paper are available in the supplementary
655 information. Any other datasets used directly or indirectly for this study are available from the
656 authors upon reasonable request.

657 **Competing interests**

658 No competing interests declared.

659 **Literature cited**

660 Alexander, A. J. (1968). Forward Speed Effects on Annular Jet Cushions. *The Aeronautical
661 Journal*, 72(689), 438-441.

662 Andersen, K. H., Berge, T., Gonçalves, R. J., Hartvig, M., Heuschele, J., Hylander, S., ... &
663 Kiørboe, T. (2016). Characteristic sizes of life in the oceans, from bacteria to whales.
664 *Annual review of marine science*, 8(1), 217-241.

665 Bi, X., & Zhu, Q. (2019). Dynamics of a squid-inspired swimmer in free swimming. *Bioinspiration
666 & Biomimetics*, 15(1), 016005.

667 Bi, X., Tang, H., & Zhu, Q., 2022. Feasibility of hydrodynamically activated valves for 416 salp-
668 like propulsion. *Physics of Fluids*, 34(10), 101903.

669 Biggs, D. C. (1977). Respiration and ammonium excretion by open ocean gelatinous zooplankton
670 1. *Limnology and Oceanography*, 22(1), 108-117.

671 Bone, Q., Anderson, P. A. V., & Pulsford, A. (1980). Morphology of salp chain communication.
672 *Proceedings of the Royal Society of London. Series B. Biological Sciences*, 210(1181),
673 549-558.

674 Bone, Q., & Trueman, E. R. (1983). Jet propulsion in salps (Tunicata: Thaliacea). *Journal of
675 Zoology*, 201(4), 481-506.

676 Cetta, C. M., Madin, L. P., & Kremer, P. (1986). Respiration and excretion by oceanic salps.
677 *Marine Biology*, 91, 529-537.

678 Chao, S., Guan, G., & Hong, G. S., 2017, September. Design of a finless torpedo-shaped micro
679 AUV with high maneuverability. In OCEANS 2017-Anchorage (pp. 425 1-6). IEEE.

680 Colin, S. P., Gemmell, B. J., Costello, J. H., & Sutherland, K. R. (2022). In situ high-speed
681 brightfield imaging for studies of aquatic organisms. *Protocols.io*.

- 682 Costello, J. H., Colin, S. P., Gemmell, B. J., Dabiri, J. O., & Sutherland, K. R., 2015. 429 Multi-jet
683 propulsion organized by clonal development in a colonial siphonophore. 430 *Nature*
684 communications, 6(1), 8158.
- 685 Dabiri, J. O., Colin, S. P., Katija, K., & Costello, J. H. (2010). A wake-based correlate of
686 swimming performance and foraging behavior in seven co-occurring jellyfish species.
687 *Journal of experimental biology*, 213(8), 1217-1225.
- 688 Damian-Serrano, A., & Sutherland, K. R. (2023). A developmental ontology for the colonial
689 architecture of salps. *The Biological Bulletin*, 245(1), 9-18..
- 690 Damian-Serrano, A., Hughes, M., & Sutherland, K. R. (2023). A new molecular phylogeny of salps
691 (Tunicata: thalicea: salpida) and the evolutionary history of their colonial architecture.
692 *Integrative Organismal Biology*, 5(1), obad037.
- 693 Décima, M., Stukel, M. R., Nodder, S. D., Gutiérrez-Rodríguez, A., Selph, K. E., Dos Santos, A.
694 L., ... & Pinkerton, M. (2023). Salp blooms drive strong increases in passive carbon export
695 in the Southern Ocean. *Nature communications*, 14(1), 425.
- 696 Di Santo, V., Goerig, E., Wainwright, D. K., Akanyeti, O., Liao, J. C., Castro-Santos, T., & Lauder,
697 G. V. (2021). Convergence of undulatory swimming kinematics across a diversity of fishes.
698 *Proceedings of the National Academy of Sciences*, 118(49), e2113206118.
- 699 Du Clos, K. T., Gemmell, B. J., Colin, S. P., Costello, J. H., Dabiri, J. O., and Sutherland, K. R.
700 2022. Distributed propulsion enables fast and efficient swimming modes in physonect
701 siphonophores. *Proceedings of the National Academy of Sciences*. 119:e2202494119.
- 702 Felsenstein, J. (1985). Phylogenies and the comparative method. *The American
703 Naturalist*, 125(1), 1-15.
- 704 Gemmell, B. J., Dabiri, J. O., Colin, S. P., Costello, J. H., Townsend, J. P., & Sutherland, K. R.
705 (2021). Cool your jets: biological jet propulsion in marine invertebrates. *Journal of
706 Experimental Biology*, 224(12), jeb222083.
- 707 Gohardani, A. S. *Distributed Propulsion Technology* Nova Science Publishers (2014).
- 708 Haddock, S. H. (2004). A golden age of gelata: past and future research on planktonic
709 ctenophores and cnidarians. *Hydrobiologia*, 530, 549-556.
- 710 Haddock, S. H., & Heine, J. N. (2005). Scientific blue-water diving.
- 711 Hamner, W. M., Madin, L. P., Alldredge, A. L., Gilmer, R. W., & Hamner, P. P. (1975). Underwater
712 observations of gelatinous zooplankton: Sampling problems, feeding biology, and
713 behavior 1. *Limnology and Oceanography*, 20(6), 907-917.

- 714 Henschke, N., Cherel, Y., Cotté, C., Espinasse, B., Hunt, B.P. and Pakhomov, E.A., 2021. Size
715 and stage specific patterns in *Salpa thompsoni* vertical migration. *Journal of Marine*
716 *Systems*, 222, p.103587.
- 717 Krummel, G. M. (2019). Locomotion and Control of Cnidarian-Inspired Robots (Doctoral
718 dissertation, Virginia Tech).
- 719 Mackie, G. O. (1986). From aggregates to integrates: physiological aspects of modularity in
720 colonial animals. *Philosophical Transactions of the Royal Society of London. B, Biological*
721 *Sciences*, 313(1159), 175-196.
- 722 Madin, L. P. (1990). Aspects of jet propulsion in salps. *Canadian Journal of Zoology*, 68(4), 765-
723 777.
- 724 Madin, L. P., & Deibel, D. (1998). Feeding and energetics of Thaliacea. *The biology of pelagic*
725 *tunicates*, 81-104.
- 726 Madin, L. P., Kremer, P., & Hacker, S. (1996). Distribution and vertical migration of salps
727 (Tunicata, Thaliacea) near Bermuda. *Journal of Plankton Research*, 18(5), 747-755.
- 728 Madin, L.P., Kremer, P., Wiebe, P.H., Purcell, J.E., Horgan, E.H. and Nemazie, D.A., 2006.
729 Periodic swarms of the salp *Salpa aspera* in the Slope Water off the NE United States:
730 Biovolume, vertical migration, grazing, and vertical flux. *Deep Sea Research Part I:*
731 *Oceanographic Research Papers*, 53(5), pp.804-819.
- 732 Marut, K. J. (2014). Underwater Robotic Propulsors Inspired by Jetting Jellyfish (Doctoral
733 dissertation, Virginia Tech).
- 734 Mayzaud, P., Boutoute, M., Gasparini, S., Mousseau, L., & Lefevre, D. (2005). Respiration in
735 marine zooplankton—the other side of the coin: CO₂ production. *Limnology and*
736 *Oceanography*, 50(1), 291-298.
- 737 Mohensi, K., 2006. Pulsatile vortex generators for low-speed maneuvering of small 482
738 underwater vehicles. *Ocean Eng.* 33, 2209–2223.
- 739 Pascual, M., Acuña, J.L., Sabatés, A., Raya, V. and Fuentes, V., 2017. Contrasting diel vertical
740 migration patterns in *Salpa fusiformis* populations. *Journal of Plankton Research*, 39(5),
741 pp.836-842.
- 742 R Core Team, R. (2021). R: A language and environment for statistical computing.
- 743 Rubio-Gracia, F., García-Berthou, E., Guasch, H., Zamora, L., & Vila-Gispert, A. (2020). Size-
744 related effects and the influence of metabolic traits and morphology on swimming
745 performance in fish. *Current Zoology*, 66(5), 493-503.

- 746 Schneider, G. (1992). A comparison of carbon-specific respiration rates in gelatinous and non-
747 gelatinous zooplankton: a search for general rules in zooplankton metabolism.
748 *Helgoländer Meeresuntersuchungen*, 46, 377-388.
- 749 Seibel, B. A., & Drazen, J. C. (2007). The rate of metabolism in marine animals: environmental
750 constraints, ecological demands and energetic opportunities. *Philosophical Transactions of the Royal Society B: Biological Sciences*, 362(1487), 2061-2078.
- 751 Stone, J. P., & Steinberg, D. K. (2014). Long-term time-series study of salp population dynamics
752 in the Sargasso Sea. *Marine Ecology Progress Series*, 510, 111-127.
- 753 Sutherland, K. R., & Weihs, D. (2017). Hydrodynamic advantages of swimming by salp chains.
754 *Journal of The Royal Society Interface*, 14(133), 20170298.
- 755 Sutherland, K. R., Damian-Serrano, A., Du Clos, K. T., Gemmell, B. J., Colin, S. P., Costello, J.
756 H. (2024). Spinning and corkscrewing of oceanic macroplankton revealed through in situ
757 imaging. *Science Advances* 10(20).
- 758 Sutherland, K. R., & Madin, L. P. (2010). Comparative jet wake structure and swimming
759 performance of salps. *Journal of Experimental Biology*, 213(17), 2967-2975.
- 760 Trueblood, L. A. (2019). Salp metabolism: temperature and oxygen partial pressure effect on the
761 physiology of *Salpa fusiformis* from the California Current. *Journal of Plankton Research*,
762 41(3), 281-291.
- 763 Trueman, E. R., Bone, Q., & Braconnor, J. C. (1984). Oxygen consumption in swimming salps
764 (Tunicata: Thaliacea). *Journal of Experimental Biology*, 110(1), 323-327.
- 765 Uyeda, J. C., Zenil-Ferguson, R., & Pennell, M. W. (2018). Rethinking phylogenetic comparative
766 methods. *Systematic Biology*, 67(6), 1091-1109.
- 767 Vogel, S. (1981). Life in moving fluids. *Princeton University Press*, Princeton, NJ.
- 768 Vogel, S. (2008). Modes and scaling in aquatic locomotion. *Integrative and Comparative Biology*,
769 48(6), 702-712.
- 770 Wiebe, P. H., Madin, L. P., Haury, L. R., Harbison, G. R., & Philbin, L. M. (1979). Diel vertical
771 migration by *Salpa aspera* and its potential for large-scale particulate organic matter
772 transport to the deep-sea. *Marine Biology*, 53, 249-255.
- 773 World Register of Marine Species (WoRMS). (2024). WoRMS Editorial Board. Accessed January
774 30, 2024. Available online at <http://www.marinespecies.org>
- 775 Yue, C. et al., 2015. Mechantronic system and experiments of a spherical underwater 510 robot:
776 SUR-II. *J. Intell. Robot Syst.* Doi:10.1007/s10846-015-0177-3.